Electronic Supplementary Material (ESI) for Chemical Science.

Supporting Information

A Novel Tyrosine Hyperoxidation Enables Selective Peptide Cleavage

*Shengping Zhang,[a,b] Luis M. De Leon Rodriguez,[a] Freda F. Li,[a] Renjie Huang,[a] Ivanhoe K. H. Leung,[a c] Paul W.R. Harris, *[a,b,c] Margaret A. Brimble *[a,b,c]*

[a] School of Chemical Sciences, The University of Auckland, 23 Symonds St, Auckland, 1010, New Zealand

[b] School of Biological Sciences, The University of Auckland, 3A Symonds Street, Auckland 1010, New Zealand

[c] Maurice Wilkins Centre for Molecular Biodiscovery, The University of Auckland, Auckland, 1142, New Zealand

Table of Contents

1. Supporting items mentioned in the main discussion of the paper

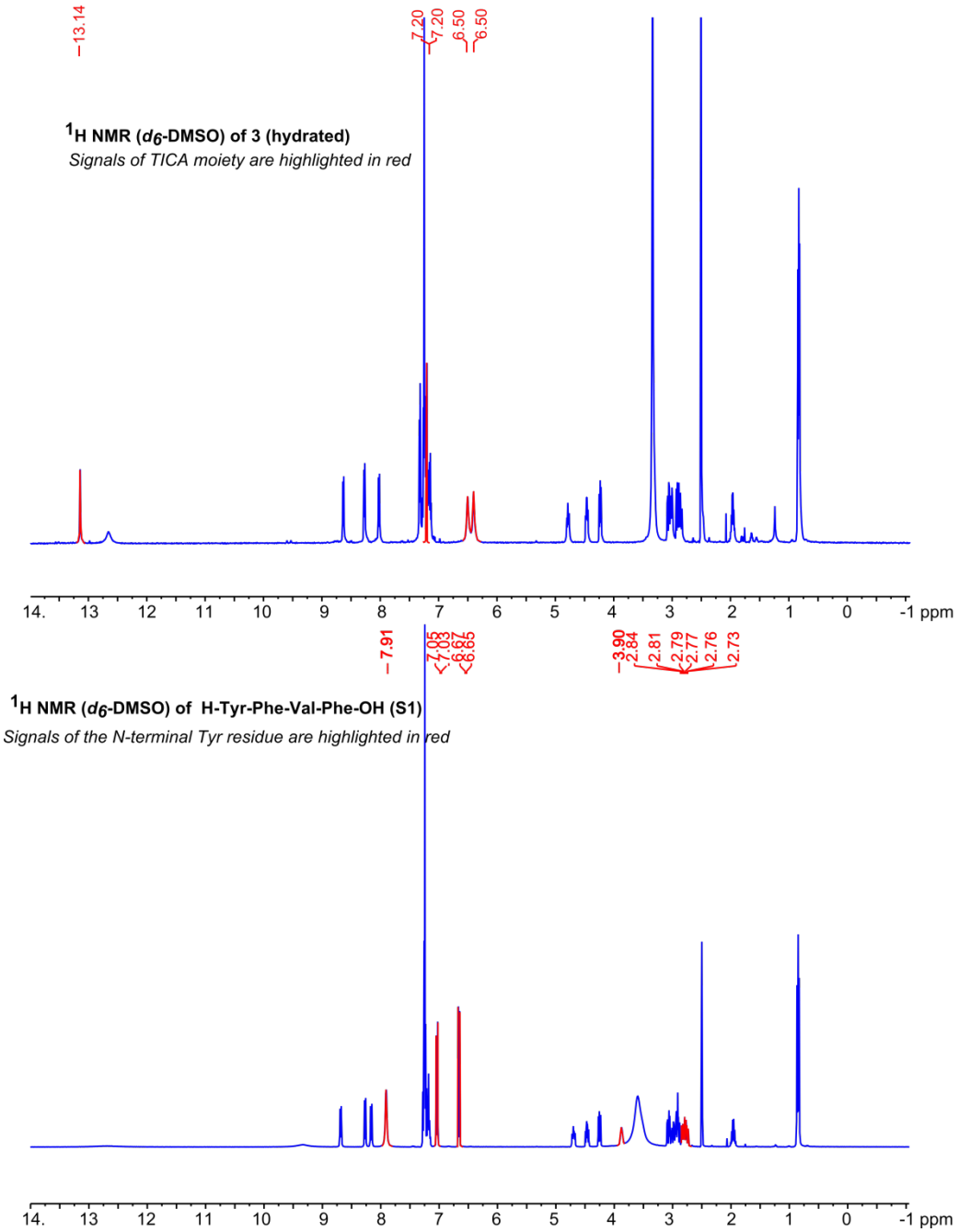

Figure S1. The stacked ^{1}H-NMR (500 MHz, d_6-DMSO) of **3** (top) and H-Tyr-Phe-Val-Phe-OH (**S1**) (bottom). The signals of the tyrosine residue in **S1** and the TICA moiety in **3** are highlighted in red.

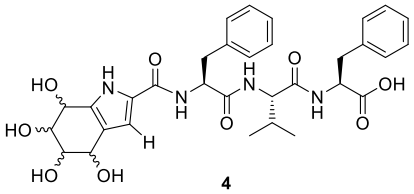

4

(4,5,6,7-tetrahydroxy-4,5,6,7-tetrahydro-1*H*-indole-2-carbonyl)- Phe-Val-Phe-OH (**4**) To a solution of peptide **3a** (5 mg, 8 μmol) in MeOH (5 mL) was added sodium borohydride (3 mg, 76 μmol). The mixture was stirred at RT for 2 h, followed by concentration under vacuum. The resulting residue was re-dissolved in 50% MeCN aqueous solution and then subjected to semi-preparative RP-HPLC purification to afford a diastereomeric mixture **4** as a white powder (3.0 mg, 63%). MS (ESI+): $C_{32}H_{38}N_4O_9$ [M+Na]$^+$ calcd./found 645.2531/645.2519.

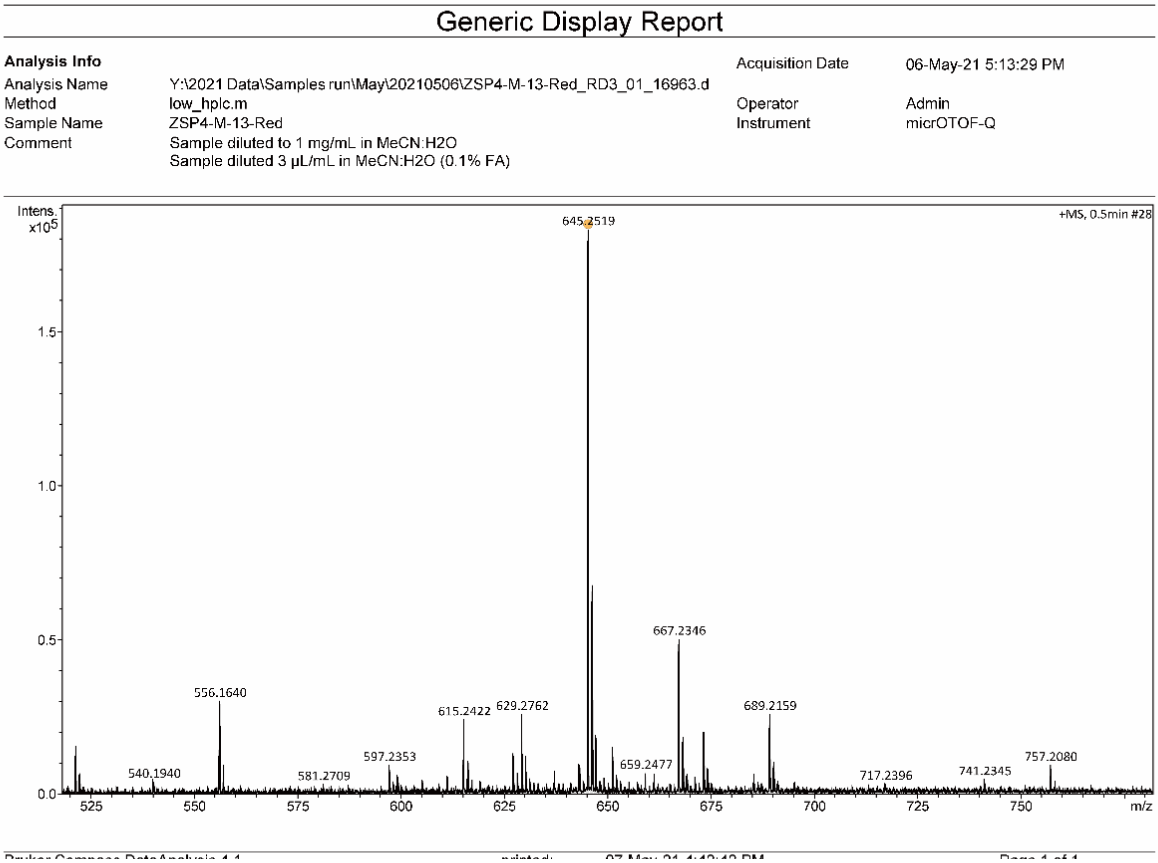

Figure S2. The HRMS of the diastereomeric mixture of **4** ([M+Na]$^+$ calcd./found 645.2531/645.2519).

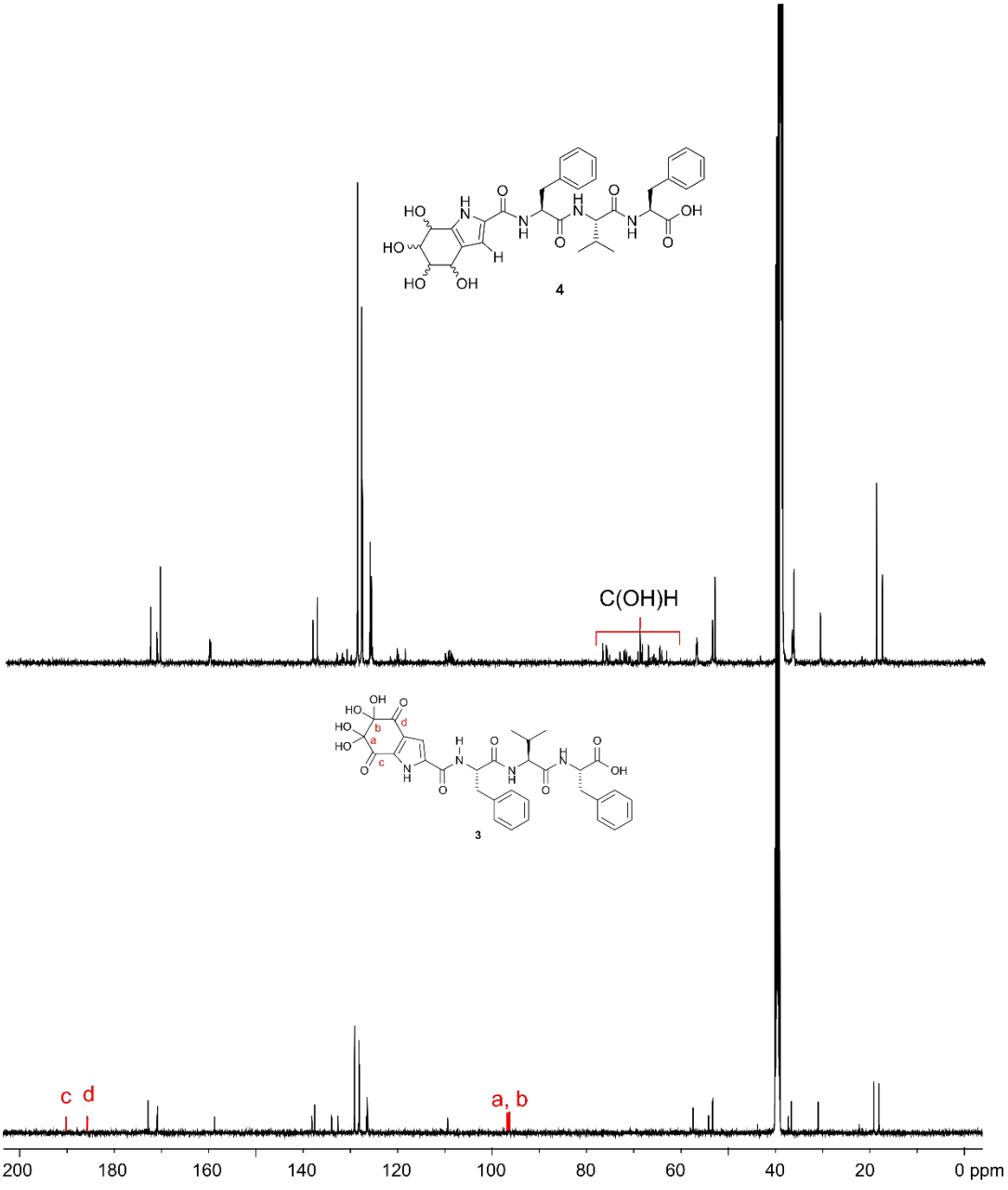

Figure S3. The stacked ^{13}C NMR (125 MHz, d_6-DMSO) of the diastereomeric mixture of **4** (top) and **3** (bottom).

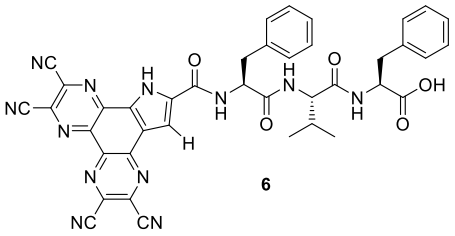

6

(2,3,6,7-tetracyano-9*H*-pyrazino[2,3-*f*]pyrrolo[2,3-*h*]quinoxaline-10-carbonyl)-Phe-Val-Phe-OH (**6**). To peptide **3a** (7 mg, 11 μmol) dissolved in EtOH (7 mL) was added with diaminomaleonitrile (25 mg, 230 μmol) and formic acid (70 μL). The mixture was stirred at RT for 24 h, followed by concentration under vacuum. The resulting residue was re-dissolved in 50% MeCN aqueous solution and then subjected to semi-preparative RP-HPLC purification to afford **6** as a yellow powder (5 mg, 62%). Anal. RP-HPLC: t_R = 24.4 min, purity: >95% (HPLC analysis at 210 nm). ^{1}H NMR (500 MHz, DMSO-d_6) δ 14.28 (s, 1H), 8.98 (d, *J* = 8.5 Hz, 1H), 8.29 (d, *J* = 7.8 Hz, 1H), 8.17 (d, *J* = 2.0 Hz, 1H), 8.15 (d, *J* = 9.1 Hz, 1H), 7.39 (d, *J* = 7.3 Hz, 2H), 7.25 (m, 6H), 7.11 – 7.20 (m, 2H), 4.92 (ddd, *J* = 11.8, 8.5, 3.7 Hz, 1H), 4.47 (m, 1H), 4.26 (dd, *J* = 9.0, 7.0 Hz, 1H), 3.07 (dd, *J* = 14.0, 4.7 Hz, 2H), 2.92 (m, 2H), 1.98 (dt, *J* = 13.7, 6.8 Hz, 1H), 0.85 (dd, *J* = 6.7, 4.6 Hz, 6H). ^{13}C NMR (125 MHz, DMSO-d_6) δ 172.8, 170.9, 170.8, 158.6, 142.4, 138.1, 137.5, 137.4, 137.4, 136.7, 136.5, 134.2, 133.8, 130.6, 130.0, 129.8, 129.2, 129.2, 129.1, 129.1, 128.2, 128.2, 128.1, 128.1, 126.4, 126.3, 123.9, 114.6, 114.6, 114.5, 114.3, 108.3, 57.5, 54.4, 53.3, 37.4, 36.6, 30.9, 19.2, 18.1. MS (ESI+): $C_{32}H_{35}N_4O_{11}$ $[M+H]^+$ calcd./found 781.2354/781.2352.

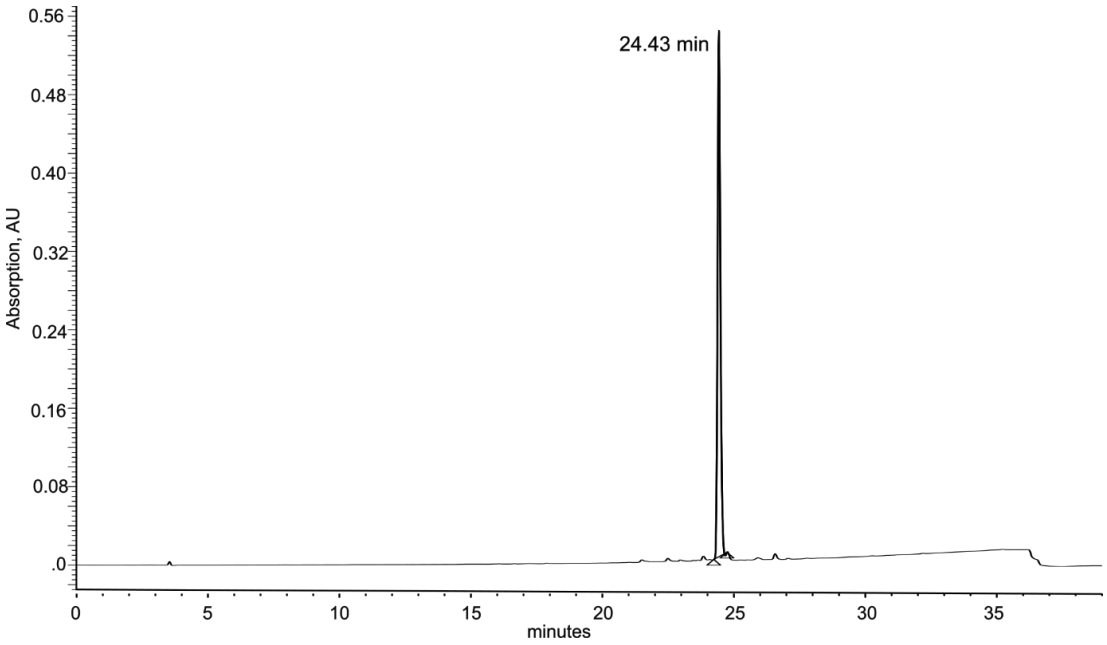

Figure S4. HPLC-MS profile of **6**, t_R = 24.4 min (purity >95% as judged by peak area of RP-HPLC at 210 nm); Waters XTerra MS C_{18} column (125 Å 4.6 mm × 150 mm, 5 μm) using a linear gradient of 5% B-95% B over 30 min (ca. 3 % B•min^{-1}) at a flow rate of 1 mL•min^{-1} (A = 0.1% TFA in H_2O and B = 0.1 %TFA MeCN).

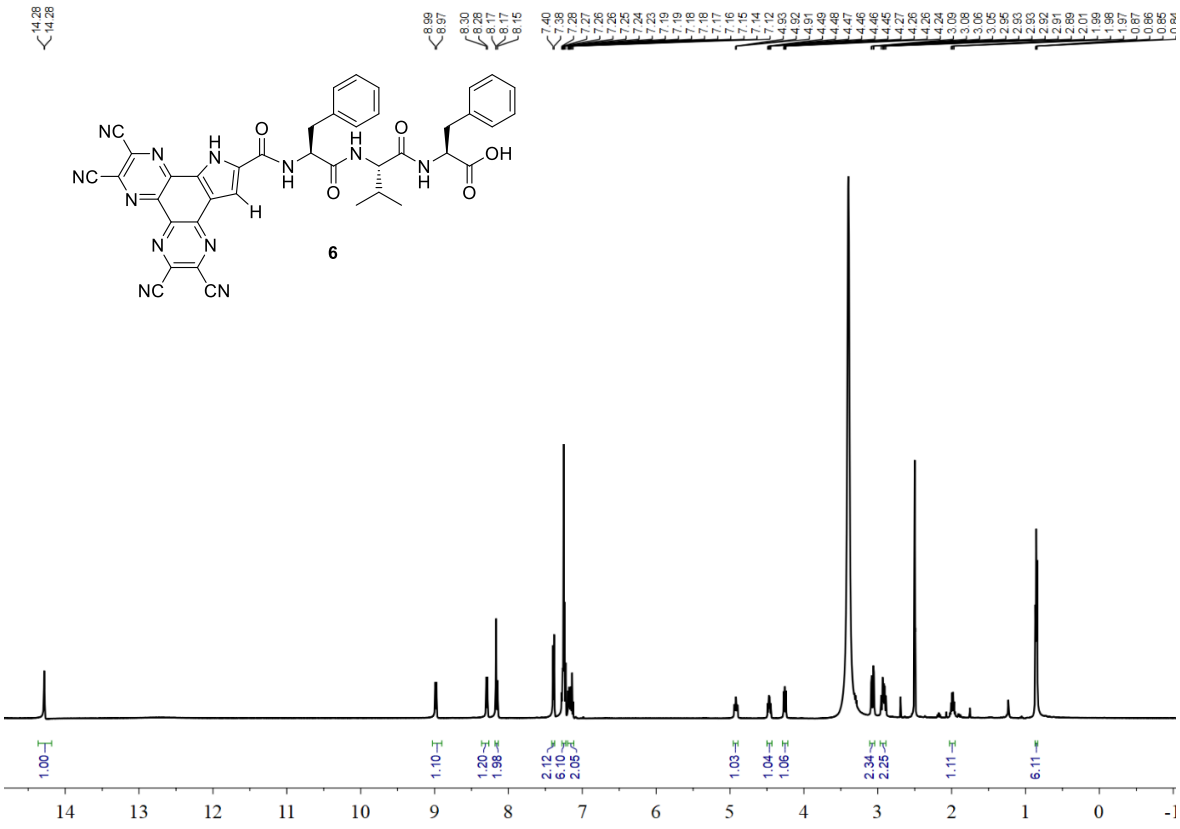

Figure S5. The ^{1}H-NMR (500 MHz, d_6-DMSO) of **6.**

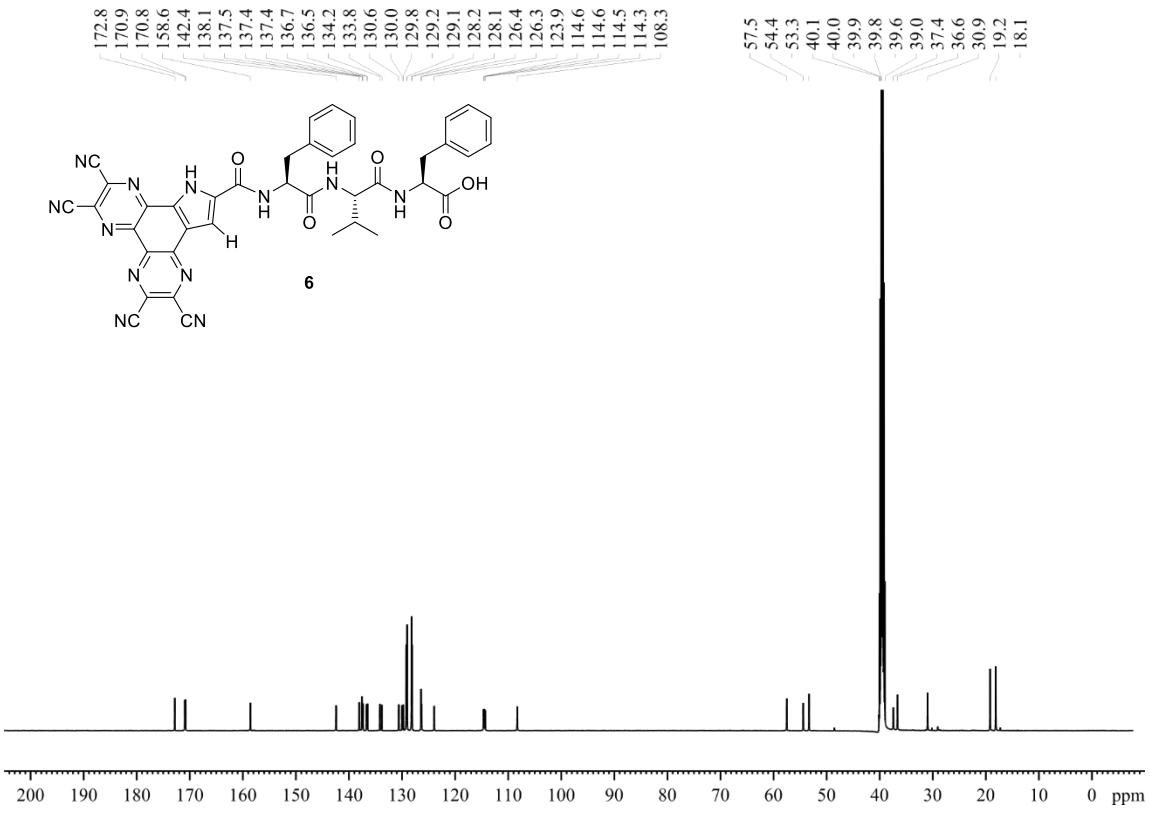

Figure S6. The ^{13}C NMR (125 MHz, d_6-DMSO) of **6**.

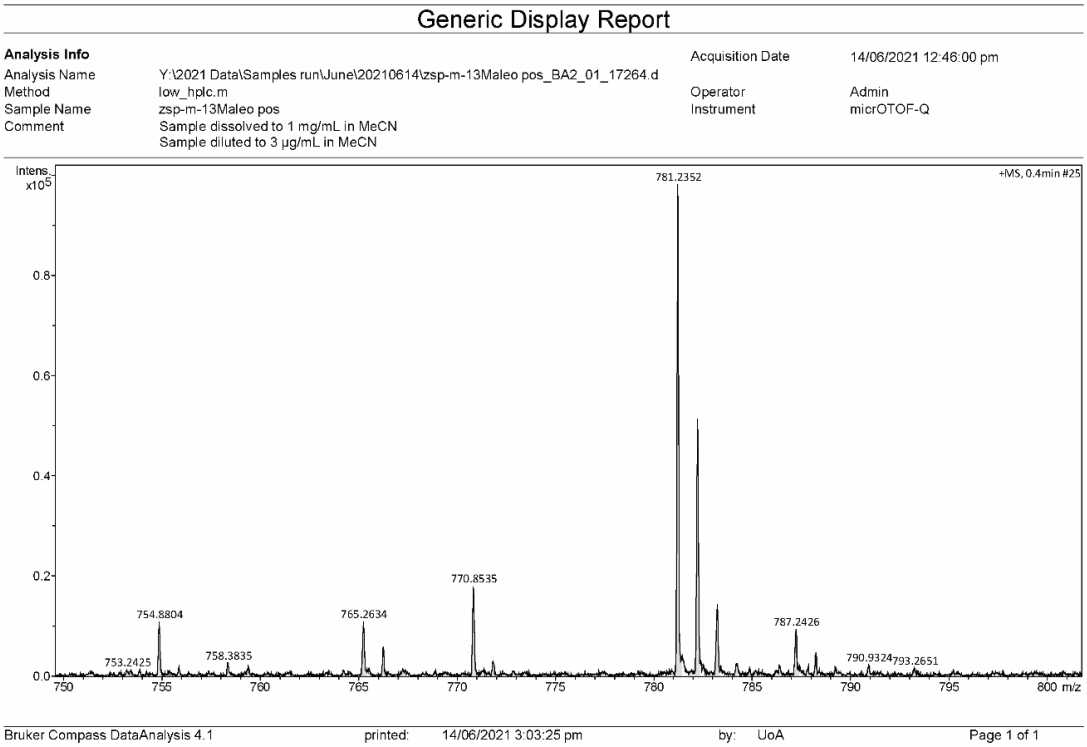

Figure S7. The HRMS of **6** ([M+Na]$^+$ calcd./found 781.2354/781.2352).

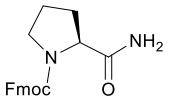

20

Fmoc-Pro-NH_2(**20**) To a solution of Fmoc-Pro-Ser-Phe-Pro-Ile-OH (7 mg, 9 µmol) in DMSO (0.7 mL) was added DMP (38 mg, 90 µmol) in DMSO (0.7 mL) and the reaction mixture was stirred at 40 ºC for 2 days. The resulting mixture was then diluted with water (10 mL) and subjected to purification using semi-preparative HPLC to give **20** as a white powder (1.2 mg, 36%). Anal. RP-HPLC: t_R = 20.3 min, purity: >95% (HPLC analysis at 210 nm). ^{1}H NMR (400 MHz, DMSO-d_6) δ 7.89 (t, *J* = 6.7 Hz, 2 H), 7.68 (t, *J* = 6.1 Hz, 2 H), 7.52 (br s, 0.5 H), 7.42 (t, *J* = 7.3, 2 H), 7.33 (m, 2.5 H), 7.10 (br s, 0.5 H), 6.93 (br s, 0.5 H), 4.33 – 4.22 (m, 2 H), 4.22 – 4.14 (m, 1 H), 4.14 – 4.05 (m, 1 H), 3.47 (dt, *J* = 10.3, 6.4 Hz, 1 H), 3.42 – 3.27 (m, 1 H), 2.20 (m, 0.5 H), 2.07 (td, *J* = 8.4, 4.0 Hz, 0.5 H), 1.94 – 1.88 (m, 0.5 H), 1.87 – 1.76 (m, 2.5 H). ^{13}C NMR (100 MHz, DMSO-d_6) δ 174.2, 173.8, 154.1, 143.9, 143.8, 143.8, 143.7, 140.7, 140.6, 127.7, 127.2, 127.1, 125.5, 125.2, 120.1, 67.0, 66.5, 59.8, 59.5, 47.1, 46.7, 46.4, 31.4, 30.0, 23.9, 23.0. A 1:1 mixture of *cis*-Fmoc-L-Pro-NH_2 and *trans*-Fmoc-L-Pro-NH_2 were found in the ^{1}H and ^{13}C-NMR spectrum. The NMR spectral data of **20** matched those previously reported in the literature.[1] MS (ESI+): $C_{20}H_{20}N_2O_3Na$ [M+H]$^+$ calcd./found 359.1366/359.1362.

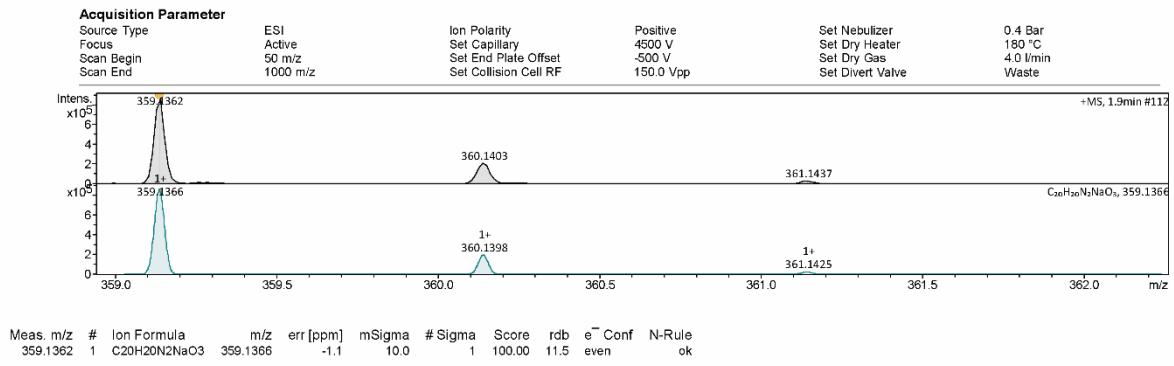

Figure S8. HRMS characterization of **20** in H_2O/MeCN (*v/v*, 1;1). HRMS (ESI+): $C_{20}H_{20}N_2O_3Na$ [M+H]$^+$ calcd./found 359.1366/359.1362.

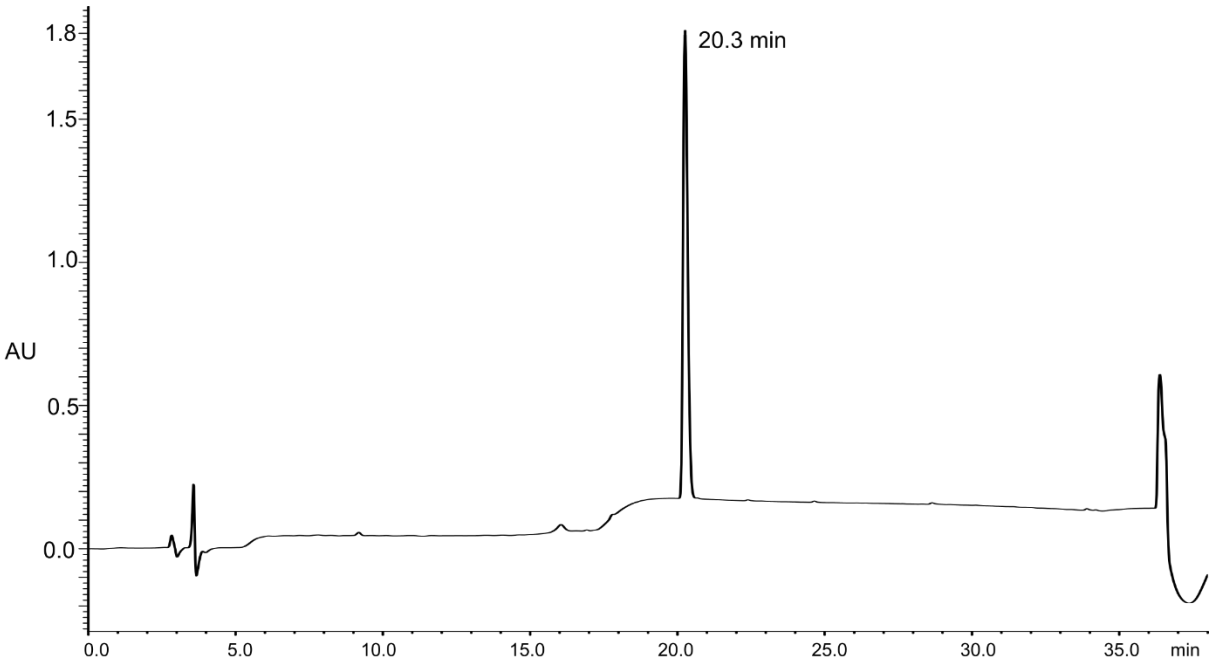

Figure S9. HPLC-MS profile of **20**, t_R = 20.3 min (purity >95% as judged by peak area of RP-HPLC at 210 nm); Phenomenex Luna, C_{18} column (100 Å, 4.6 x 250 mm, 5 µm) using a linear gradient of 5% B-95% B over 30 min (*ca.* 3 % B•min^{-1}) at a flow rate of 1 mL•min^{-1} (A = 0.1% TFA in H_2O and B = 0.1 %TFA MeCN).

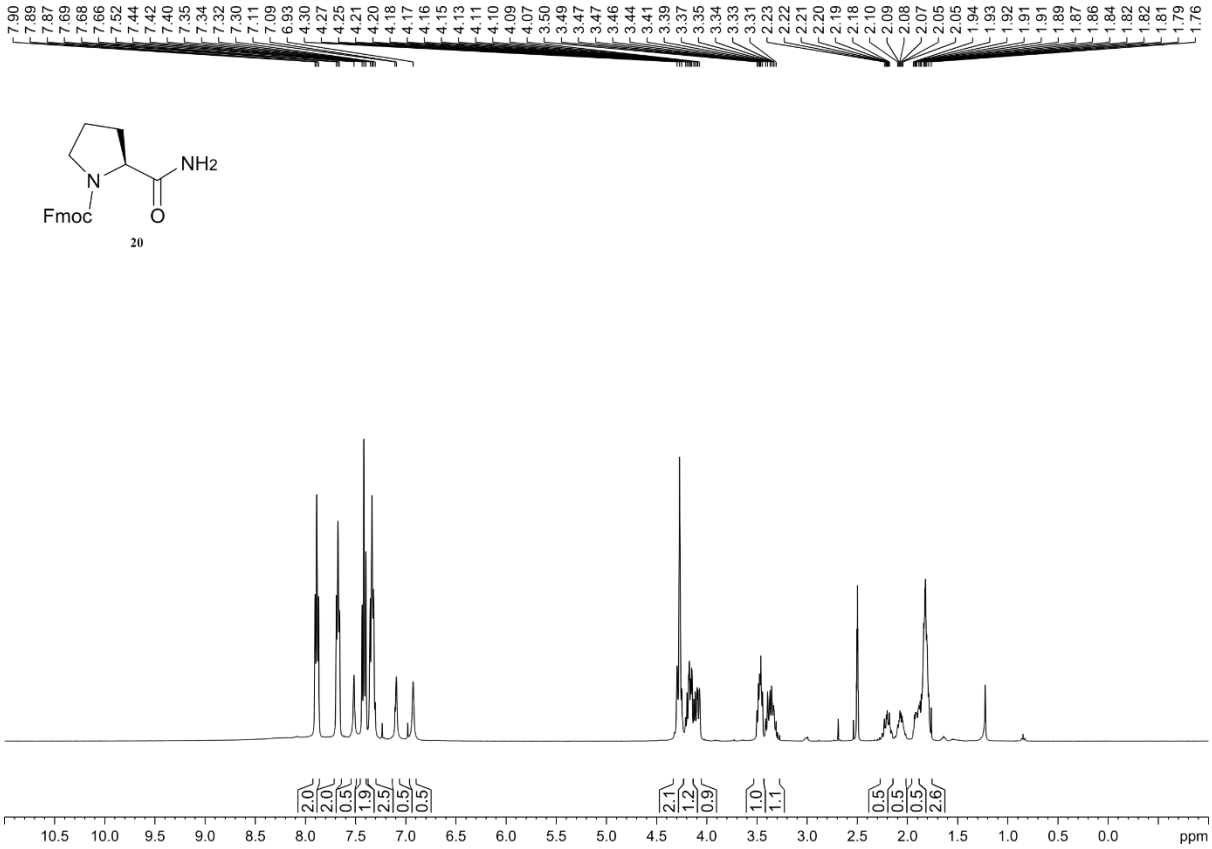

Figure S10. The ^{1}H-NMR (400 MHz, d_6-DMSO) of **20**.

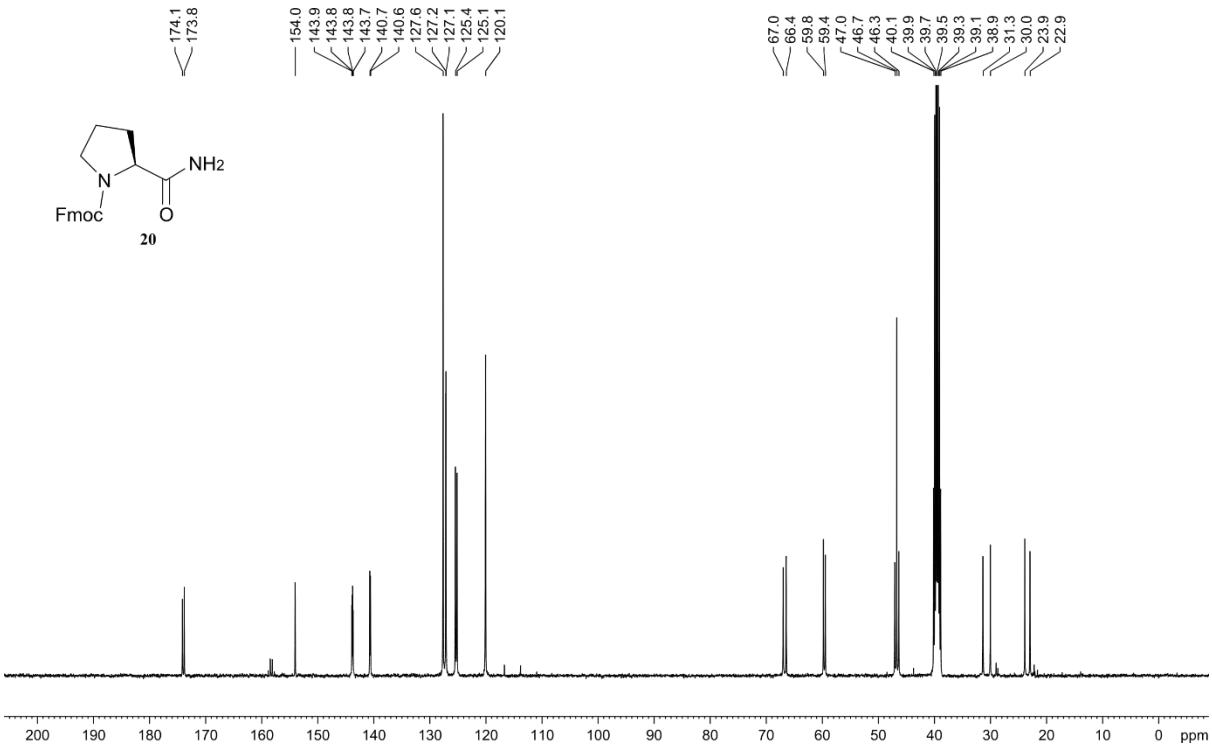

Figure S11. The ^{13}C NMR (100 MHz, d_6-DMSO) of **20**.

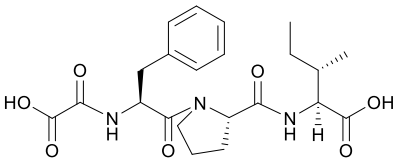

S2

(carboxycarbonyl)-Phe-Pro-Ile-OH(**S2**) To a solution of Fmoc-Pro-Ser-Phe-Pro-Ile-OH (7 mg, 9 µmol) in DMSO (0.7 mL) was added DMP (38 mg, 90 µmol) in DMSO (0.7 mL) and the reaction mixture was stirred at 40 ºC for 2 days. The resutlng mixture was then diluted with water (10 mL) and subjected to purification using semi-preparative HPLC to give **S2** as a white powder (0.7 mg, 18%). Anal. RP-HPLC: t_R = 15.8 min, purity: >95% (HPLC analysis at 210 nm). ^1H NMR (400 MHz, DMSO-d_6) δ 8.68 (d, J = 8.1 Hz, 1 H), 8.01 (d, J = 8.4 Hz, 1 H), 7.33 – 7.15 (m, 5 H), 4.73 – 4.63 (m, 1 H), 4.54 – 4.43 (m, 1 H), 4.20 (dd, J = 8.4, 5.71 Hz, 1 H), 3.68 – 3.60 (m, 1 H), 3.56 (dd, J = 14.2, 7.21 Hz, 1 H), 3.02 – 2.94 (m, 2 H), 2.08 – 1.97 (m, 1 H), 1.97 – 1.66 (m, 4 H), 1.44 (ddd, J = 11.8, 7.4, 4.4 Hz, 1 H), 1.20 (dt, J = 18.8, 7.3 Hz, 1 H), 0.86 (ddd, J = 13.9, 8.6, 5.1 Hz, 6 H). ^{13}C NMR (100 MHz, DMSO-d_6) δ 172.9, 171.4, 168.5, 161.6, 157.8, 137.2, 129.4,129.4, 128.1, 128.1, 126.4, 59.1, 56.2, 52.6, 46.8, 36.5, 35.8, 28.8, 24.6, 24.5, 15.6, 11.4. MS (ESI+): $C_{22}H_{29}N_3O_7$ $[M+H]^+$ calcd./found 448.2078/448.2069.

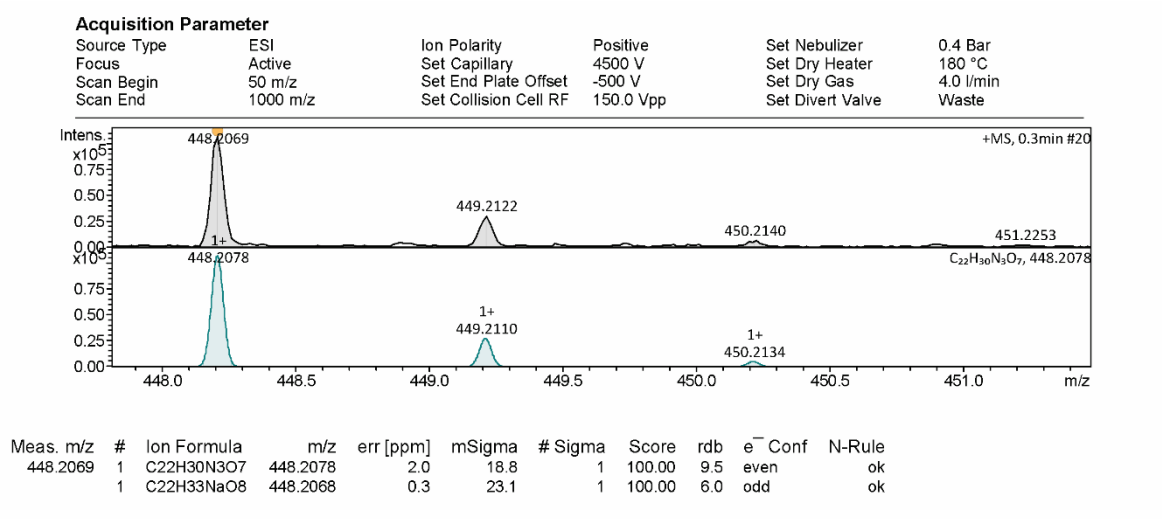

Meas. m/z	#	Ion Formula	m/z	err [ppm]	mSigma	# Sigma	Score	rdb	e⁻ Conf	N-Rule
448.2069	1	C22H30N3O7	448.2078	2.0	18.8	1	100.00	9.5	even	ok
	1	C22H33NaO8	448.2068	0.3	23.1	1	100.00	6.0	odd	ok

Figure S12. HRMS characterization of **S2** in H_2O/MeCN (*v/v*, 1;1). HRMS (ESI+): $C_{22}H_{29}N_3O_7$ $[M+H]^+$ calcd./found 448.2078/448.2069.

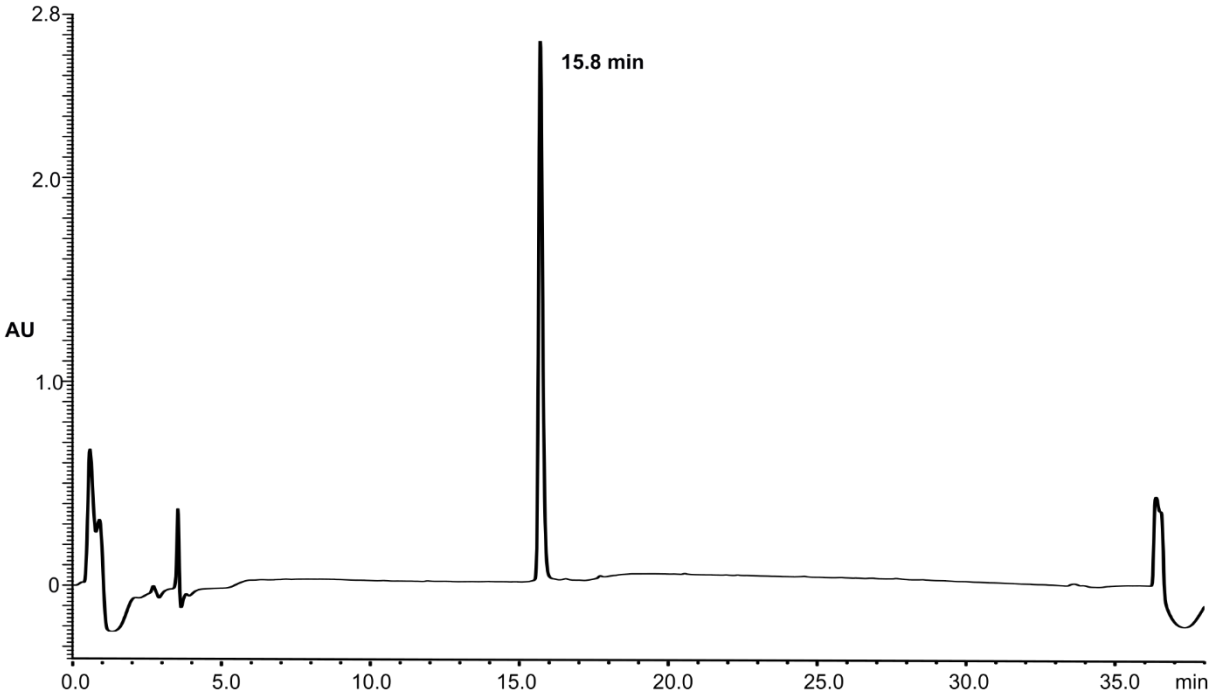

Figure S13. HPLC-MS profile of **S2**, t_R = 15.8 min (purity >95% as judged by peak area of RP-HPLC at 210 nm); Phenomenex Luna, C_{18} column (100 Å, 4.6 x 250 mm, 5 µm) using a linear gradient of 5% B-95% B over 30 min (*ca.* 3 % B•min^{-1}) at a flow rate of 1 mL•min^{-1} (A = 0.1% TFA in H_2O and B = 0.1 %TFA MeCN)

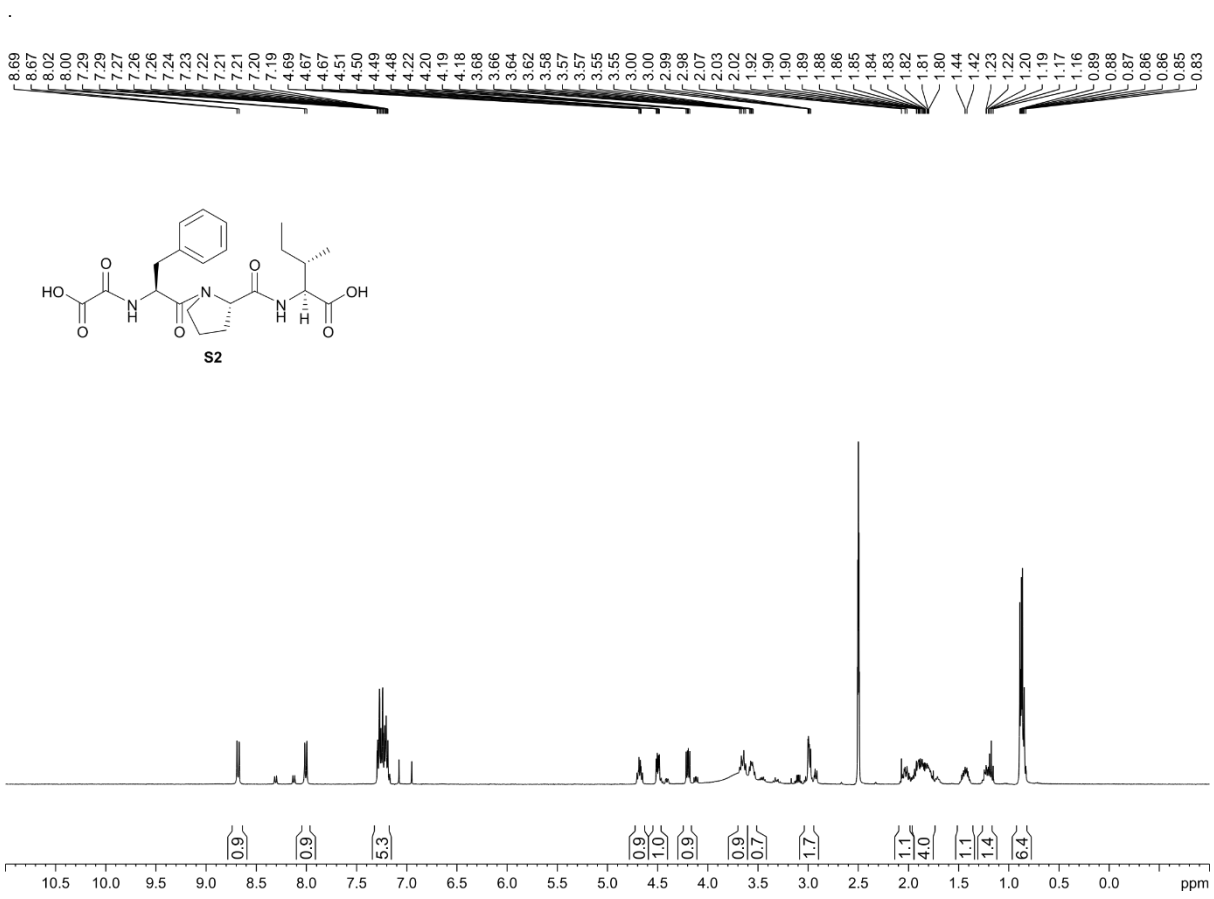

Figure S14. The ^{1}H-NMR (400 MHz, d_6-DMSO) of **S2**.

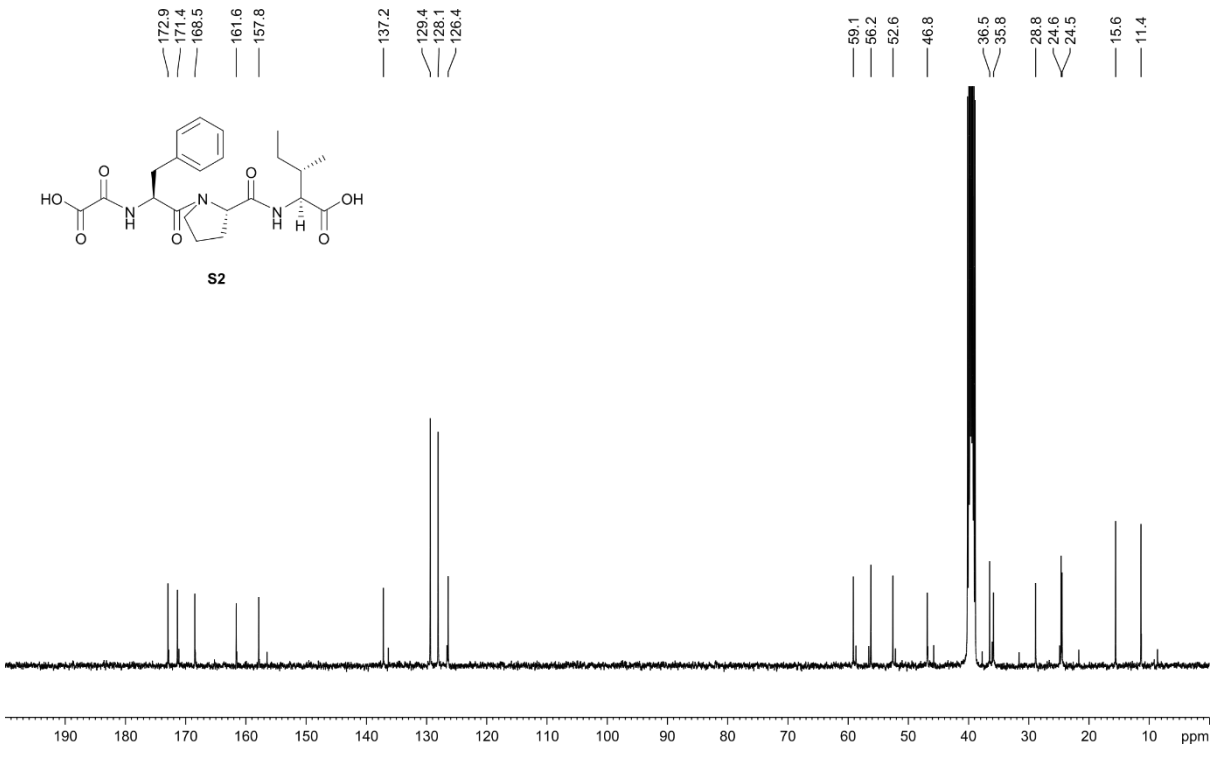

Figure S15. The ^{13}C NMR (100 MHz, d_6-DMSO) of **S2**.

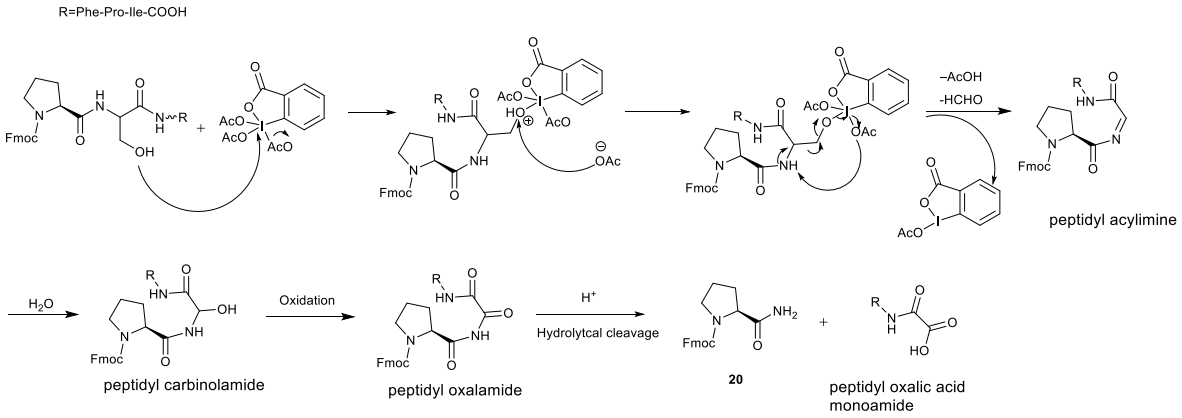

Scheme S1. The proposed mechanism of the DMP-mediated peptide cleavage at a serine residue.

Table S1. Optimization of the cleavage reaction conditions using peptide **21**[a]

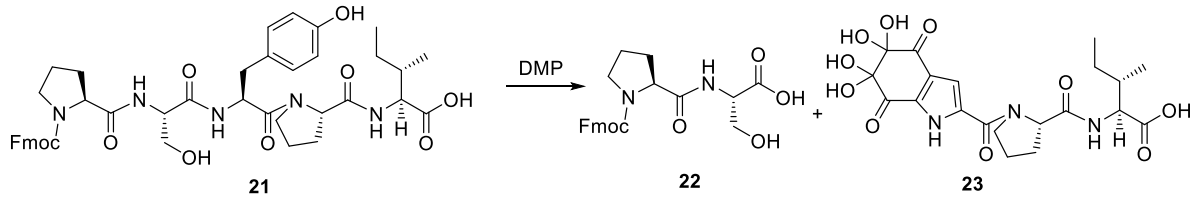

21 **22** **23**

Entry	Equiv. of DMP	Ratio of DMSO/phosphate buffer (*v*/*v*)	Temperature	Conversion (%)[b]
1	10	2:1	40 ºC	76
2	20	2:1	40 ºC	69
3	50	2:1	40 ºC	55
4	10	10:1	40 ºC	18
5	10	4:1	40 ºC	49
6	10	1:1	40 ºC	67
7	10	1:2	40 ºC	61
8	10	2:1	RT	66
9	10	2:1	60 ºC	58

[a]Reaction conditions: peptide **21** (1 mg, 1.2 μmol) in a mixture of DMSO and 0.1 M phosphate buffer (pH =7) was treated with DMP for 2 h. [b] Conversion percentage from peptide **21** to the *N*-terminal fragment **22** was calculated from the HPLC peak area at 254 nm.

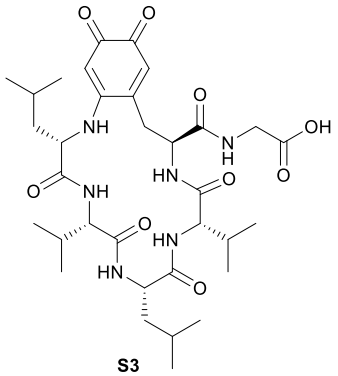

S3

Cyclized **24l** (**S3**). To a solution of **24l** (10 mg, 15 µmol) in DMSO (2 mL) was treated with DMP (63 mg, 150 µmol), followed by addition of 0.1 M phosphate buffer at pH 7 (1 mL). The mixture was stirred at RT at 30 min. The resulting mixture was diluted with water and subjected semi-preparative RP-HPLC purification to afford **S3** as a red powder (6.8 mg, 67%). Anal. RP-HPLC: t_R = 19.6 min, purity: >95% (HPLC analysis at 210 nm). ^{1}H NMR (500 MHz, DMSO-d_6) δ 8.10 (t, *J* = 5.8 Hz, 1 H), 7.90 (d, *J* = 4.7 Hz, 1 H,), 7.78 (d, *J* = 10.0 Hz, 1 H), 7.35 (d, *J* = 8.4 Hz, 1 H), 7.26 (d, *J* = 9.6 Hz, 1 H), 6.64 (s, 1 H), 6.39 (d, *J* = 9.1 Hz, 1 H), 5.44 (s, 1 H), 4.53 (ddd, *J* = 12.6, 8.4, 3.7 Hz, 1 H), 4.36 (td, *J* = 9.9, 3.7 Hz, 1 H), 4.19 (dd, *J* = 9.9, 4.3 Hz, 1 H), 3.84 – 3.82 (m, 1 H), 3.80 (d, *J* = 5.8 Hz, 2 H), 3.32 (dd, *J* = 8.4, 4.7 Hz, 1 H), 3.00 (t, *J* = 13.5 Hz, 1 H), 2.45 (d, *J* = 14.1 Hz, 1 H), 2.33 (td, *J* = 6.9, 4.3 Hz, 1 H), 1.92 – 1.84 (m, 1 H), 1.83 – 1.74 (m, 1 H), 1.67 (m, 2 H), 1.50 (dtd, *J* = 11.1, 6.9, 4.5 Hz, 1 H), 1.31 (ddd, *J* = 13.7, 9.9, 3.7 Hz, 1 H), 1.10 (ddd, *J* = 14.0, 10.5, 4.3 Hz, 1 H), 0.95 (d, *J* = 6.5, 3 H), 0.91 – 0.78 (m, 21 H). ^{13}C NMR (125 MHz, DMSO-d_6): δ 185.4, 183.9, 172.0, 171.2, 171.0, 170.5, 169.3, 147.3, 145.7, 130.3, 99.5, 60.6, 57.1, 56.7, 52.7, 48.9, 41.7, 10.7, 28.9, 28.5, 24.7, 24.1, 23.5, 22.3, 21.9, 21.2, 19.3, 19.3, 19.0, 16.7. HRMS (ESI+): $C_{33}H_{50}N_6O_9Na$. $[M+Na]^+$ calcd./found 697.3531/697.3529.

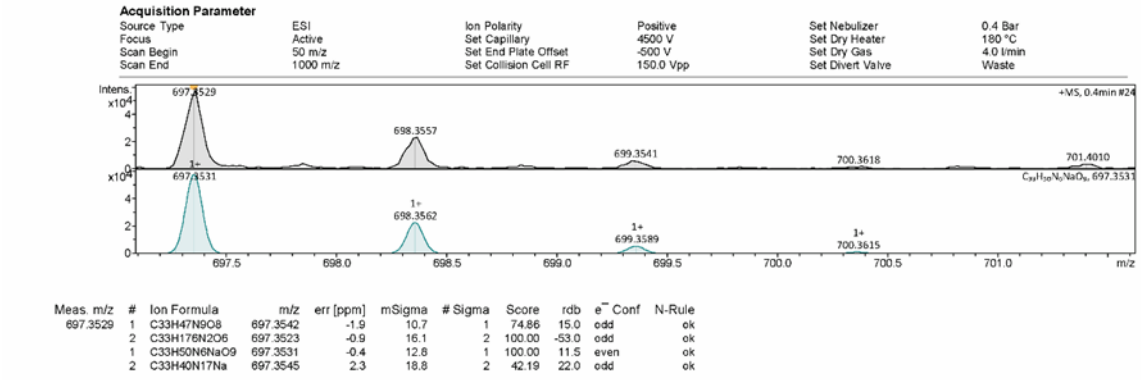

Meas. m/z	#	Ion Formula	m/z	err [ppm]	mSigma	# Sigma	Score	rdb	e⁻ Conf	N-Rule
697.3529	1	C33H47N9O8	697.3542	-1.9	10.7	1	74.86	15.0	odd	ok
	2	C33H176N2O6	697.3523	-0.9	16.1	2	100.00	-53.0	odd	ok
	1	C33H50N6NaO9	697.3531	-0.4	12.8	1	100.00	11.5	even	ok
	2	C33H40N17Na	697.3545	2.3	18.8	2	42.19	22.0	odd	ok

Figure S16. HRMS characterization of **S3** in H_2O/MeCN (*v/v*, 1;1). HRMS (ESI+): $C_{33}H_{50}N_6O_9Na$. $[M+Na]^+$ calcd./found 697.3531/697.3529.

.

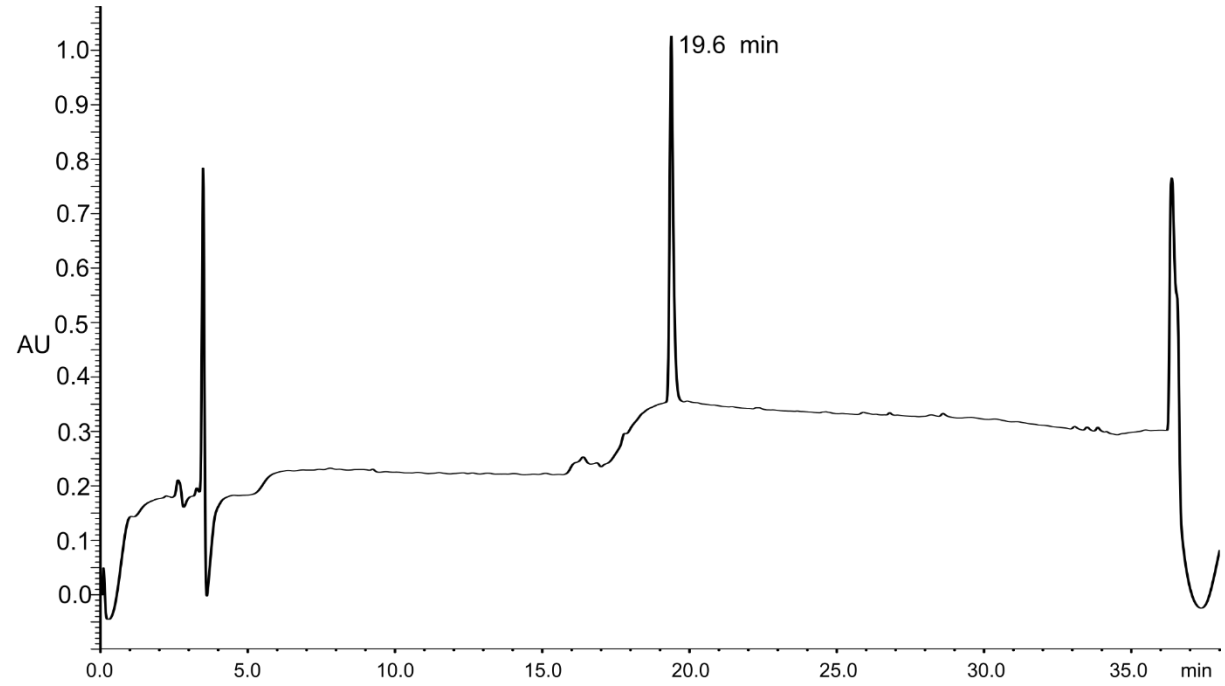

Figure S17. HPLC-MS profile of **S3**, t_R = 19.6 min (purity >95% as judged by peak area of RP-HPLC at 210 nm); Phenomenex Luna, C_{18} column (100 Å, 4.6 x 250 mm, 5 µm) using a linear gradient of 5% B-95% B over 30 min (*ca.* 3 % B•min^{-1}) at a flow rate of 1 mL•min^{-1} (A = 0.1% TFA in H_2O and B = 0.1 %TFA MeCN).

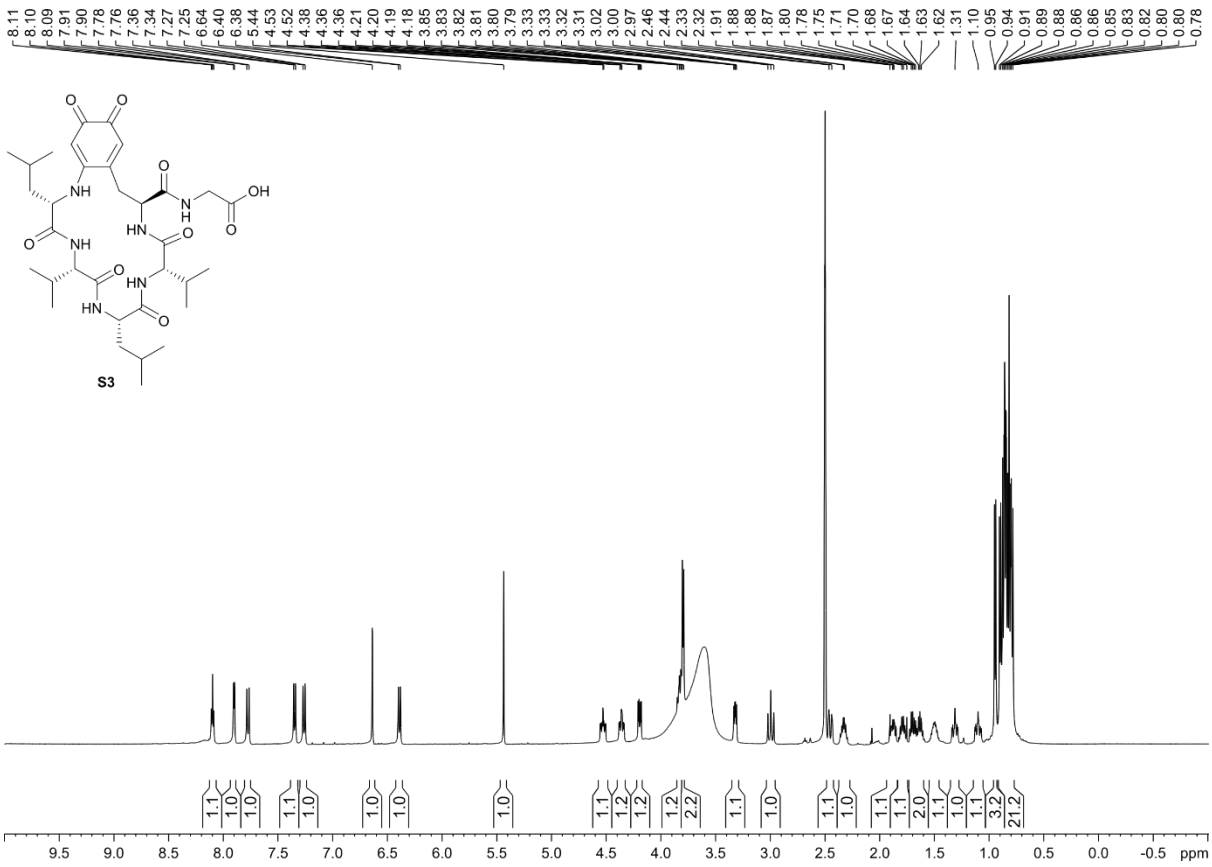

Figure S18. The ^{1}H-NMR (500 MHz, d_6-DMSO) of **S3.**

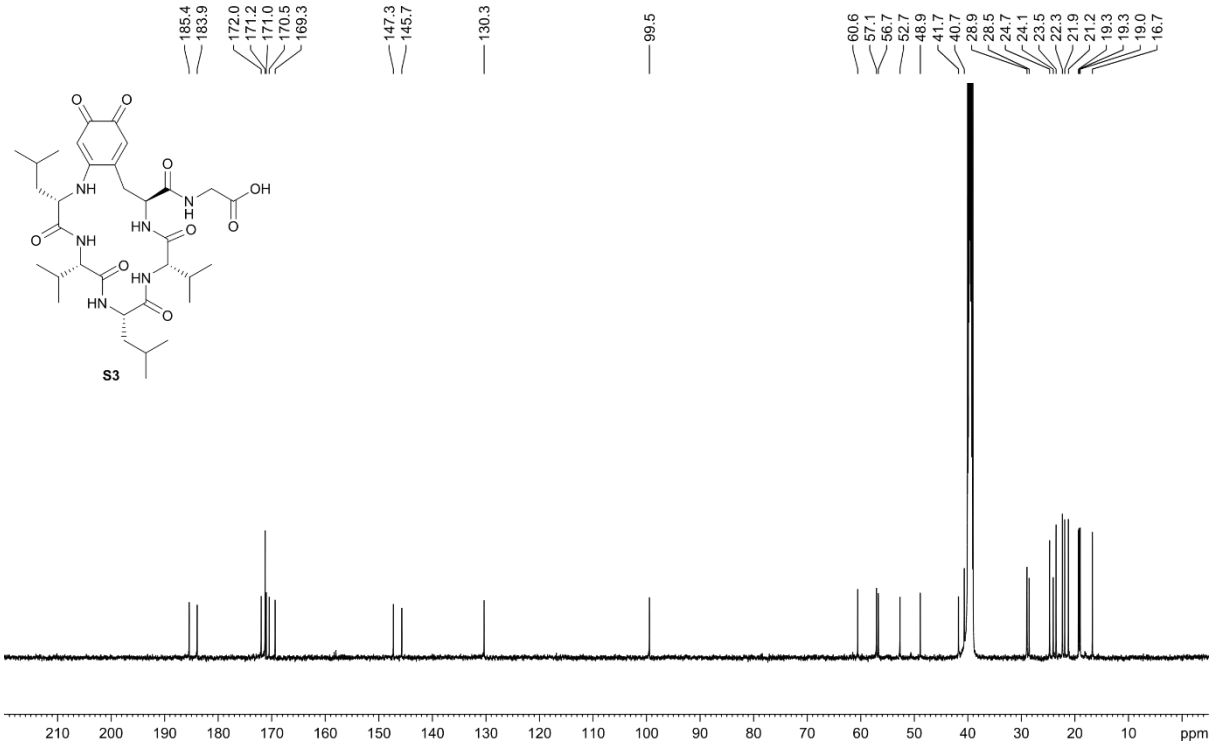

Figure S19. The ^{13}C NMR (125 MHz, d_6-DMSO) of **S3.**

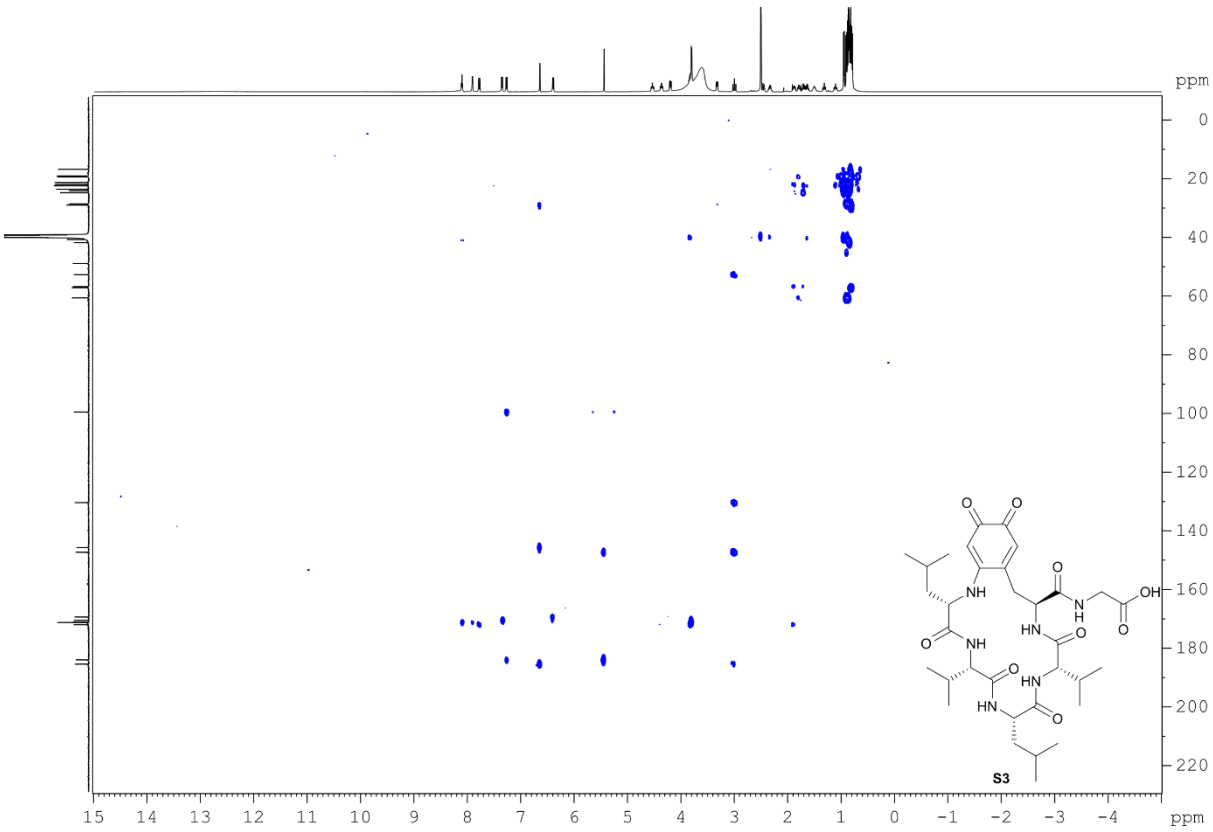

Figure S20. The HMBC spectrum (500MHz, DMSO-d_6) of **S3.**

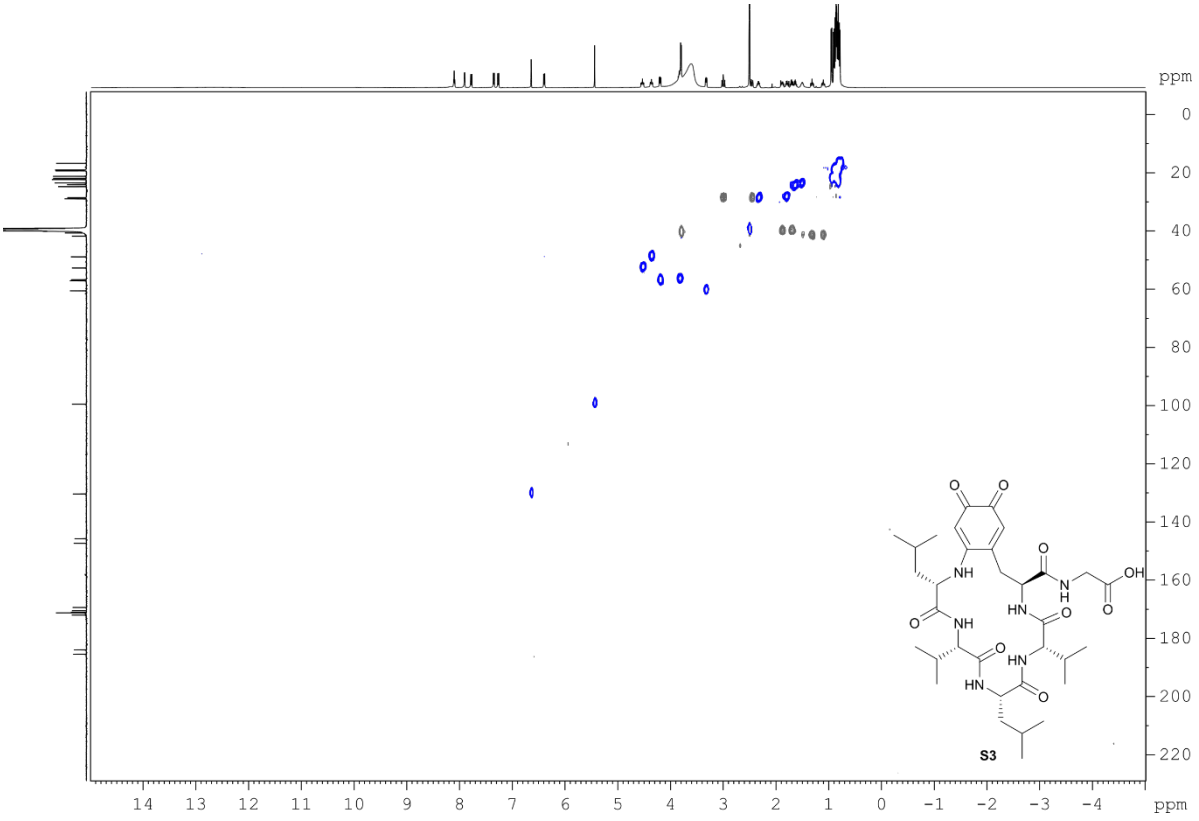

Figure S21. The HSQC spectrum (500MHz, DMSO-d_6) of **S3.**

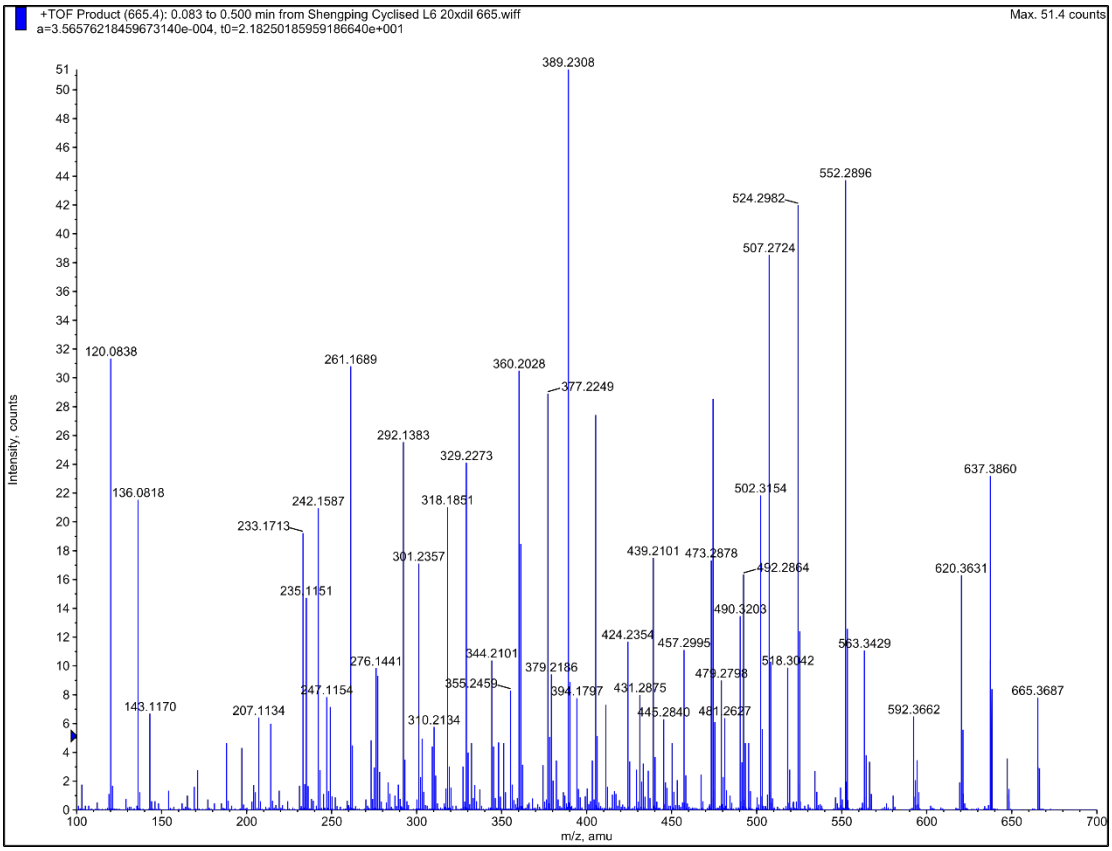

Figure S22. The MS/MS spectrum of dichotomin J (**30**).

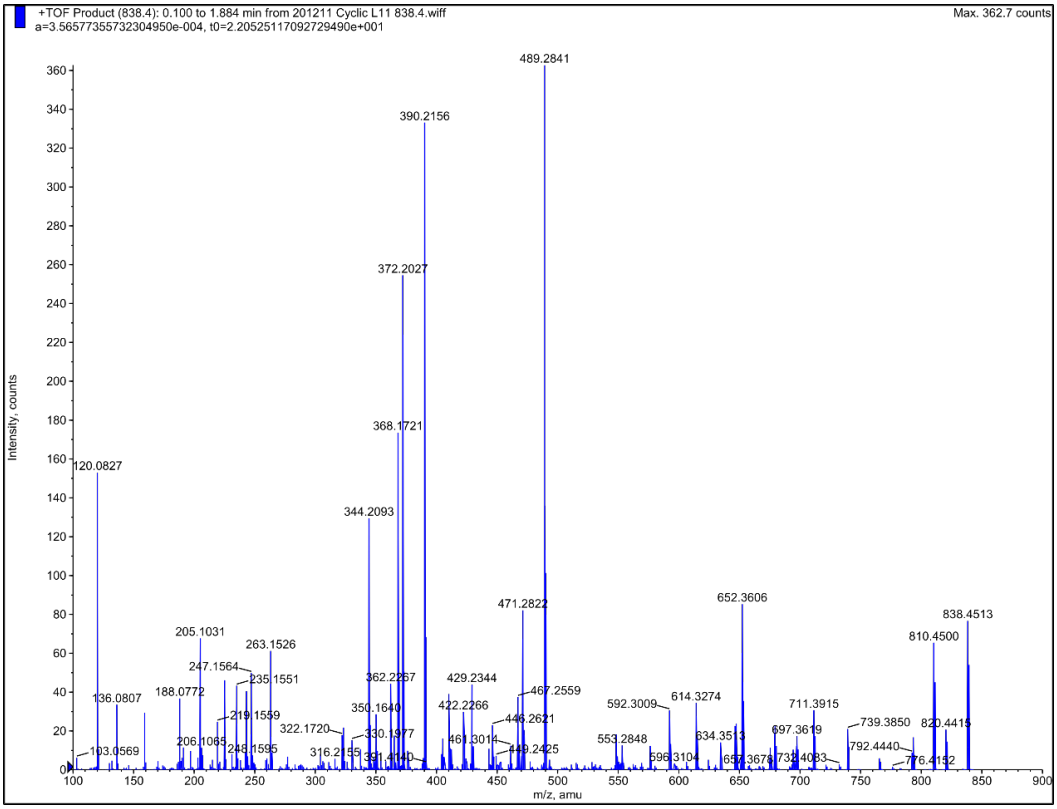

Figure S23. The MS/MS spectrum of szentiamide (**31**).

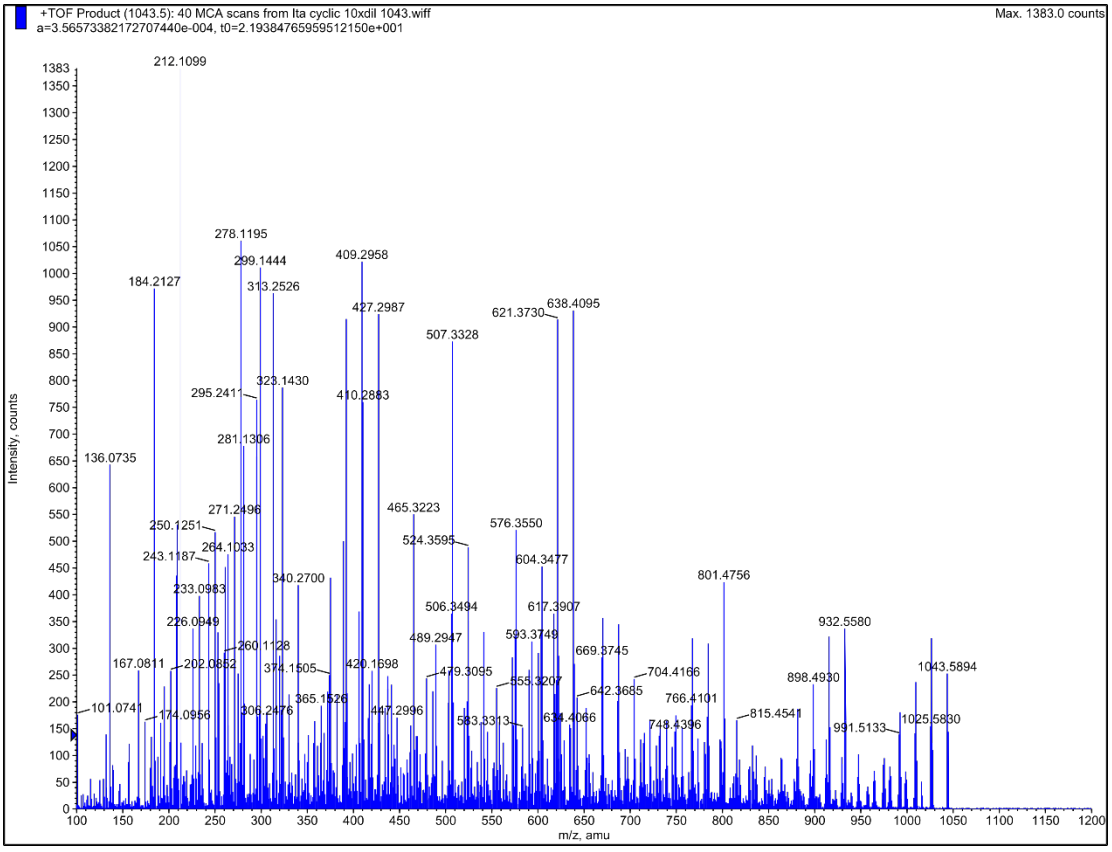

Figure S24. The MS/MS spectrum of iturin A (**32**).

2. General Information

All the reagents purchased from commercial sources were reagent grade and were used without further purification. Solvents for peptide synthesis and RP-HPLC were purchased as synthesis grade and HPLC grade, respectively. 2-Chlorotrityl chloride polystyrene resin (2-CTC, 0.9 mmol/g) was purchased from Novabiochem (Merck, Germany). TentaGel™ S-NH_2 resin was purchased from Rapp Polymere (Tübingen, Germany). *O*-(7-azabenzotriazol-1-yl)-*N*,*N*,*N*',*N*'-tetramethyluronium hexafluorophosphate (HATU) was supplied by Chempep (Wellington, USA). 6-Chloro-1-hydroxytriazole (6-Cl-HOBt), (benzotriazol-1-yloxy)tripyrrolidinophosphonium hexafluorophosphate (PyBOP) and (7-azabenzotriazol-1-yloxy)tripyrrolidinophosphonium hexafluorophosphate (PyAOP) were purchased from Aapptec (Louisville, KY, USA). Diethyl ether (Et_2O), Dess-Martin periodinane (DMP), piperidine, *N,N*-diisopropylethylamine (DIPEA), triisopropylsilane (*i*Pr_3SiH), formic acid, *N*-methylmorpholine (NMM), triethylamine (Et_3N), benzoyl chloride, *N*,*N*'-diisopropylcarbodiimide (DIC) and iturin A from *Bacillus subtilis* were purchased from Sigma-Aldrich (St. Louis, MO, USA). *N*,*N*-dimethyl-4-aminopyridine (DMAP) was purchased from AK Scientific (Union City, CA, USA). Dimethylformamide (DMF, AR grade), acetonitrile (CH_3CN, HPLC grade) and trifluoroacetic acid (TFA) were purchased from Scharlau (Barcelona, Spain). Dichloromethane (CH_2Cl_2), sodium dihydrogen phosphate dihydrate and disodium hydrogen phosphate were obtained from ECP Limited (Auckland, New Zealand). Dimethyl sulfoxide (DMSO) was provided by ChemSupply (Gillman, Australia). 4-[(*R*,*S*)-α-[1-(9*H*-fluoren-9-yl)]-methoxycarbonylamino]-2,4-dimethoxy]phenoxyacetic acid (Rink amide linker) and all Fmoc-amino acids were purchased from GL Biochem (Shanghai, China).

^1H and ^{13}C NMR experiments were performed on either a Bruker (Billerica, MA, USA) AVANCE III HD 500 (^1H 500 MHz; ^{13}C 125 MHz) or 400 (^1H 400 MHz; ^{13}C 100 MHz) spectrometer in deuterated DMSO-d_6, deuterated acetone-d_6 or deuterated pyridine-d_5. Chemical shifts were recorded in parts per million (ppm). The ^1H values were referenced to the residual DMSO signal at 2.50 ppm, or residual acetone signal at 2.09 ppm or residual pyridine signal at 7.21 ppm for the experiment at 298K. The ^{13}C values were presented relative to the signal of residual DMSO at 39.5 ppm, residual acetone at 29.84 ppm or residual pyridine at 135.5 ppm. ^1H NMR spectral data were reported as follows: chemical shift (δ_H), relative integral, multiplicity (s, singlet; d, doublet; t, triplet; q, quartet; m, multiplet; dd, doublet of doublets; dq, doublet of quartets; ddd, doublet of doublet of doublets) and coupling constant (*J* in Hz).

High-resolution mass spectra were obtained on a QSTAR XL Quadrupole-Time-of-Flight mass spectrometer (Sciex, CA, USA) using electrospray ionization (ESI) under either positive or negative mode. For the MS/MS experiments, TOF-MS scans were performed to confirm the precursor ion *m/z*, followed by product ion scans of the relevant precursor ion in each case, using collision energies ramping from 20-70 V.

Analytical RP-HPLC experiments were carried out using one of the following set of conditions:
1. Waters (Milford, MAUSA) XTerra MS C18 column (125 Å 4.6 mm × 150 mm, 5 µm) with a linear gradient of 5% B-95% B over 45 min (ca. 2 % B•min^{-1}) at a flow rate of 1 mL•min^{-1} (A = 0.1% TFA in H_2O and B = 0.1 %TFA MeCN) on a Waters e2695 System.
2. Waters XTerra MS C18 column (125 Å 4.6 mm × 150 mm, 5 µm) with using a linear gradient of 5% B-65% B over 30 min (ca. 2 % B•min^{-1}) at a flow rate of 1 mL•min^{-1} (A = 0.1% TFA in H_2O and B = 0.1 %TFA MeCN) on a Waters e2695 System or a Dionex (Torrance, CA, USA) Ultimate 3000 System.
3. Waters XTerra MS C18 column (125 Å, 4.6 mm × 150 mm, 5 µm) using a linear gradient of 5% B-60% B over 55 min (*ca.* 1 % B•min^{-1}) at a flow rate of 1 mL•min^{-1} (A = 0.1% TFA in H_2O and B = 0.1 %TFA MeCN) on a Dionex Ultimate 3000 System.
4. Phenomenex Luna, C_{18} column (100 Å, 4.6 x 250 mm, 5 µm) with using a linear gradient of 5% B-95% B over 45 min (ca. 2 % B•min^{-1}) at a flow rate of 1 mL•min^{-1} (A = 0.1% TFA in H_2O and B = 0.1 %TFA MeCN) on a Waters e2695 System.
5. Phenomenex Luna, C_{18} column (100 Å, 4.6 x 250 mm, 5 µm) with using a linear gradient of 5% B-65% B over 30 min (ca. 2 % B•min^{-1}) at a flow rate of 1 mL•min^{-1} (A = 0.1% TFA in H_2O and B = 0.1 %TFA MeCN) on a Waters e2695 System.
6. Phenomenex Luna, C_{18} column (100 Å, 4.6 x 250 mm, 5 µm) with using a linear gradient of 5% B-95% B over 30 min (ca. 3 % B•min^{-1}) at a flow rate of 1 mL•min^{-1} (A = 0.1% TFA in H_2O and B = 0.1 %TFA MeCN) on a Waters e2695 System.

The UV-Vis detector was set at a wavelength of 210 and 254 nm when Waters e2695 System was used and was set at wavelengths 210, 225, 254 and 280 nm when a Dionex Ultimate 3000 System was employed. Conversion to the *N*-terminal peptide fragment was determined by taking the ratio of A_{prod}/A_{total} where A_{prod} = area in mAU*min of the product peak and A_{total} = area in mAU*min of the combined peptide-containing species (product, starting material and side products) detected at a wavelength of 254 nm.

Semi-preparative RP-HPLC was carried out on a Waters 600 system using a semi-preparative column (XTerra MS C_{18} Prep Column, 125 Å, 19 mm × 300 mm, 10 µm) at a flow rate of 10 mL•min^{-1} using an adjusted gradient of 5-95% solvent B according to the elution profiles obtained from analytical RP-HPLC chromatography. LC/MS analysis was conducted on an Agilent Technologies (Santa Clara, CA, USA)1260 Infinity LC equipped with an Agilent Technologies 6120

Quadrupole mass spectrometer using an analytical column (Agilent ZORBAX C_3, 300 Å, 3.0 mm × 150 mm, 3.5 µm) with a 30 min linear gradient of 5-95% solvent B at a flow rate of 0.3 mL•min^{-1}.

3. Model Peptide Synthesis and Characterization

General protocol for Fmoc solid phase peptide synthesis (Fmoc-SPPS).
Peptide synthesis was performed manually at a 0.1 mmol scale using either 2-chlorotrityl chloride polystyrene (2-CTC) or TentaGel™ S-NH_2 resin. For 2-CTC resin, the first amino acid (0.2 mmol) in CH_2Cl_2 was mixed with the resin in the presence of DIPEA (78 µL, 0.5 mmol) for 1 h. For TentaGel™ S-NH_2 resin, the Rink amide linker (108 mg, 0.2 mmol) was coupled to the resin using DIC (33 µL, 0.2 mmol) in 3 mL of DMF/CH_2Cl_2 (1:2, *v*/*v*) for 1 h. Fmoc-protected amino acids (0.4 mmol) were sequentially coupled using HATU (0.38 mmol each) and DIPEA (139 µL, 0.8 mmol) for 30 min at room temperature after removal of each Fmoc group with 20% piperidine in DMF for 2 x 5 min. After peptide assembly, the final peptide was cleaved from the resin by TFA in the presence of *i*Pr$_3$SiH and water (95:2.5:2.5, *v*/*v*/*v*) for 60 min at room temperature, concentrated under a flow of nitrogen, and precipitated with diethyl ether. The resulting product was dissolved with 50% aqueous acetonitrile containing 0.1% TFA and lyophilized. The crude product was purified using semi-preparative HPLC and lyophilized to give the desired peptide as a white powder.

General protocol for disulfide bond formation
Linear peptide precursors (4 mM) was dissolved in a 6 M guanidine hydrochloride buffer (pH 8.2) containing 200 mM Na_2HPO_4, 8 mM cysteine, 1 mM cystine and 0.1 mM EDTA. The resulting solution was then diluted four folds by water and stirred at RT overnight. The mixture was then subjected semi-preparative HPLC purification, followed by lyophilization to furnish the corresponding cyclic peptides as a white powder.

Substrate characterization
Fmoc-Gly-Tyr-Phe-Val-Phe-OH (**1**). Anal. RP-HPLC: t_R = 31.8 min, MS (ESI+): $C_{49}H_{51}N_5O_9$ $[M+H]^+$ calcd./found 854.4/854.3.Purity: >95% (HPLC analysis at 210 nm).

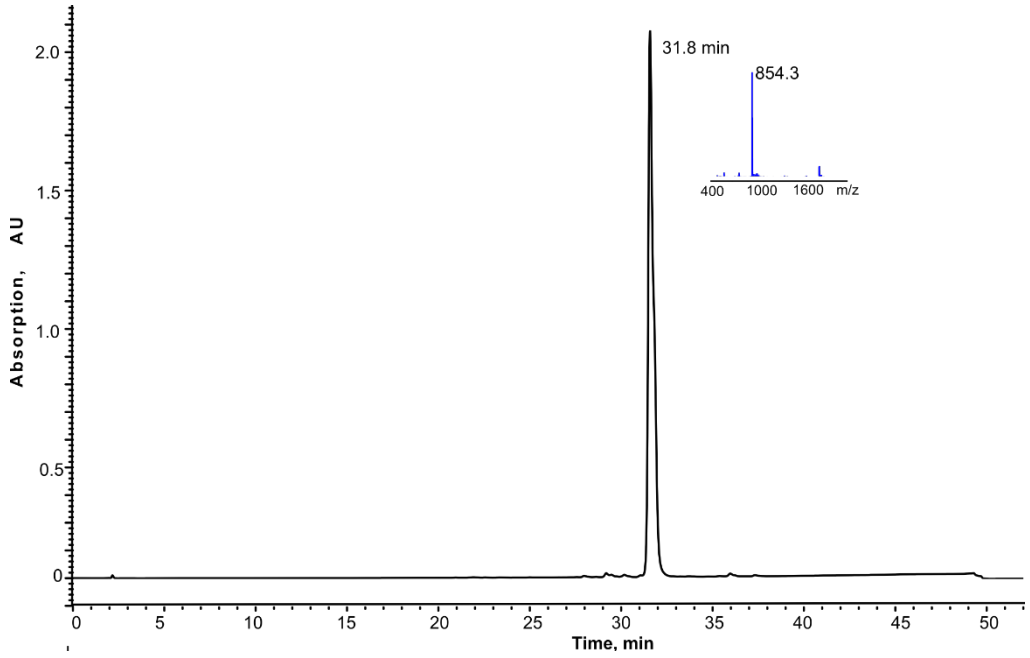

Figure S25. HPLC-MS profile of **1**, t_R = 31.8 min (purity >95% as judged by peak area of RP-HPLC at 210 nm); Waters XTerra MS C18 column (125 Å 4.6 mm × 150 mm, 5 µm) with a linear gradient of 5% B-95% B over 45 min (*ca.* 2 % B•min^{-1}) at a flow rate of 1 mL•min^{-1} (A = 0.1% TFA in H_2O and B = 0.1 %TFA MeCN).

Fmoc-Pro-Ser-Tyr-Pro-Ile-OH (**21**). Anal. RP-HPLC: t_R = 37.1 min, MS (ESI+): $C_{43}H_{51}N_5O_{10}$ $[M+H]^+$ calcd./found 798.4/798.2.Purity: 91% (HPLC analysis at 210 nm).

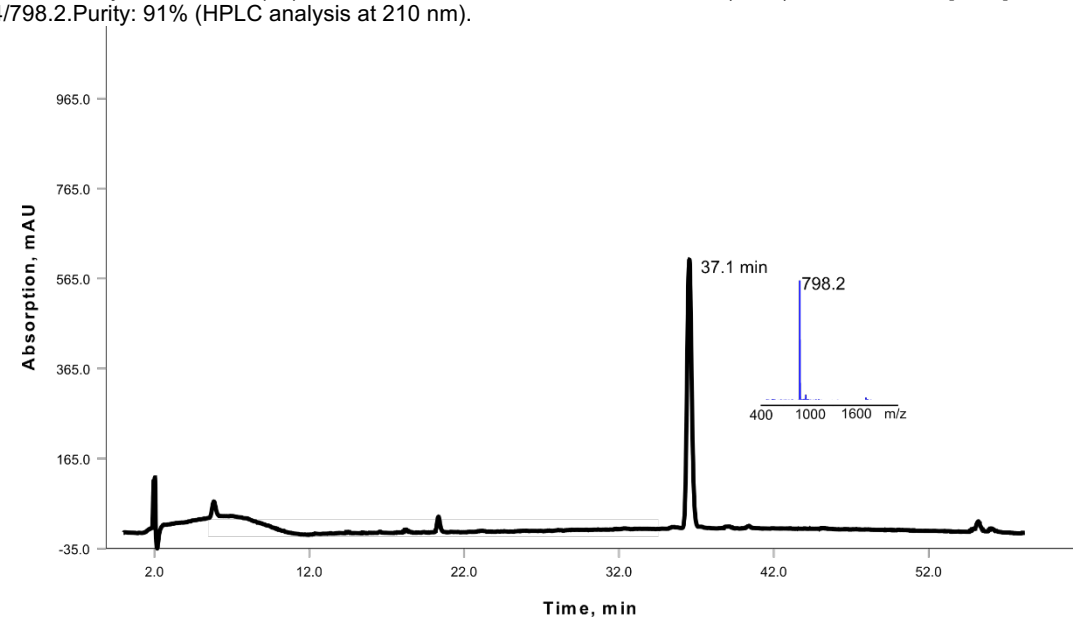

Figure S26. HPLC-MS profile of **21**, t_R = 37.1 min (purity 91% as judged by peak area of RP-HPLC at 210 nm); Waters XTerra MS C18 column (125 Å, 4.6 mm × 150 mm, 5 µm) using a linear gradient of 5% B-60% B over 55 min (*ca.* 1 % B•min^{-1}) at a flow rate of 1 mL•min^{-1} (A = 0.1% TFA in H_2O and B = 0.1 %TFA MeCN).

Fmoc-Pro-Leu-Tyr-Pro-Ile-OH (**24a**). Anal. RP-HPLC: t_R = 32.2 min, MS (ESI+): $C_{46}H_{57}N_5O_9$ $[M+H]^+$ calcd./found 824.4/824.2.Purity: >95% (HPLC analysis at 210 nm).

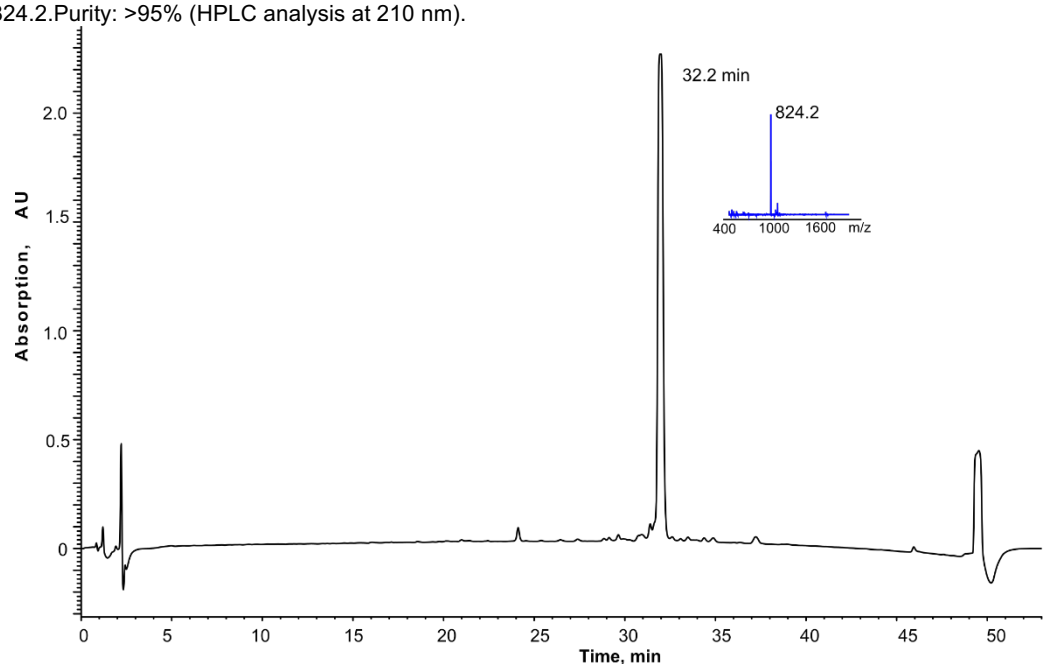

Figure S27. HPLC-MS profile of **24a**, t_R = 32.2 min (purity >95% as judged by peak area of RP-HPLC at 210 nm); Waters XTerra MS C18 column (125 Å 4.6 mm × 150 mm, 5 µm) with a linear gradient of 5% B-95% B over 45 min (*ca.* 2 % B•min^{-1}) at a flow rate of 1 mL•min^{-1} (A = 0.1% TFA in H_2O and B = 0.1 %TFA MeCN).

Fmoc-Pro-Arg-Tyr-Pro-Ile-OH (**24b**). Anal. RP-HPLC: t_R = 36.7 min, MS (ESI+): $C_{46}H_{58}N_8O_9$ $[M+H]^+$ calcd./found 867.4/867.0.Purity: >95% (HPLC analysis at 210 nm).

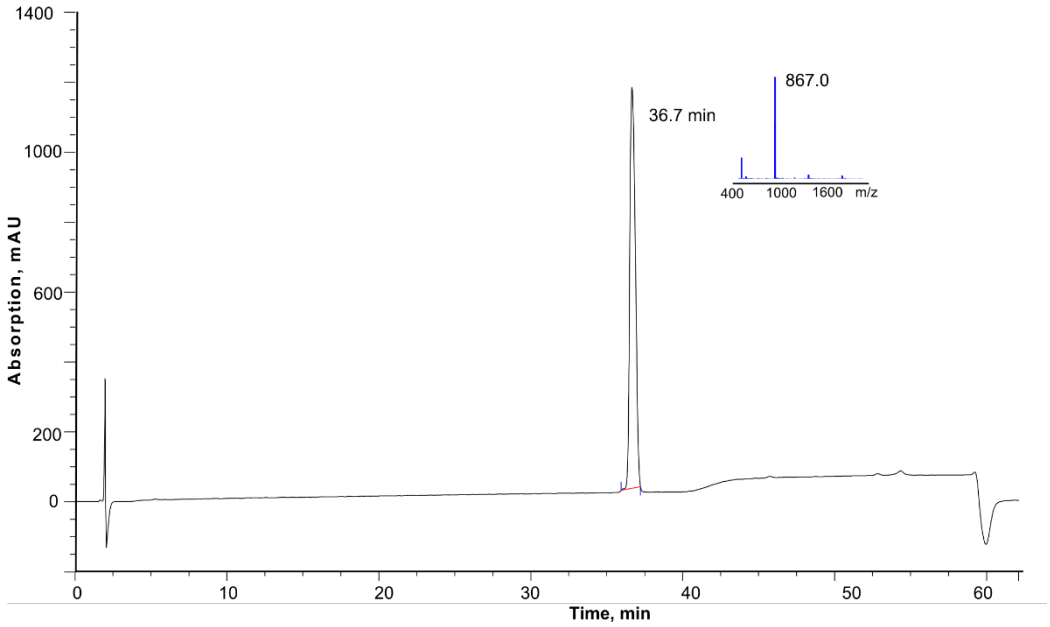

Figure S28. HPLC-MS profile of **24b**, t_R = 36.7 min (purity >95% as judged by peak area of RP-HPLC at 210 nm); Waters XTerra MS C18 column (125 Å, 4.6 mm × 150 mm, 5 µm) using a linear gradient of 5% B-60% B over 55 min (*ca.* 1 % B•min^{-1}) at a flow rate of 1 mL•min^{-1} (A = 0.1% TFA in H_2O and B = 0.1 %TFA MeCN).

Fmoc-Pro-Asp-Tyr-Pro-Ile-OH (**24c**). Anal. RP-HPLC: t_R = 36.2 min, MS (ESI+): $C_{44}H_{51}N_5O_{11}$ $[M+H]^+$ calcd./found 826.3/826.2.Purity: >95% (HPLC analysis at 210 nm).

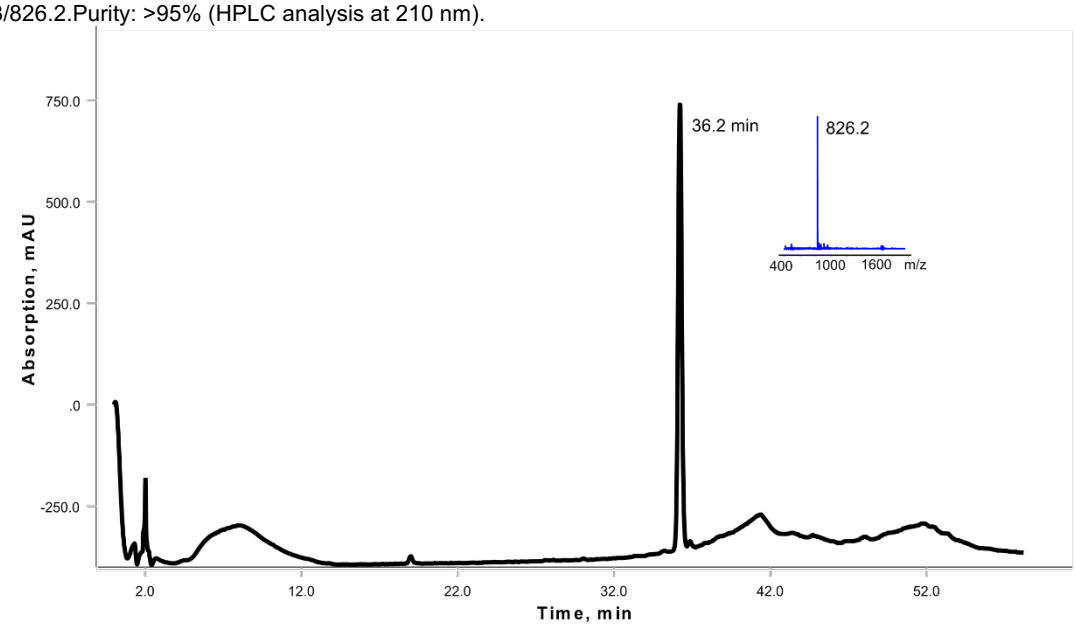

Figure S29 HPLC-MS profile of **24c**, t_R = 36.2 min (purity >90% as judged by peak area of RP-HPLC at 210 nm); Waters XTerra MS C18 column (125 Å, 4.6 mm × 150 mm, 5 µm) using a linear gradient of 5% B-60% B over 55 min (*ca.* 1 % B•min^{-1}) at a flow rate of 1 mL•min^{-1} (A = 0.1% TFA in H_2O and B = 0.1 %TFA MeCN).

Fmoc-Pro-Gln-Tyr-Pro-Ile-OH (**24d**). Anal. RP-HPLC: t_R = 35.3 min, MS (ESI+): $C_{45}H_{54}N_6O_{10}$ $[M+H]^+$ calcd./found 839.4/839.2.Purity: 93% (HPLC analysis at 210 nm).

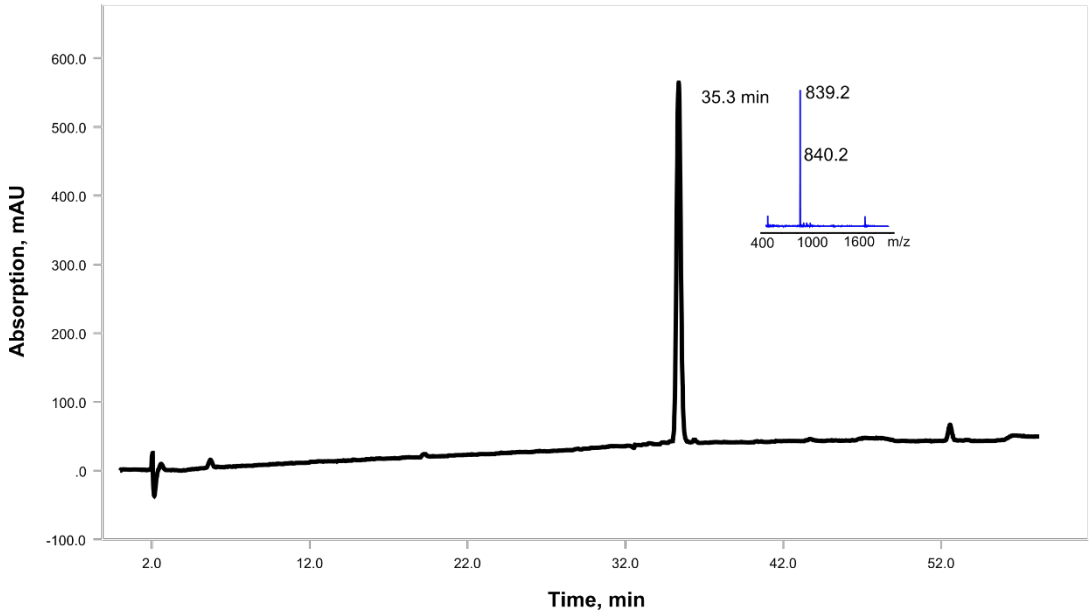

Figure S30. HPLC-MS profile of **24d**, t_R = 35.3 min (purity 93% as judged by peak area of RP-HPLC at 210 nm); Waters XTerra MS C18 column (125 Å, 4.6 mm × 150 mm, 5 µm) using a linear gradient of 5% B-60% B over 55 min (*ca.* 1 % B•min^{-1}) at a flow rate of 1 mL•min^{-1} (A = 0.1% TFA in H_2O and B = 0.1 %TFA MeCN).

Fmoc-Pro-Thr-Tyr-Pro-Ile-OH (**24e**). Anal. RP-HPLC: t_R = 37.5 min, MS (ESI+): $C_{44}H_{53}N_5O_{10}$ $[M+H]^+$ calcd./found 812.4/812.2.Purity: 89% (HPLC analysis at 210 nm).

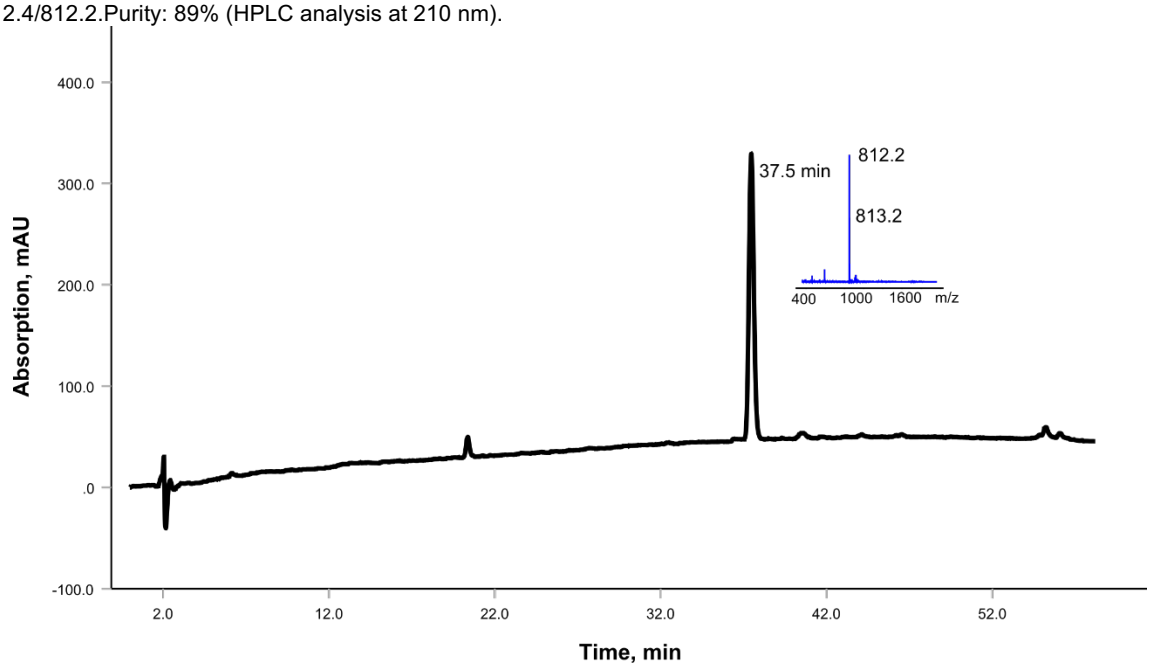

Figure S31. HPLC-MS profile of **24e**, t_R = 37.5 min (purity 89% as judged by peak area of RP-HPLC at 210 nm); Waters XTerra MS C18 column (125 Å, 4.6 mm × 150 mm, 5 µm) using a linear gradient of 5% B-60% B over 55 min (*ca.* 1 % B•min^{-1}) at a flow rate of 1 mL•min^{-1} (A = 0.1% TFA in H_2O and B = 0.1 %TFA MeCN).

Fmoc-Pro-Lys-Tyr-Pro-Ile-OH (**24f**). Anal. RP-HPLC: t_R = 35.4 min, MS (ESI+): $C_{46}H_{58}N_6O_9$ $[M+H]^+$ calcd./found 839.4/839.2.Purity: >95% (HPLC analysis at 210 nm).

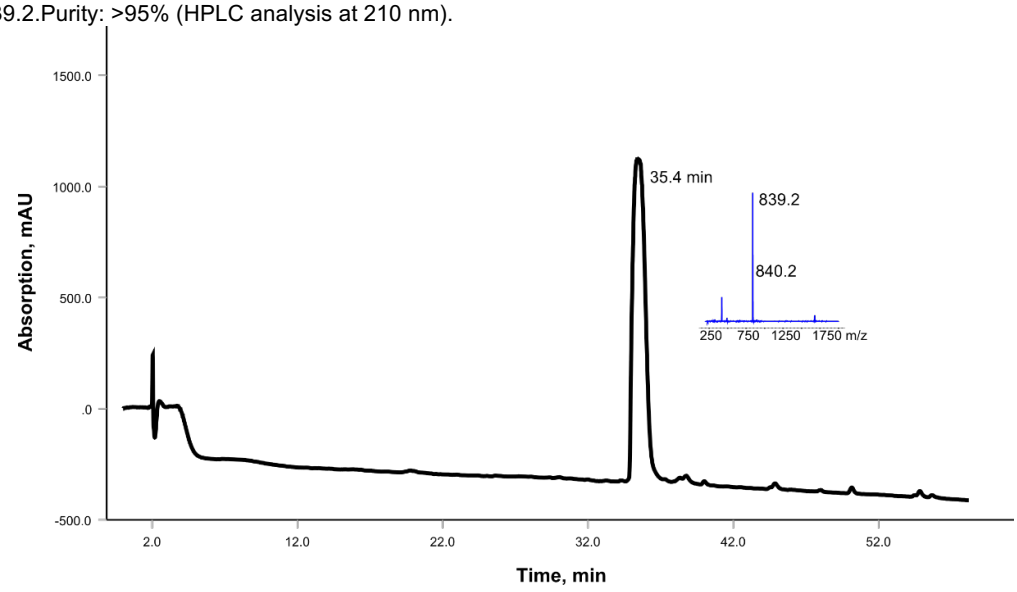

Figure S32. HPLC-MS profile of **24f**, t_R = 35.4 min (purity >95% as judged by peak area of RP-HPLC at 210 nm); Waters XTerra MS C18 column (125 Å, 4.6 mm × 150 mm, 5 µm) using a linear gradient of 5% B-60% B over 55 min (*ca.* 1 % B•min^{-1}) at a flow rate of 1 mL•min^{-1} (A = 0.1% TFA in H_2O and B = 0.1 %TFA MeCN).

Fmoc-Pro-His-Tyr-Pro-Ile-OH (**24g**). Anal. RP-HPLC: t_R = 36.4 min, MS (ESI+): $C_{46}H_{53}N_7O_9$ $[M+H]^+$ calcd./found 848.4/848.0.Purity: 85% (HPLC analysis at 210 nm).

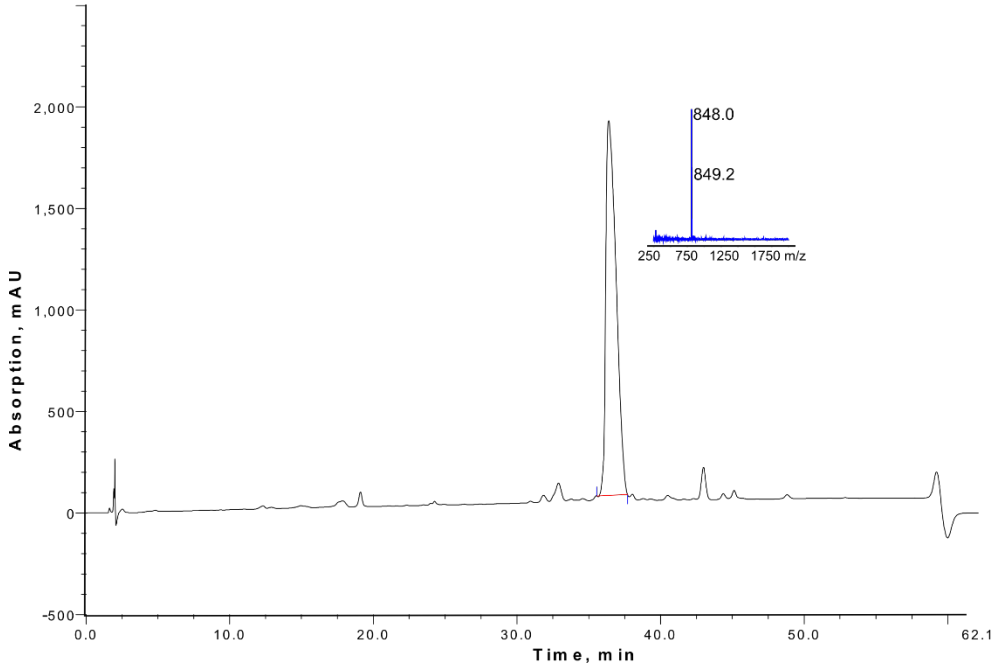

Figure S33. HPLC-MS profile of **24g**, t_R = 36.4 min (purity 84% as judged by peak area of RP-HPLC at 210 nm); Waters XTerra MS C18 column (125 Å, 4.6 mm × 150 mm, 5 µm) using a linear gradient of 5% B-60% B over 55 min (*ca.* 1 % B•min^{-1}) at a flow rate of 1 mL•min^{-1} (A = 0.1% TFA in H_2O and B = 0.1 %TFA MeCN).

Fmoc-Pro-Cys-Tyr-Pro-Ile-OH (**24h**). Anal. RP-HPLC: t_R = 39.5 min, MS (ESI+): $C_{43}H_{51}N_5O_9S$. $[M+H]^+$ calcd./found 814.3/814.2.Purity: >95% (HPLC analysis at 210 nm).

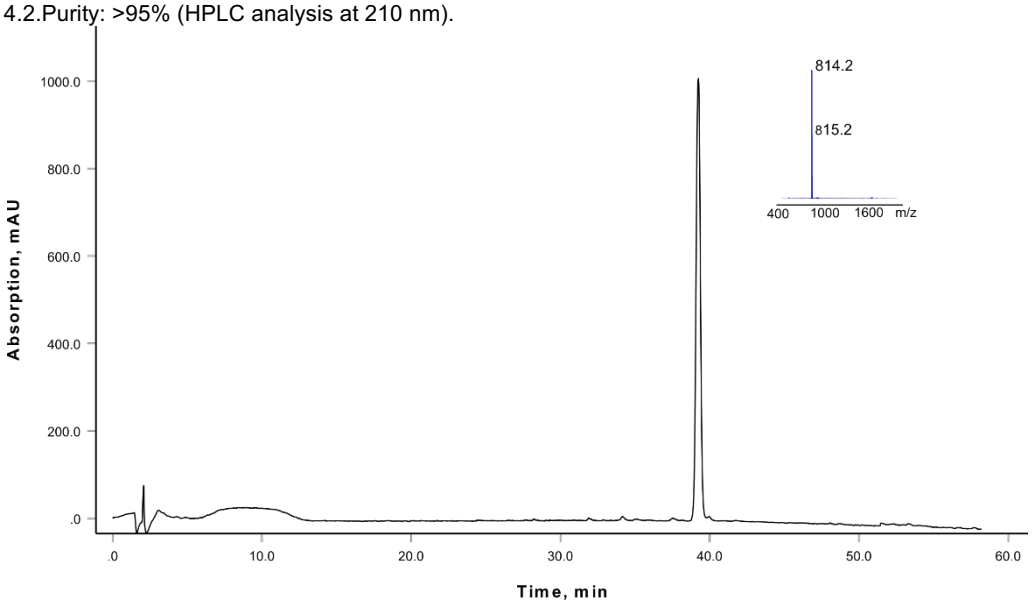

Figure S34. HPLC-MS profile of **24h**, t_R = 39.5 min (purity >95% as judged by peak area of RP-HPLC at 210 nm); Waters XTerra MS C18 column (125 Å, 4.6 mm × 150 mm, 5 µm) using a linear gradient of 5% B-60% B over 55 min (*ca.* 1 % B•min^{-1}) at a flow rate of 1 mL•min^{-1} (A = 0.1% TFA in H_2O and B = 0.1 %TFA MeCN).

Fmoc-Pro-Cys(CH_2CONH_2)-Tyr-Pro-Ile-OH (**24i**). Anal. RP-HPLC: t_R = 36.1 min, MS (ESI+): $C_{45}H_{54}N_6O_{10}S$. $[M+H]^+$ calcd./found 871.4/871.3.Purity: 76% (HPLC analysis at 210 nm).

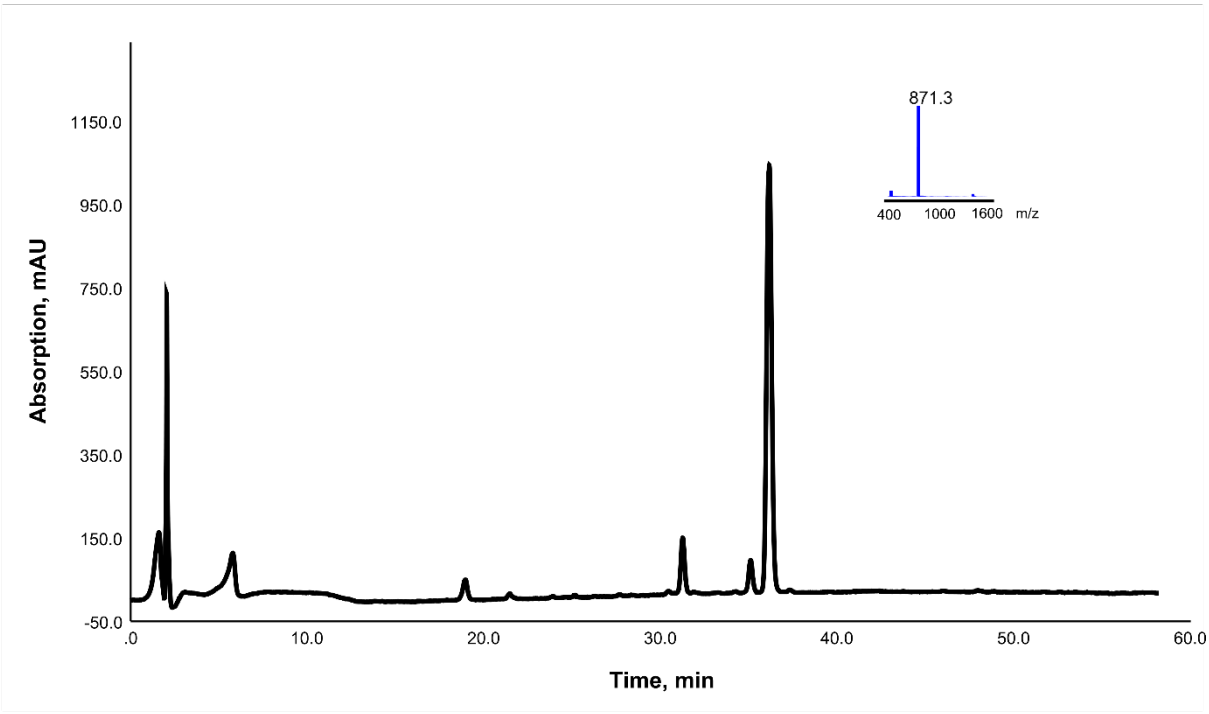

Figure S35. HPLC-MS profile of **24i**, t_R = 36.1 min (purity 76% as judged by peak area of RP-HPLC at 210 nm); Waters XTerra MS C18 column (125 Å, 4.6 mm × 150 mm, 5 µm) using a linear gradient of 5% B-60% B over 55 min (*ca.* 1 % B•min^{-1}) at a flow rate of 1 mL•min^{-1} (A = 0.1% TFA in H_2O and B = 0.1 %TFA MeCN).

Fmoc-Pro-Met-Tyr-Pro-Ile-OH (**24j**). Anal. RP-HPLC: t_R = 31.1 min, MS (ESI+): $C_{45}H_{55}N_5O_9S$. $[M+H]^+$ calcd./found 842.4/842.2.Purity: 87% (HPLC analysis at 210 nm).

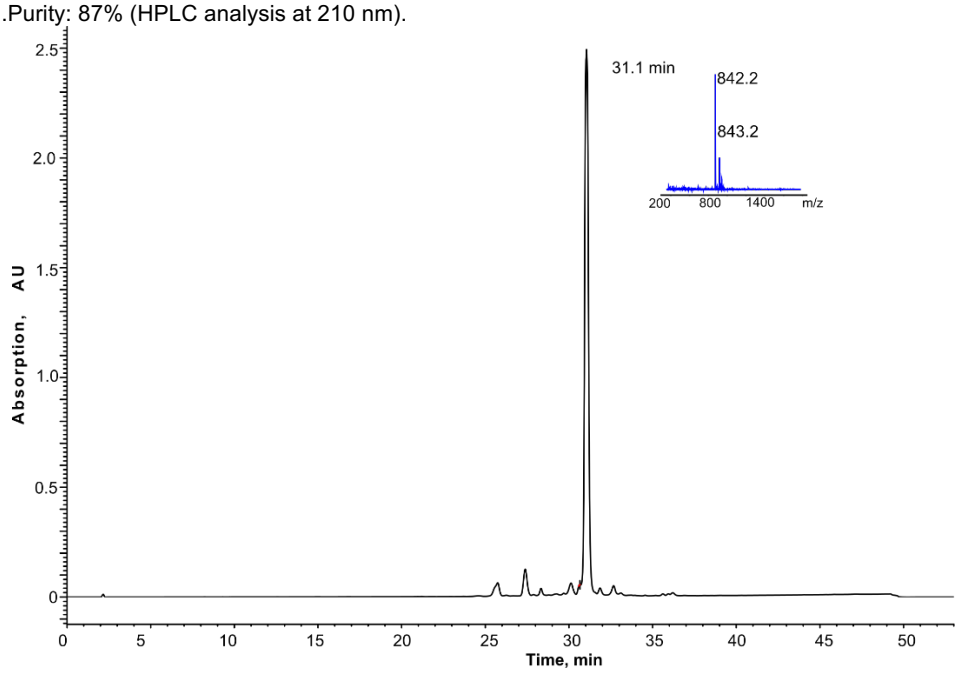

Figure S36. HPLC-MS profile of **22j**, t_R = 31.1 min (purity 86% as judged by peak area of RP-HPLC at 210 nm); Waters XTerra MS C18 column (125 Å 4.6 mm × 150 mm, 5 µm) with a linear gradient of 5% B-95% B over 45 min (*ca.* 2 % B•min^{-1}) at a flow rate of 1 mL•min^{-1} (A = 0.1% TFA in H_2O and B = 0.1 %TFA MeCN).

Fmoc-Pro-Trp-Tyr-Pro-Ile-OH (**24k**). Anal. RP-HPLC: t_R = 33.4 min, MS (ESI+): $C_{51}H_{56}N_6O_9$. $[M+H]^+$ calcd./found 897.4/897.2.Purity: >95% (HPLC analysis at 210 nm).

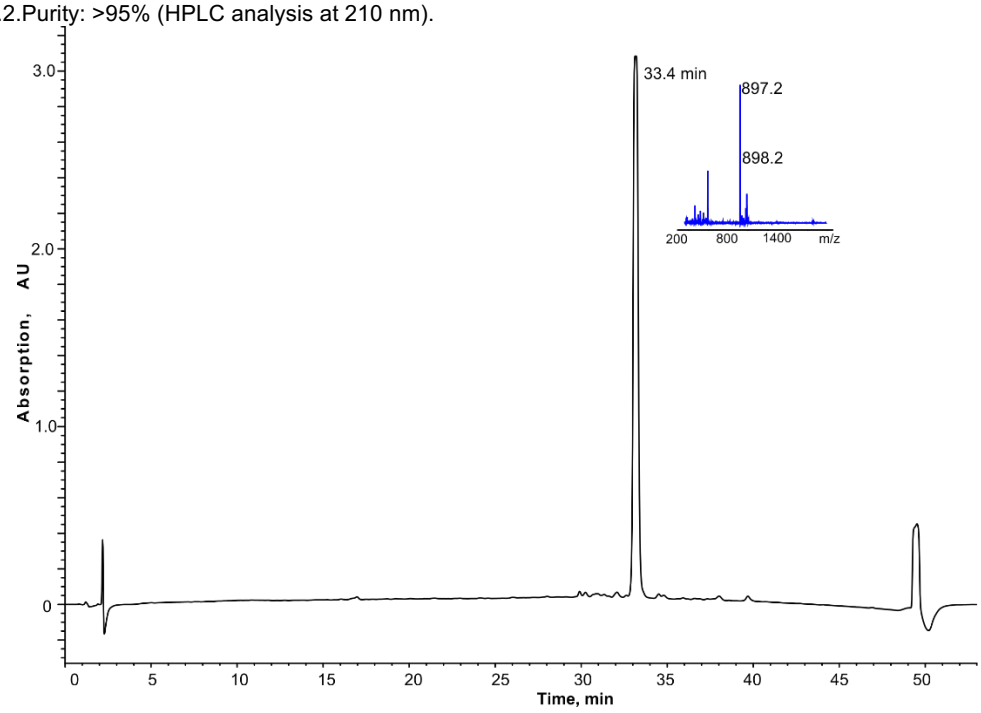

Figure S37. HPLC-MS profile of **24k**, t_R = 33.4 min (purity >95% as judged by peak area of RP-HPLC at 210 nm); Waters XTerra MS C18 column (125 Å 4.6 mm × 150 mm, 5 µm) with a linear gradient of 5% B-95% B over 45 min (*ca.* 2 % B•min^{-1}) at a flow rate of 1 mL•min^{-1} (A = 0.1% TFA in H_2O and B = 0.1 %TFA MeCN).

H-Leu-Val-Leu-Val-Tyr-Gly-OH (**24l**). Anal. RP-HPLC: t_R = 11.0 min, MS (ESI+): $C_{33}H_{54}N_6O_8$. $[M+H]^+$ calcd./found 663.4/663.2.Purity: >95% (HPLC analysis at 210 nm).

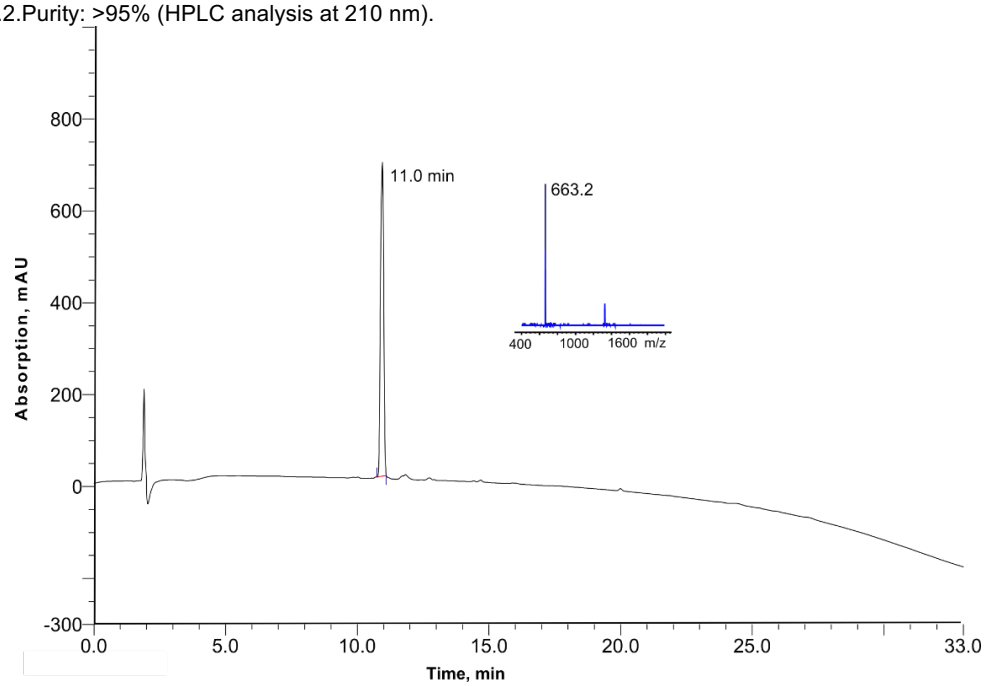

Figure S38. HPLC-MS profile of **24l**, t_R = 11.0 min (purity >95% as judged by peak area of RP-HPLC at 210 nm); Waters XTerra MS C18 column (125 Å 4.6 mm × 150 mm, 5 µm) with a linear gradient of 5% B-65% B over 30 min (*ca.* 2 % B•min^{-1}) at a flow rate of 1 mL•min^{-1} (A = 0.1% TFA in H_2O and B = 0.1 %TFA MeCN).).

Fmoc-Gly-DTyr-DAsp-Phe-Gly-OH (**24m**). Anal. RP-HPLC: t_R = 35.0 min, MS (ESI+): $C_{41}H_{41}N_5O_{11}$. $[M+H]^+$ calcd./found 780.3/780.2.Purity: >95% (HPLC analysis at 210 nm).

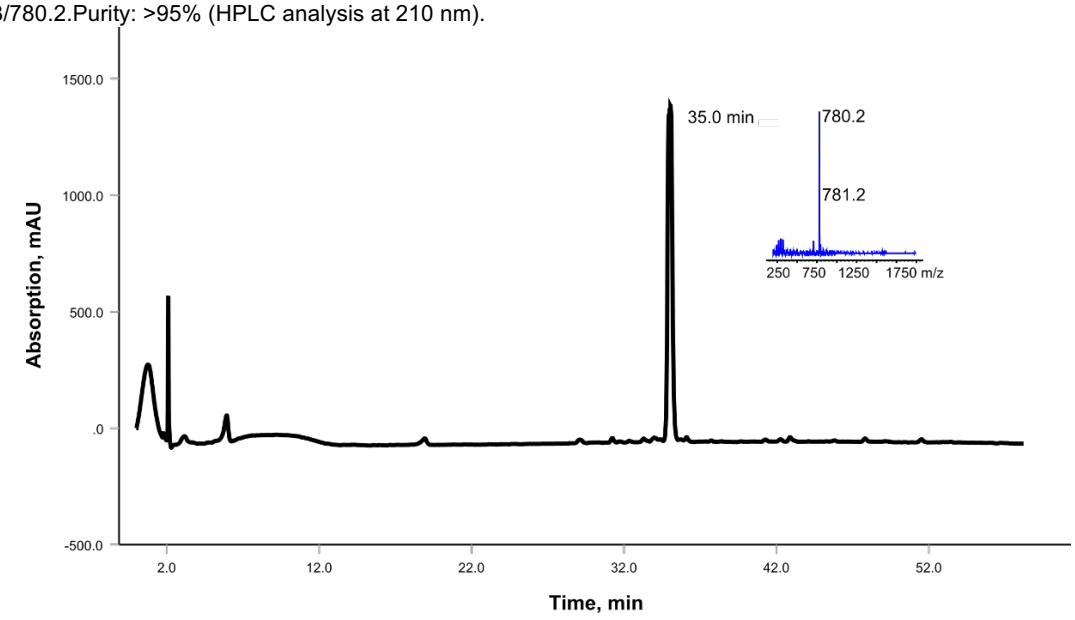

Figure S39. HPLC-MS profile of **24m**, t_R = 35.0 min (purity >95% as judged by peak area of RP-HPLC at 210 nm); Waters XTerra MS C18 column (125 Å, 4.6 mm × 150 mm, 5 µm) using a linear gradient of 5% B-60% B over 55 min (*ca.* 1 % B•min^{-1}) at a flow rate of 1 mL•min^{-1} (A = 0.1% TFA in H_2O and B = 0.1 %TFA MeCN).

Fmoc-Gly-(*N*Me)Ala-Tyr-Asn-Leu-Gly-OH (**24n**). Anal. RP-HPLC: t_R = 34.3 min, MS (ESI+): $C_{42}H_{51}N_7O_{11}$. $[M+H]^+$ calcd./found 830.4/830.2.Purity: >95% (HPLC analysis at 210 nm).

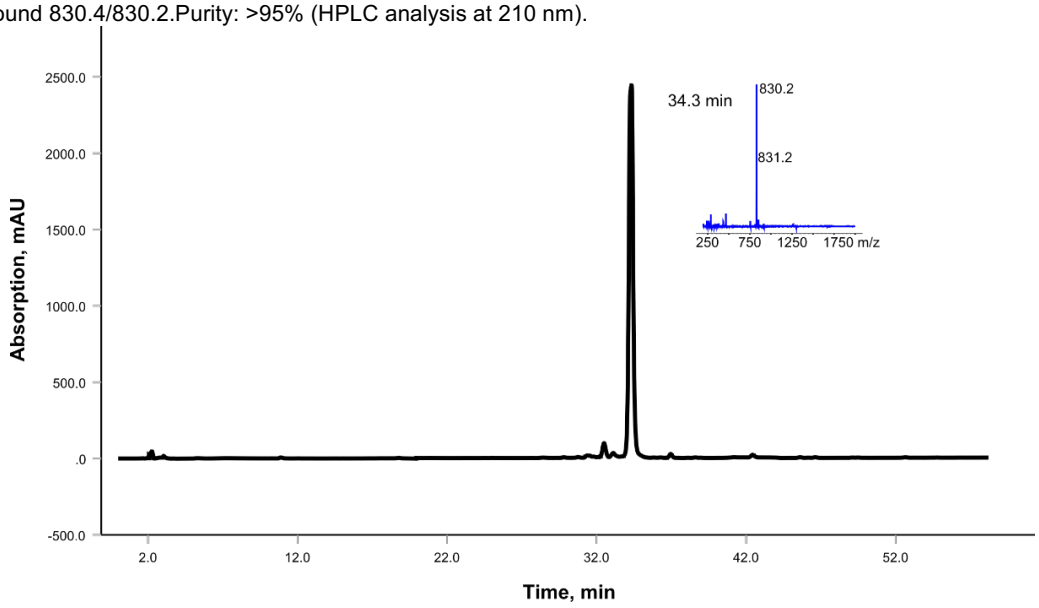

Figure S40. HPLC-MS profile of **24n**, t_R = 34.3 min (purity >95% as judged by peak area of RP-HPLC at 210 nm); Waters XTerra MS C18 column (125 Å, 4.6 mm × 150 mm, 5 µm) using a linear gradient of 5% B-60% B over 55 min (*ca.* 1 % B•min^{-1}) at a flow rate of 1 mL•min^{-1} (A = 0.1% TFA in H_2O and B = 0.1 %TFA MeCN).

Fmoc-Gly-Tyr^{phos}-Asp-Phe-Gly-OH (**24o**). Anal. RP-HPLC: t_R = 18.3 min, MS (ESI+): $C_{41}H_{42}N_5O_{14}P$. $[M+H]^+$ calcd./found 860.2/860.4.Purity: 94% (HPLC analysis at 210 nm).

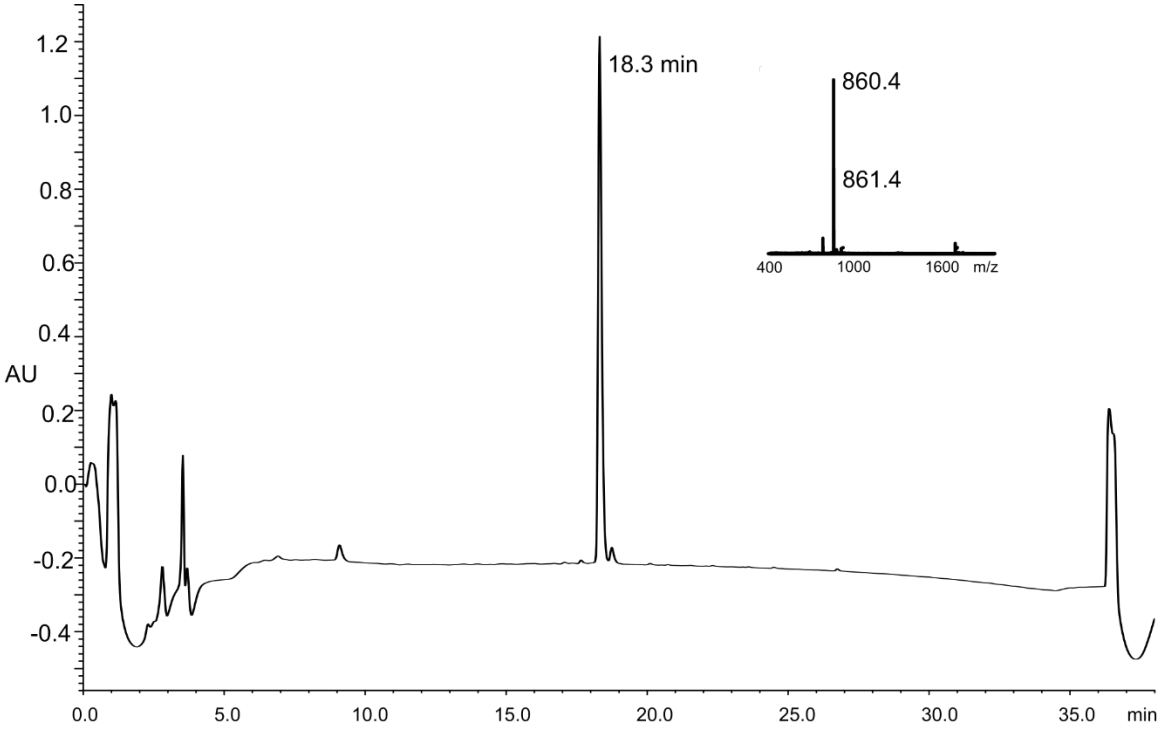

Figure S41. HPLC-MS profile of **24o**, t_R = 18.3 min (purity 94% as judged by peak area of RP-HPLC at 210 nm); Phenomenex Luna, C_{18} column (100 Å, 4.6 x 250 mm, 5 µm) using a linear gradient of 5% B-95% B over 30 min (*ca.* 3 % B•min^{-1}) at a flow rate of 1 mL•min^{-1} (A = 0.1% TFA in H_2O and B = 0.1 %TFA MeCN).

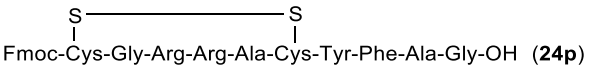

Anal. RP-HPLC: t_R = 33.4 min, MS (ESI+): $C_{61}H_{78}N_{16}O_{14}S_2$. $[M+H]^+$ calcd./found 1323.5/1323.3, $[M+2H]^{2+}$ calcd./found 662.2/662.2. Purity: 82% (HPLC analysis at 210 nm).

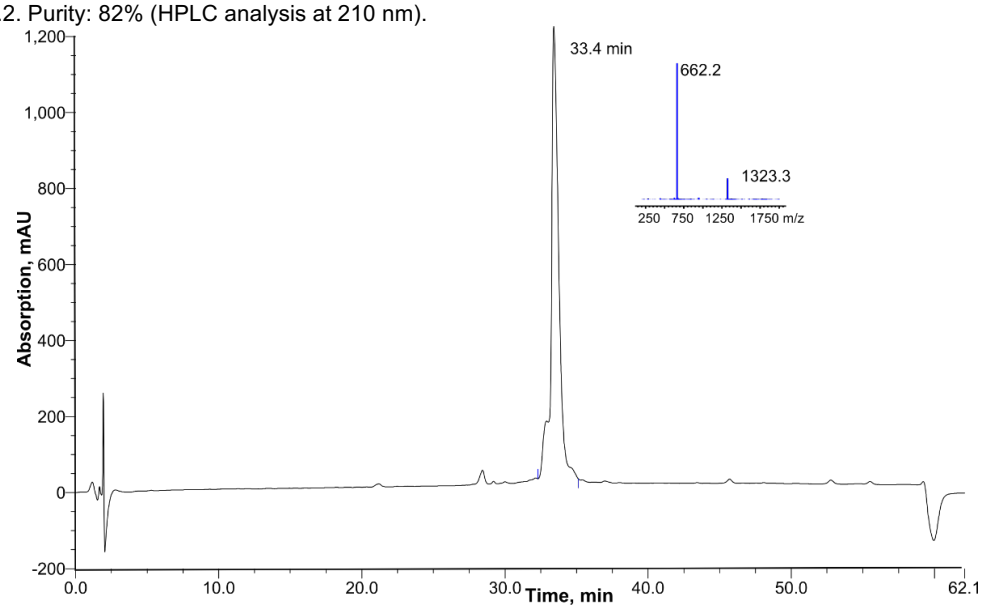

Figure S42. HPLC-MS profile of **24p**, t_R = 33.4 min (purity 82% as judged by peak area of RP-HPLC at 210 nm); Waters XTerra MS C18 column (125 Å, 4.6 mm × 150 mm, 5 µm) using a linear gradient of 5% B-60% B over 55 min (*ca.* 1 % B•min^{-1}) at a flow rate of 1 mL•min^{-1} (A = 0.1% TFA in H_2O and B = 0.1 %TFA MeCN).

Oxytocin (**24q**) Anal. RP-HPLC: t_R = 13.5 min, MS (ESI+): $C_{43}H_{66}N_{12}O_{12}S_2$. $[M+H]^+$ calcd./found 1008.2/1008.3, $[M+2H]^{2+}$ calcd./found 504.6/504.8. Purity: >95% (HPLC analysis at 210 nm).

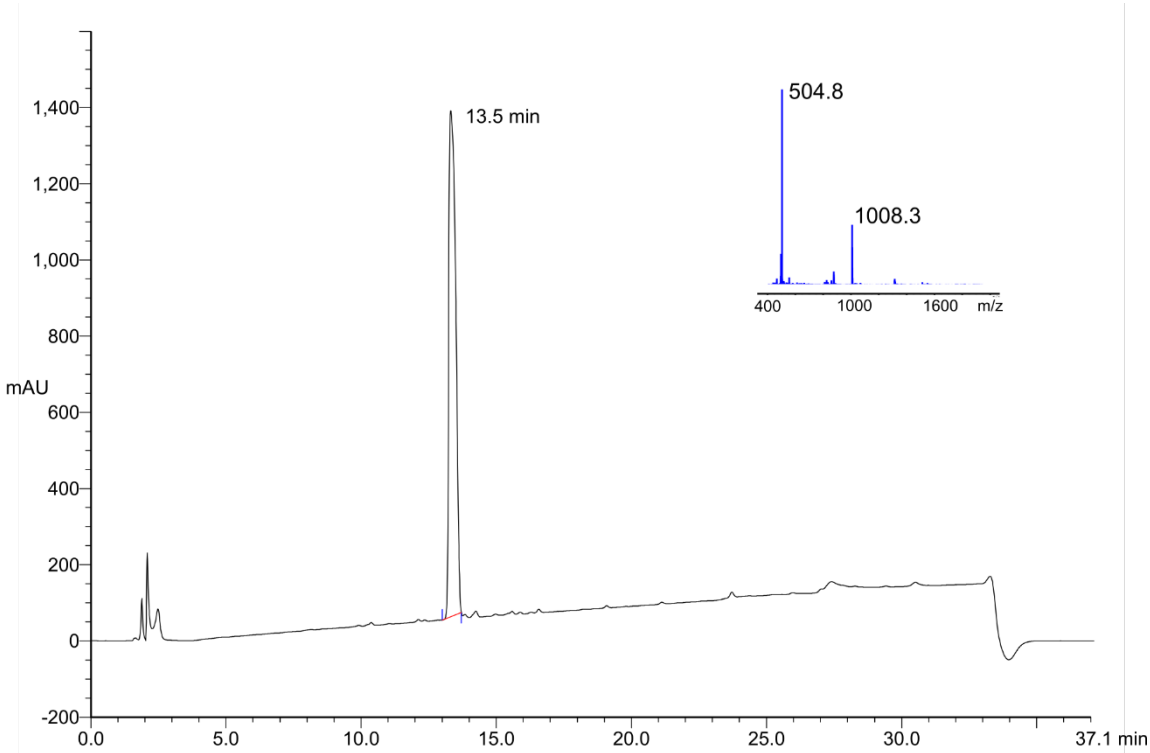

Figure S43. HPLC-MS profile of **24q**, t_R = 13.5 min (purity >95% as judged by peak area of RP-HPLC at 210 nm); Phenomenex Lunar, C_{18} column (100 Å, 4.6 x 250 mm, 5 µm) with using a linear gradient of 5% B-95% B over 30 min (ca. 3 % B•min^{-1}) at a flow rate of 1 mL•min^{-1} (A = 0.1% TFA in H_2O and B = 0.1 %TFA MeCN).

Fmoc-Gln-Gln-Arg-Leu-Ile-Tyr-Phe-Leu-Phe-Tyr-Ala-Ile-Leu-Gly-NH_2 (**25**) Anal. RP-HPLC: t_R = 38.5 min, MS (ESI+): $C_{102}H_{139}N_{19}O_{21}$. $[M+H]^+$ calcd./found 1967.0/1967.0, $[M+2H]^{2+}$ calcd./found 984.0/983.9. Purity: 93% (HPLC analysis at 210 nm).

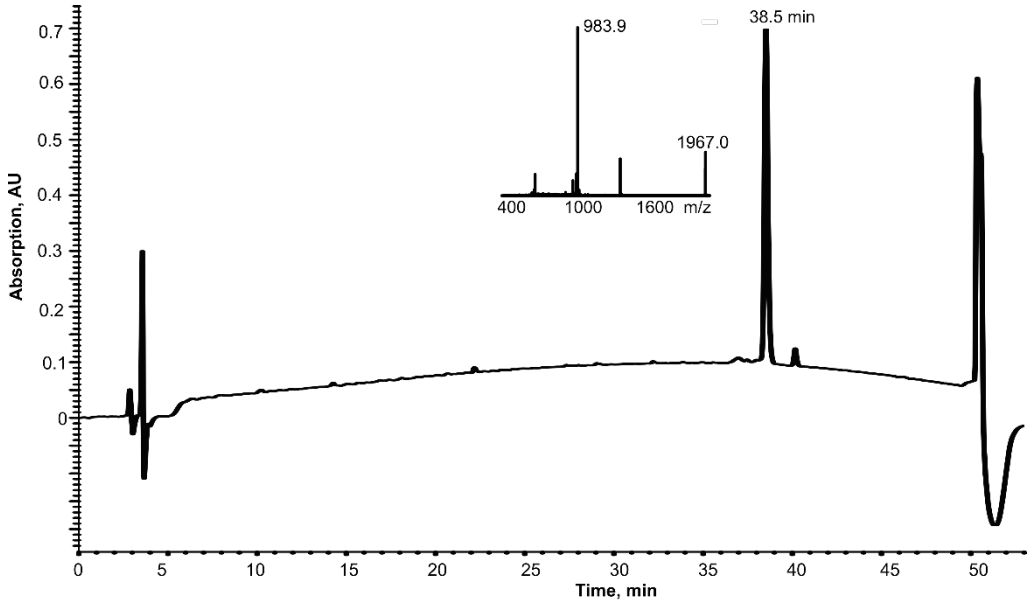

Figure S44. HPLC-MS profile of **25**, t_R = 38.5 min (purity 93% as judged by peak area of RP-HPLC at 210 nm); Phenomenex Lunar, C_{18} column (100 Å, 4.6 x 250 mm, 5 µm) with using a linear gradient of 5% B-95% B over 45 min (ca. 2 % B•min^{-1}) at a flow rate of 1 mL•min^{-1} (A = 0.1% TFA in H_2O and B = 0.1 %TFA MeCN).

Fmoc-Arg-Ala-Ala-Pro-Tyr-Gly-Val-Arg-Leu-Ser-Gly-Arg-Glu-Phe-Ile-Pro-Ala-Val-Ile-Phe-Thr-Ser-Arg-OH (**26**) Anal. RP-HPLC: t_R = 23.7 min, MS (ESI+): $C_{132}H_{197}N_{35}O_{32}$. $[M+H]^{2+}$ calcd./found 929.5/929.5, $[M+H]^{3+}$ calcd./found 697.4/697.4. Purity: 88% (HPLC analysis at 210 nm).

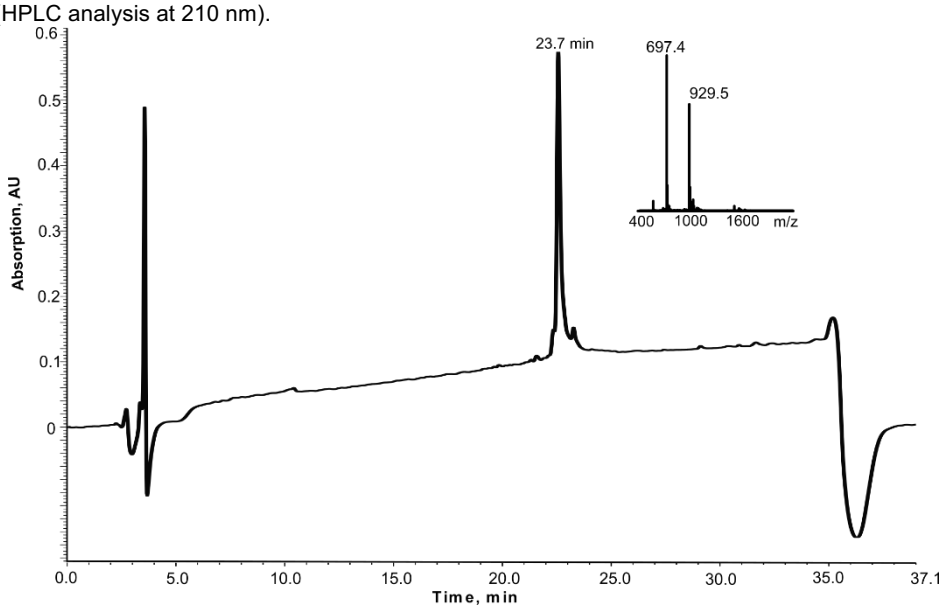

Figure S45. HPLC-MS profile of **26**, t_R = 23.7 min (purity 88% as judged by peak area of RP-HPLC at 210 nm); Phenomenex Lunar, C_{18} column (100 Å, 4.6 x 250 mm, 5 µm) with using a linear gradient of 5% B-65% B over 30 min (ca. 2 % B•min^{-1}) at a flow rate of 1 mL•min^{-1} (A = 0.1% TFA in H_2O and B = 0.1 %TFA MeCN).

Fmoc-Asp-Ala-Glu-Phe-Arg-His-Asp-Ser-Gly-Tyr-Glu-Val-His-His-Gln-Lys-Leu-Val-Phe-OH (**27**). Anal. RP-HPLC: t_R = 21.8 min, MS (ESI+): $C_{119}H_{158}N_{30}O_{33}$. $[M+2H]^{2+}$ calcd./found 1269.1/1269.3, $[M+3H]^{3+}$ calcd./found 846.4/846.6, $[M+4H]^{4+}$ calcd./found 635.0/635.2. Purity: >95% (HPLC analysis at 210 nm).

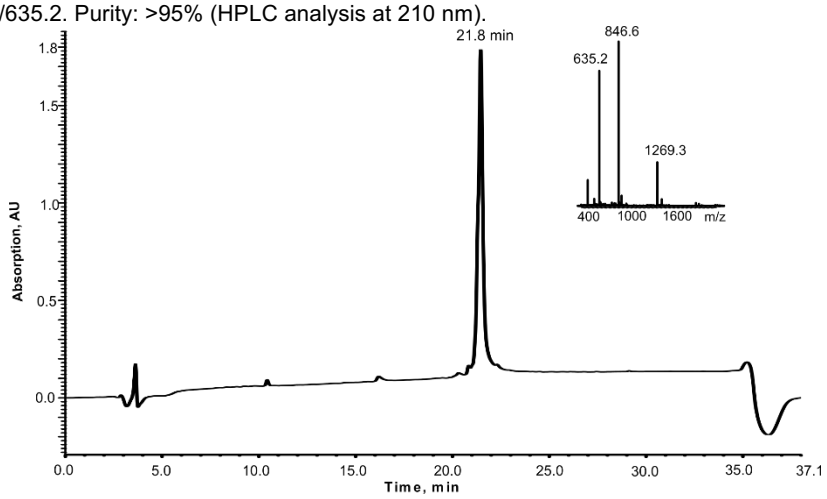

Figure S46. HPLC-MS profile of **27**, t_R = 21.8 min (purity >95% as judged by peak area of RP-HPLC at 210 nm); Phenomenex Lunar, C_{18} column (100 Å, 4.6 x 250 mm, 5 µm) with using a linear gradient of 5% B-65% B over 35 min (*ca*. 2 % B•min^{-1}) at a flow rate of 1 mL•min^{-1} (A = 0.1% TFA in H_2O and B = 0.1 %TFA MeCN).

Ac-His-Ala-Glu-Gly-Thr-Phe-Thr-Ser-Asp-Val-Ser-Ser-Tyr-Leu-Glu-Gly-Gln-Ala-Ala-Lys(Ac)-Glu-Phe-Ile-Ala-Trp-Leu-Val-Lys(Ac)-Gly-Arg-NH_2 (fully acetylated **28**). Anal. RP-HPLC: t_R = 25.7 min, MS (ESI+): $C_{155}H_{232}N_{40}O_{48}$. $[M+2H]^{2+}$ calcd./found 1712.4/1712.6, $[M+3H]^{3+}$ calcd./found 1141.9/1142.1, $[M+4H]^{4+}$ calcd./found 856.7/856.9. Purity: >90% (HPLC analysis at 210 nm).

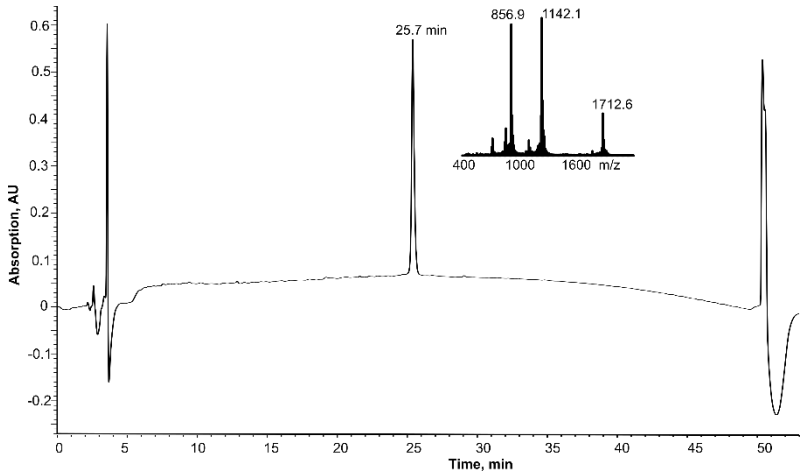

Figure S47. HPLC-MS profile of fully acetylated **28**, t_R = 25.7min (purity >95% as judged by peak area of RP-HPLC at 210 nm); Waters XTerra MS C18 column (125 Å 4.6 mm × 150 mm, 5 µm) with a linear gradient of 5% B-95% B over 45 min (*ca.* 2 % B•min^{-1}) at a flow rate of 1 mL•min^{-1} (A = 0.1% TFA in H_2O and B = 0.1 %TFA MeCN).

Ac-Gly-Ala-Trp-Lys(Ac)-Asn-Phe-Trp-Ser-Ser-Leu-Arg-Lys(Ac)-Gly-Phe-Tyr-Asp-Gly-Glu-Ala-Gly-Arg-Ala-Ile-Arg-Arg-OH (fully acetylated **29**). Anal. RP-HPLC: t_R = 16.2 min, MS (ESI+): $C_{139}H_{204}N_{42}O_{37}$. $[M+2H]^{2+}$ calcd./found 1528.2/1528.0, $[M+3H]^{3+}$ calcd./found 1019.2/1019.2, $[M+4H]^{4+}$ calcd./found 764.6/764.6. Purity: >95% (HPLC analysis at 210 nm).

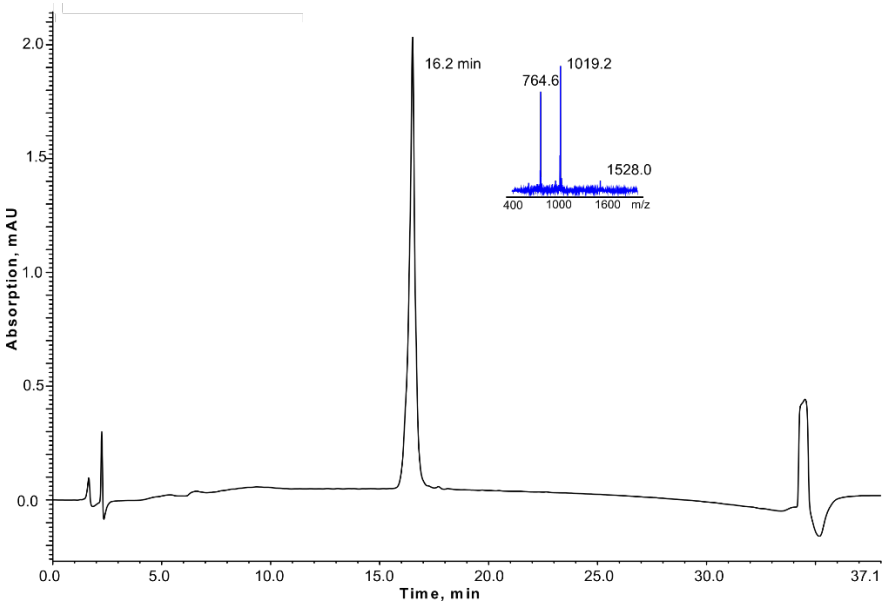

Figure S48. HPLC-MS profile of the fully acetylated **29**, t_R = 16.2 min (purity >95% as judged by peak area of RP-HPLC at 210 nm); Waters XTerra MS C18 column (125 Å 4.6 mm × 150 mm, 5 µm) with a linear gradient of 5% B-65% B over 30 min (*ca.* 2 % B•min^{-1}) at a flow rate of 1 mL•min^{-1} (A = 0.1% TFA in H_2O and B = 0.1 %TFA MeCN).

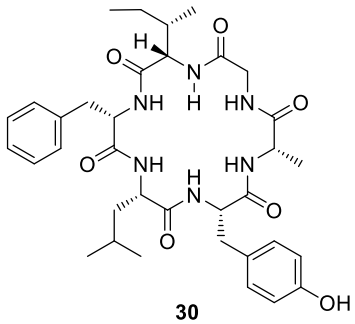

30

Dichotomin J (**30**). The linear protected peptide precursor H-Ile-Phe-Leu-Tyr(*t*Bu)-Ala-Gly-OH was prepared using the general protocol of Fmoc-SPPS on a 2-CTC resin. The fully protected linear peptide (20 mg, 29 µmol) was then cyclized using PyBOP (45 mg, 87 µmol), 6-Cl-HOBt (15 mg, 87 µmol) and DIPEA (25 µL, 145 µmol) in DMF (40 mL, 0.75 mM) overnight. The reaction mixture was then diluted with water (360 mL) and subjected to semi-preparative RP-HPLC purification. The purified peptide was finally treated with a mixture of TFA/CH_2Cl_2 (5 mL, *v*/*v*, 1:1) to furnish **30** as a white powder (14 mg, 73 %). Anal. RP-HPLC: t_R = 21.7 min, purity: >95% (HPLC analysis at 210 nm). ^{1}H NMR (500 MHz, pyridine-d_6) δ 9.57 (s, 1H), 9.22 (d, *J* = 5.7 Hz, 1H), 9.10 (d, *J* = 4.4 Hz, 1H), 9.00 (m, 2H), 8.94 (d, *J* = 8.5 Hz,1H), 7.44 (d, *J* = 6.5 Hz, 2H), 7.27 (d, *J* = 7.9 Hz, 2H), 7.15 (m, 3H), 7.10 (d, *J* = 8.0 Hz, 2H), 5.10 (m, 1H), 4.73 (m, 2H), 4.44 – 4.57 (m, 2H), 4.10 (d, *J* = 8.6 Hz, 1H), 3.73 (d, *J* = 9.1 Hz, 1H), 3.53 (d, *J* = 7.4 Hz, 2H), 3.41 (d, *J* = 8.6 Hz, 1H), 2.18 (m, 1H), 1.90 (m, 2H), 1.64 (d, *J* = 6.5 Hz, 3H), 1.59 – 1.70 (m, 1H), 1.36 (m, 1H), 1.16 (m, 1H), 0.81 (d, *J* = 6.4 Hz, 2H), 0.72 (m, 6H), 0.65 (d, *J* = 6.9 Hz, 3H). ^{13}C NMR (125 MHz, pyridine-d_6): δ 173.63, 173.61, 172.60, 172.60, 172.41, 170.96, 157.43, 138.69, 130.86, 129.70, 128.58, 128.38, 126.59, 115.99, 59.50, 57.12, 55.89, 54.41, 50.61, 44.25, 40.58, 37.60, 36.51, 35.86, 24.80, 24.68, 22.80, 21.84, 17.18, 15.69, 11.32. HRMS (ESI+): $C_{35}H_{48}N_6O_7$. $[M+H]^+$ calcd./found 665.3584/665.3687. The NMR spectral data of **30** matched those previously reported in the literature[2].

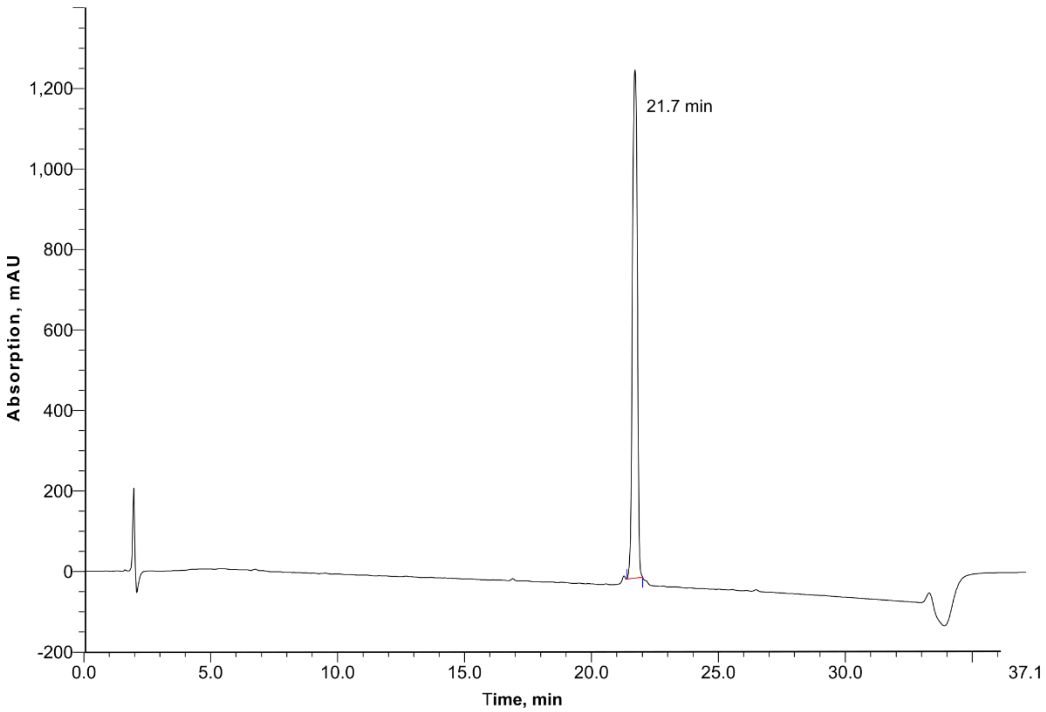

Figure S49. HPLC profile of **30**, t_R = 21.7 min (purity >95% as judged by peak area of RP-HPLC at 210 nm); Waters XTerra MS C18 column (125 Å 4.6 mm × 150 mm, 5 µm) with a linear gradient of 5% B-65% B over 30 min (*ca.* 2 % B•min^{-1}) at a flow rate of 1 mL•min^{-1} (A = 0.1% TFA in H_2O and B = 0.1 %TFA MeCN).

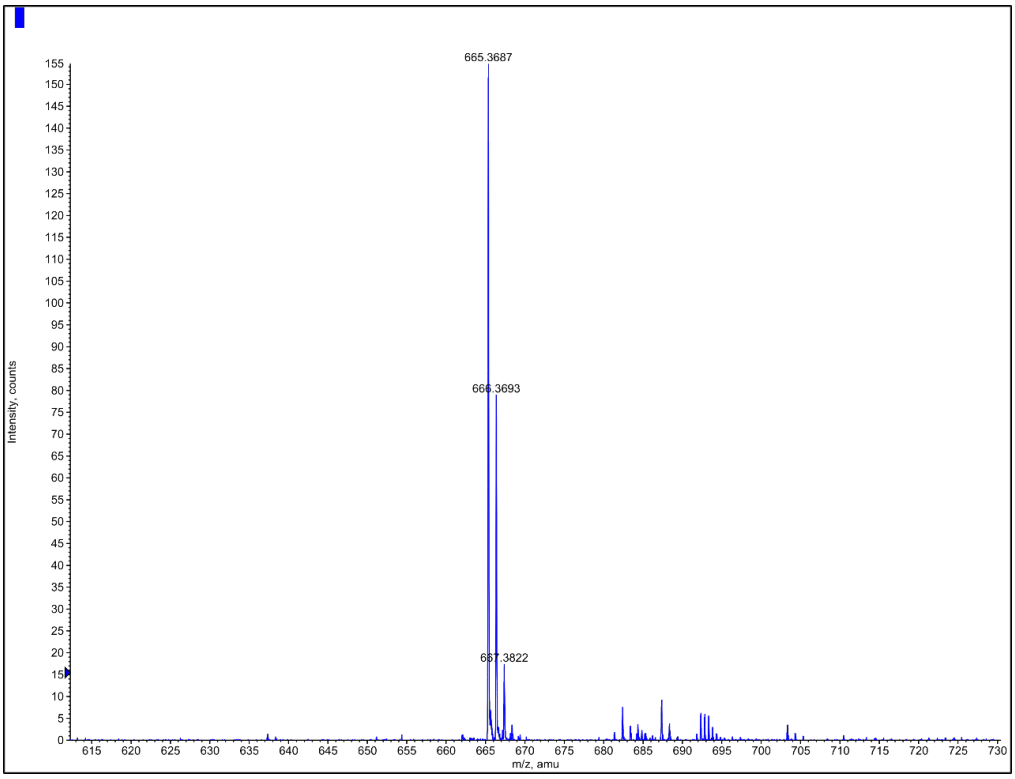

Figure S50. HRMS profile of **30**. MS (ESI$^+$): $C_{35}H_{48}N_6O_7$. $[M+H]^+$ calcd./found 665.3584/665.3687.

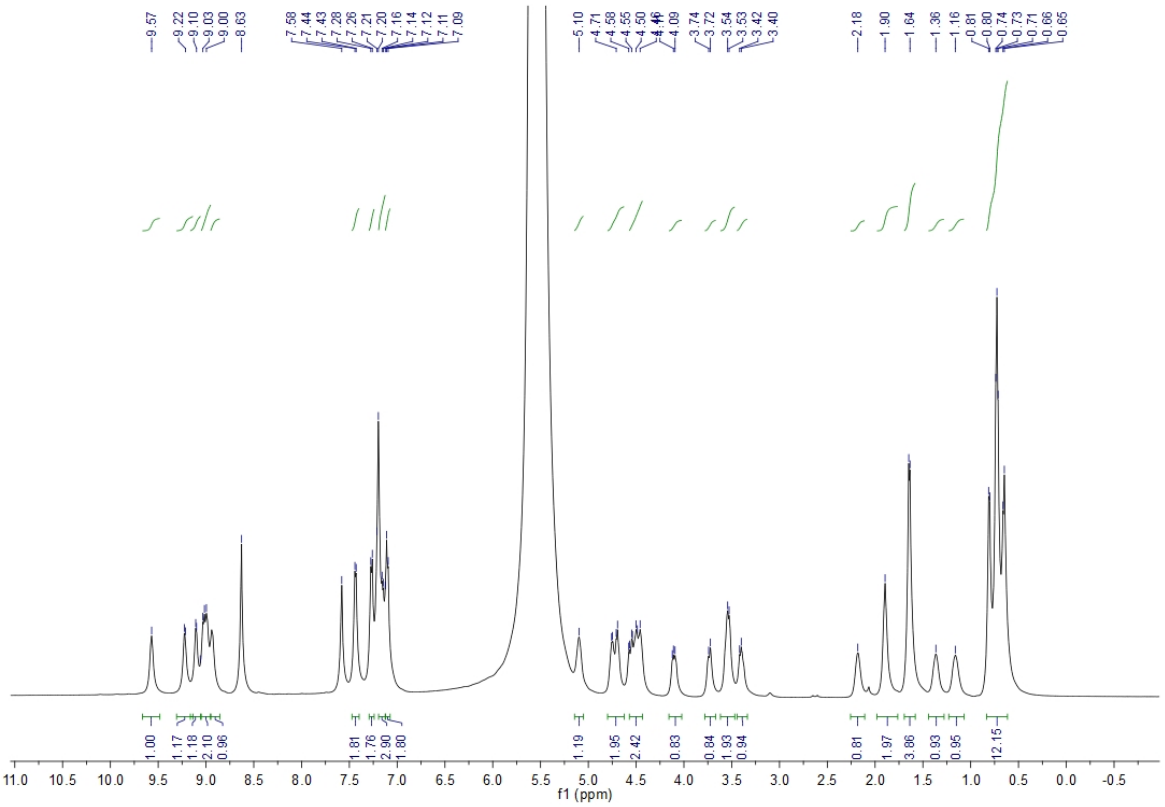

Figure S51. ^{1}H NMR (500 MHz, pyridine-d_6) spectrum of **30**.

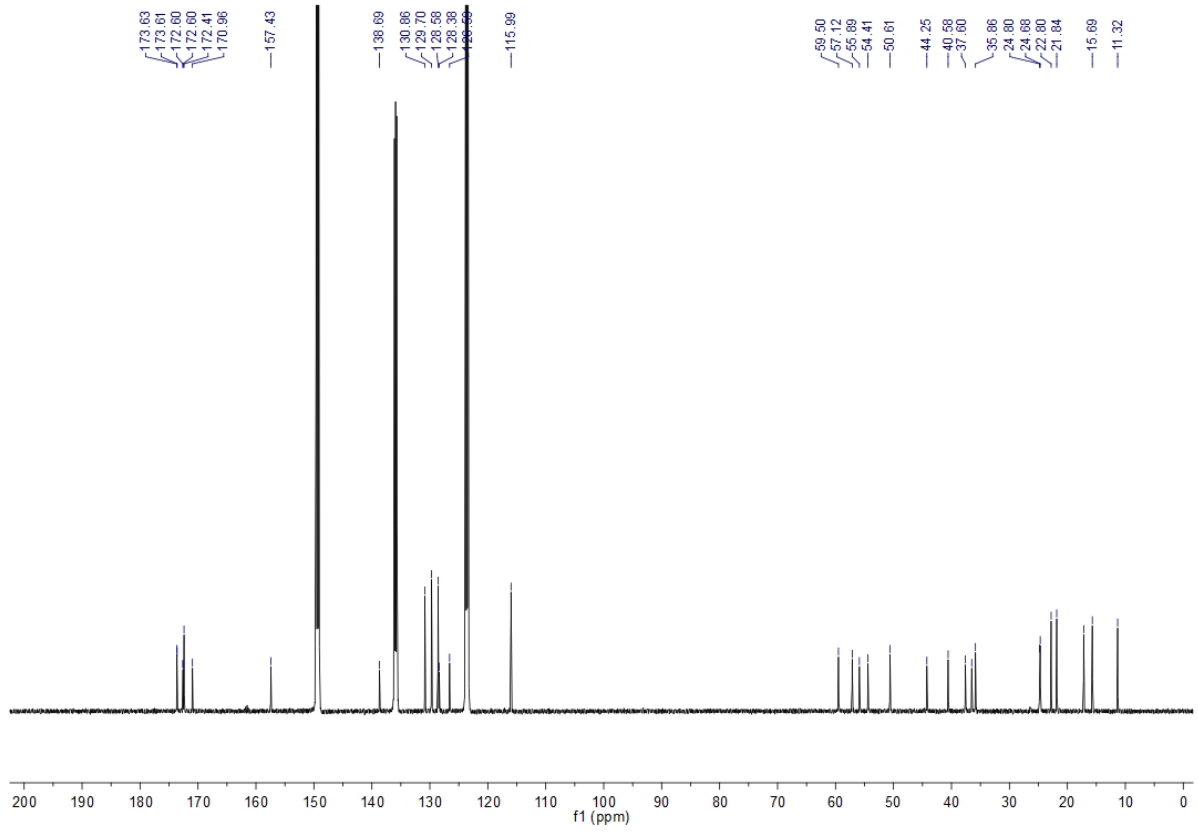

Figure S52. ^{13}C NMR (125 MHz, pyridine-d_6) spectrum of **30**.

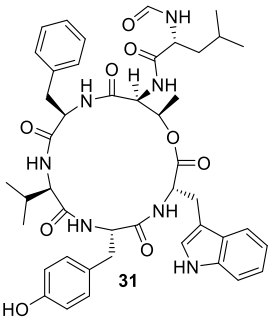

Szentiamide (**31**). Compound **31** was prepared using a method similar to that reported in literature[3]. Anal. RP-HPLC: t_R = 41.3 min, purity: >95% (HPLC analysis at 210 nm). ^{1}H NMR (500 MHz, acetone-d_6) δ 9.82 (s, 1H), 8.30 (d, *J* = 10.2 Hz, 1H), 8.29 (s, 1H), 8.20 (d, *J* = 3.7 Hz, 1H), 7.97 (d, *J* = 7.6 Hz, 1H), 7.75 (d, *J* = 9.9 Hz, 1H), 7.60 (dd, *J* = 8.1, 4.6 Hz, 2H), 7.40 (d, *J* = 8.1 Hz, 1H), 7.27 (m, 4H), 7.21 (d, *J* = 2.3 Hz, 2H), 7.11 (m, 1H), 7.10 (m, 1H), 7.05 (m, 1H), 7.00 (d, *J* = 8.4 Hz, 2H), 6.70 (d, *J* = 8.5 Hz, 2H), 5.53 (m, 1H), 4.75 (m, 3H), 4.67 (td, *J* = 8.2, 5.1 Hz, 1H), 4.49 (m, 1H), 4.05 (t, *J* = 8.0 Hz, 1H), 3.32 (m, 1H), 3.25 (m, 1H), 3.21 (d, *J* = 8.3 Hz, 2H), 3.14 (dd, *J* = 14.5, 3.4 Hz, 1H), 2.47 (dd, *J* = 14.5, 11.9 Hz, 1H), 1.76 (m, 3H), 1.64 (m, 1H), 1.20 (d, *J* = 6.4 Hz, 3H), 1.07 (d, *J* = 6.4 Hz, 3H), 0.96 (d, *J* = 6.3 Hz, 3H), 0.78 (d, *J* = 6.7 Hz, 3H), 0.60 (d, *J* = 6.8 Hz, 3H). ^{13}C NMR (125 MHz, acetone-d_6): δ 175.22, 174.29, 173.63, 171.28, 171.05, 170.18, 164.12, 157.03, 138.49, 137.49, 130.69, 129.97, 129.42, 129.32, 128.76, 128.73, 124.59, 122.17, 119.59, 119.25, 116.05, 112.29, 111.02, 71.69, 59.97, 58.77,57.26, 56.21, 54.28, 53.53, 40.71, 37.34, 35.81, 31.48, 27.98, 25.63, 22.82, 22.51, 19.41, 18.96, 16.73 . HRMS (ESI+): $C_{45}H_{55}N_7O_9$. $[M+H]^+$ calcd./found 838.4061/838.3997. The spectral data of **31** matched those previously reported in the literature[4].

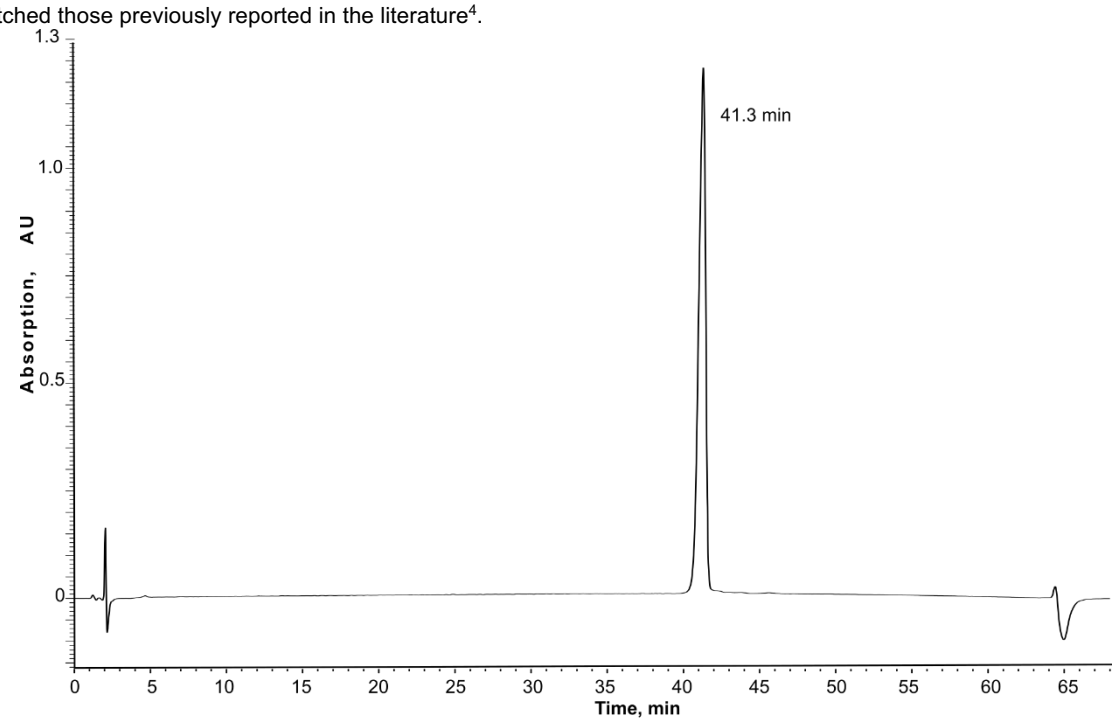

Figure S53. HPLC profile of **31**, t_R = 41.3 min (purity >95% as judged by peak area of RP-HPLC at 210 nm); Waters XTerra MS C18 column (125 Å 4.6 mm × 150 mm, 5 µm) with a linear gradient of 5% B-65% B over 60 min (*ca.* 1 % B•min^{-1}) at a flow rate of 1 mL•min^{-1} (A = 0.1% TFA in H_2O and B = 0.1 %TFA MeCN).

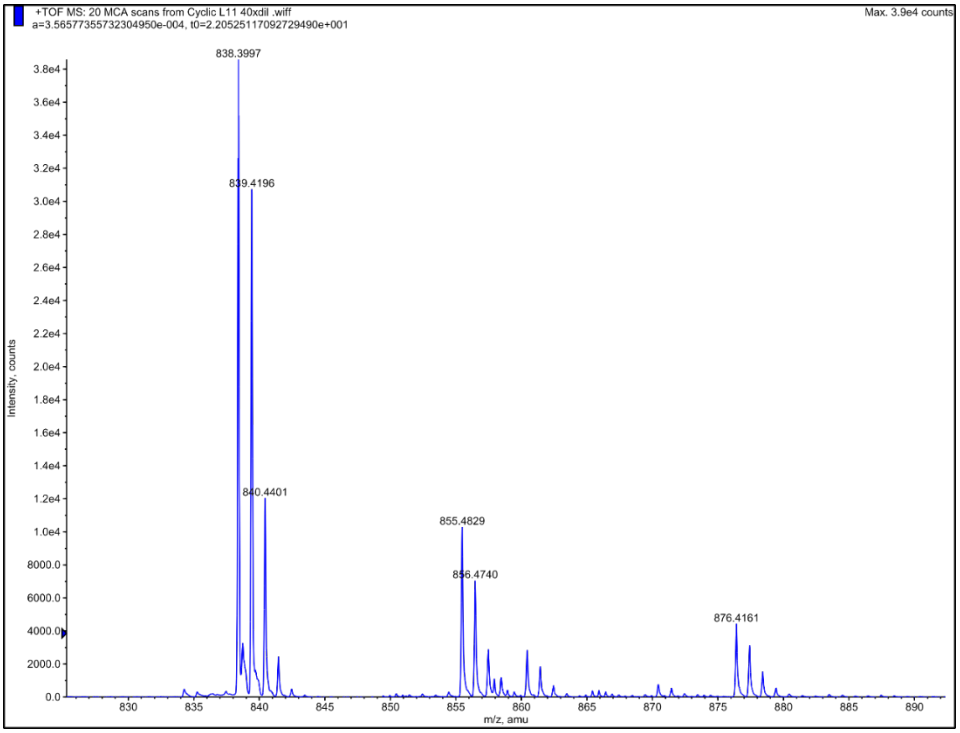

Figure S54. HRMS profile of **31**. MS (ESI+): $C_{45}H_{55}N_7O_9$. $[M+H]^+$ calcd./found 838.4061/838.3997.

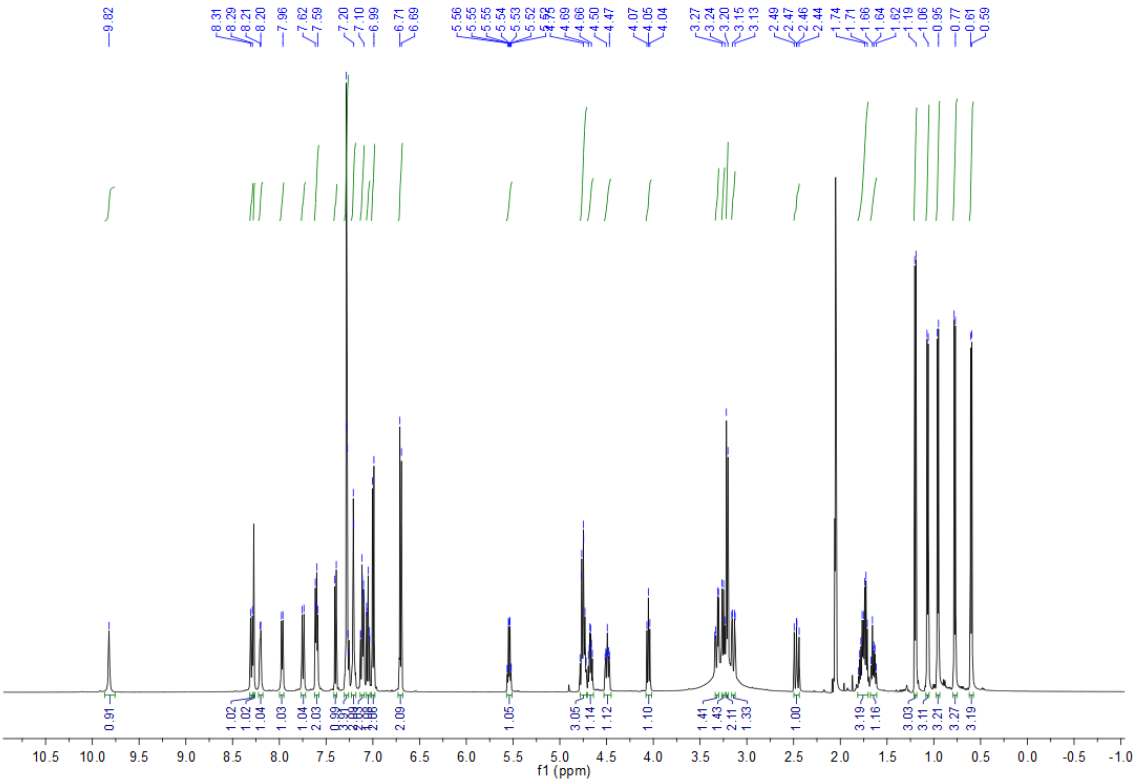

Figure S55. ^{1}H NMR (500 MHz, acetone-d_6) spectrum of **31**.

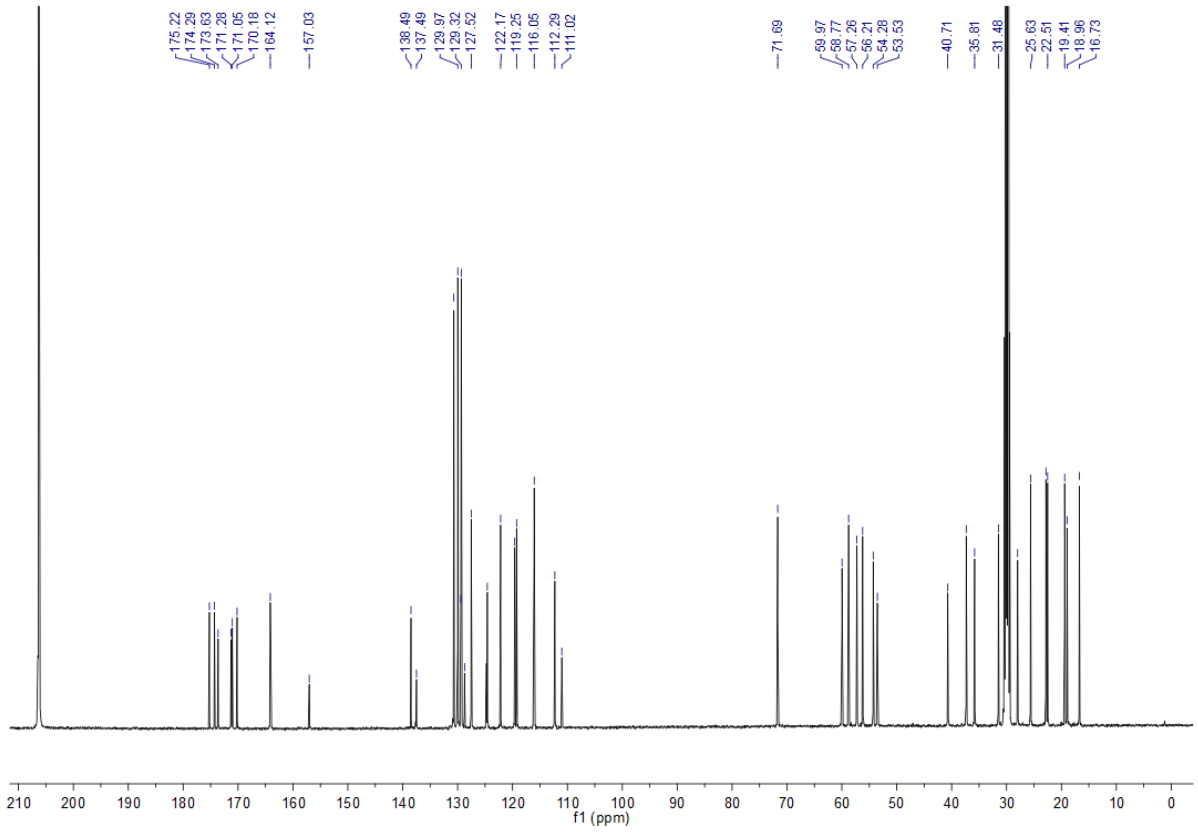

Figure S56. ^{13}C NMR (125 MHz, acetone-d_6) spectrum of **31**.

Iturin A (**32**). Compound **32** derived from *Bacillus subtilis* was purchased from Sigma-Aldrich. Anal. RP-HPLC: t_R = 41.0 min. MS (ESI+): $C_{48}H_{74}N_{12}O_{14}$. $[M+H]^+$ calcd./found 1043.5447/1043.5318.

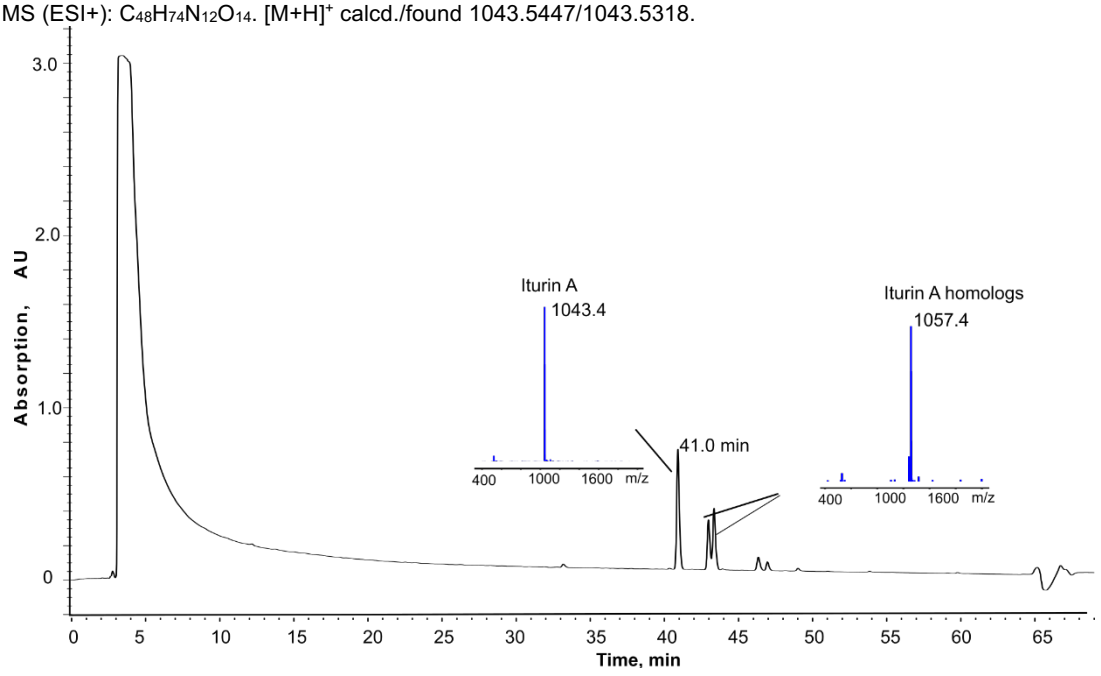

Figure S57. HPLC-MS profile of **32** purchased from Sigma-Aldrich, t_R = 41.0 min; MS (ESI+): $C_{48}H_{74}N_{12}O_{14}$. $[M+H]^+$ calcd./found 1043.5/1043.4. Waters Xterra MS C18 column (125 Å 4.6 mm × 150 mm, 5 µm) with a linear gradient of 5% B-65% B over 60 min (*ca.* 1 % B•min^{-1}) at a flow rate of 1 mL•min^{-1} (A = 0.1% TFA in H_2O and B = 0.1 %TFA MeCN).

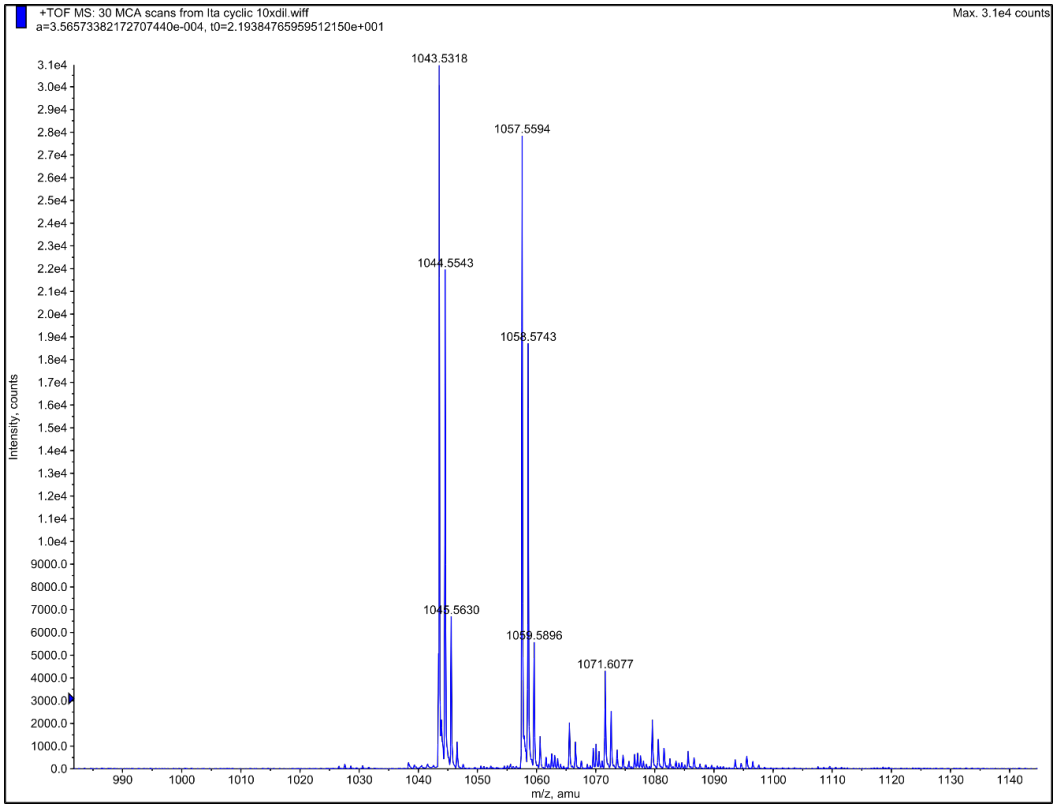

Figure S58. HRMS profile of **32**. MS (ESI+): $C_{48}H_{74}N_{12}O_{14}$. $[M+H]^+$ calcd./found 1043.5447/1043.5318.

4. Selective Peptide Cleavage at a Tyrosine Site

General protocol for the selective peptide cleavage at a tyrosine residue

A solution of peptide (1mg) in DMSO (100 µL) was mixed with a solution of DMP (10 equiv. for peptides containing less than 10 amino acids or 40 equiv. for peptides containing more than 10 amino acids and cyclic peptides) in DMSO (100 µL), followed by addition of 0.1 M phosphate buffer at pH 7 (100 µL). The resulting mixture was stirred at 40 ºC for 2 h (for peptides containing less than 10 amino acids) or 3 h (for peptides containing more than 10 amino acids and cyclic peptides). Reaction progression was analysed by analytical reverse phase HPLC-MS spectroscopy.

HPLC Chromatograms for the Tyr-selective peptide cleavage

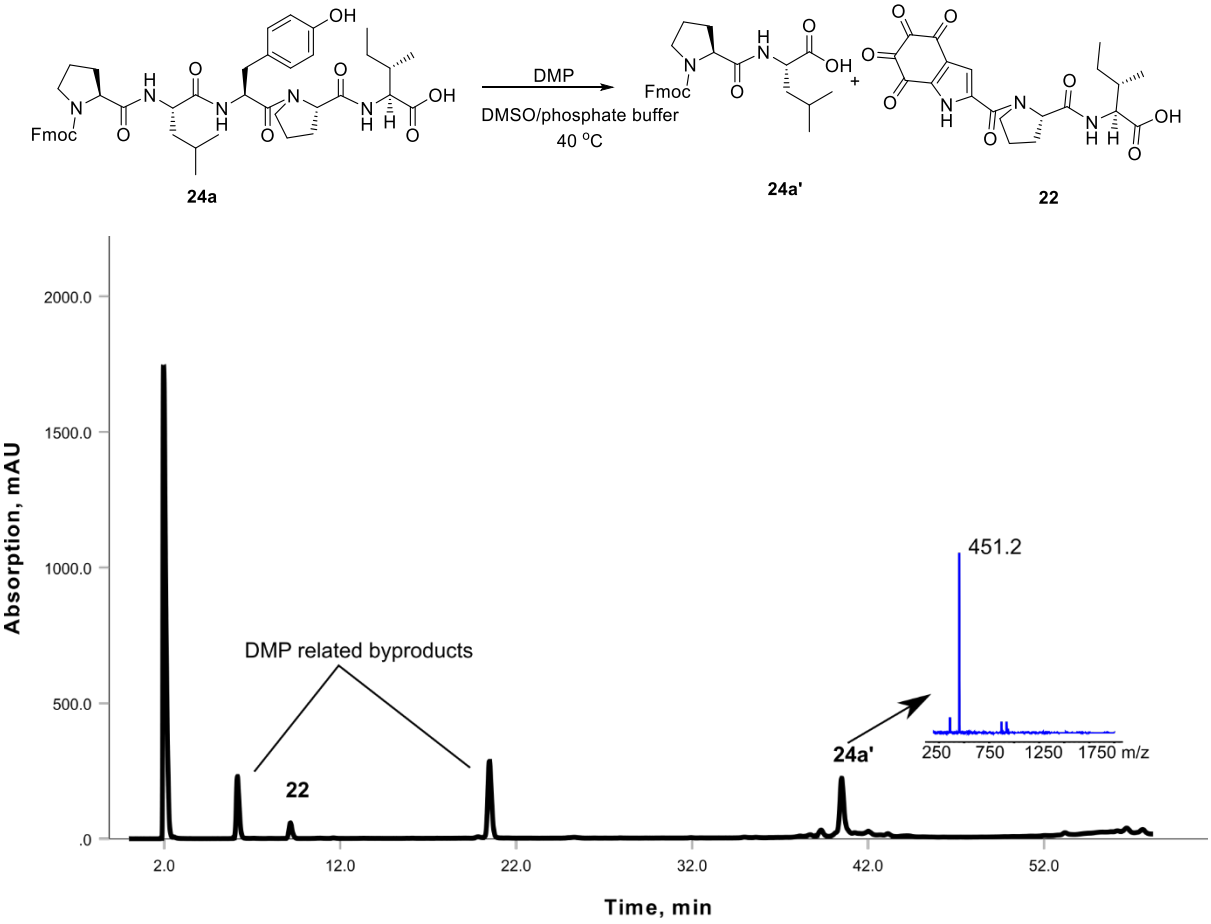

Figure S59. HPLC-MS profile of the DMP-mediated cleavage of **24a.** Waters Xterra MS C18 column (125 Å 4.6 mm × 150 mm, 5 µm) with a linear gradient of 5% B-65% B over 60 min (*ca.* 1 % B•min^{-1}) at a flow rate of 1 mL•min^{-1} (A = 0.1% TFA in H_2O and B = 0.1 %TFA MeCN). The UV-Vis detector was set at the wavelength of 254 nm. MS characterization of **24a'**: MS (ESI+): $C_{26}H_{30}N_2O_5$. $[M+H]^+$ calcd./found 451.2/451.2.

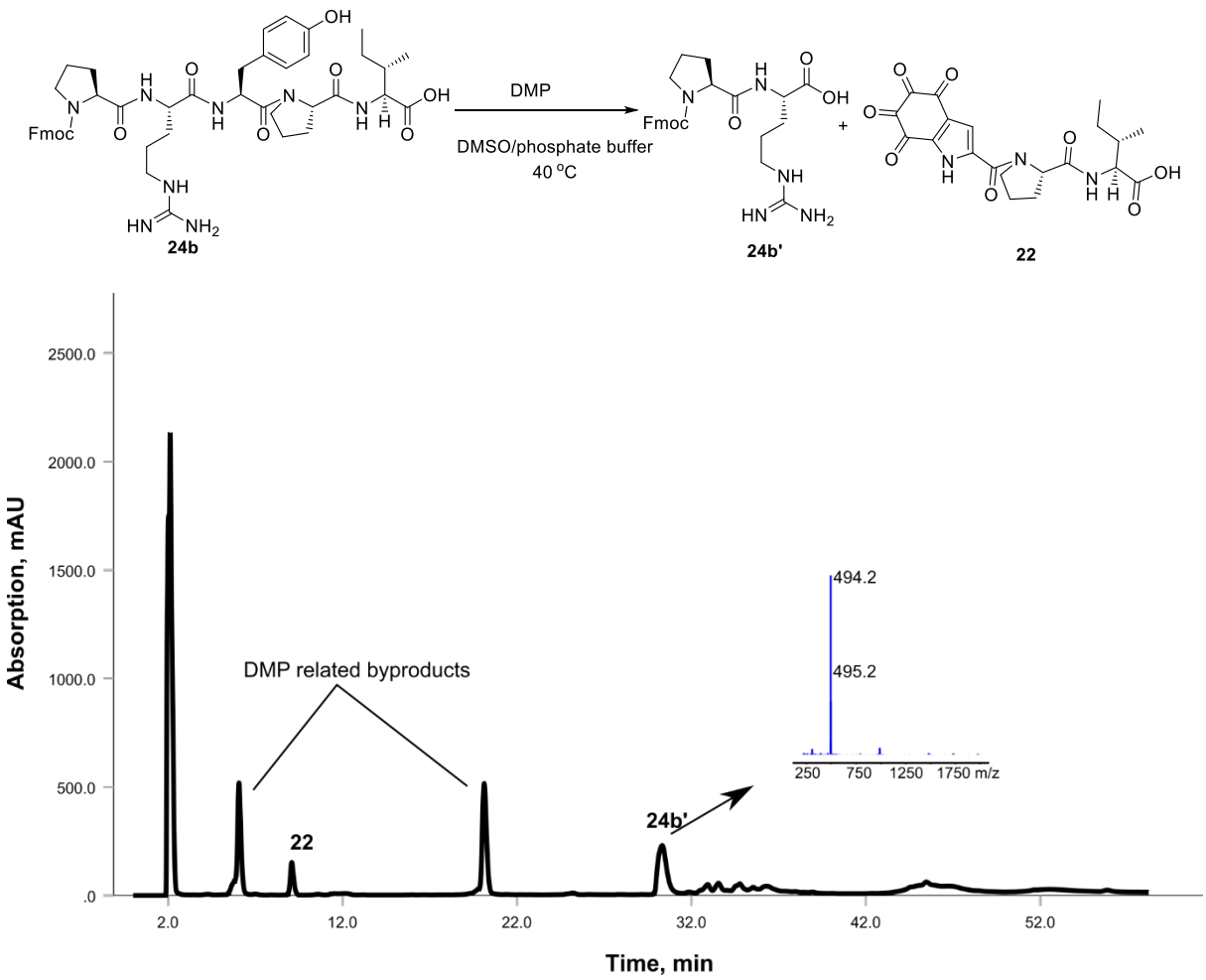

Figure S60. HPLC-MS profile of the DMP-mediated cleavage of **24b.** Waters Xterra MS C18 column (125 Å 4.6 mm × 150 mm, 5 µm) with a linear gradient of 5% B-65% B over 60 min (*ca.* 1 % B•min^{-1}) at a flow rate of 1 mL•min^{-1} (A = 0.1% TFA in H_2O and B = 0.1 %TFA MeCN). The UV-Vis detector was set at the wavelength of 254 nm. MS characterization of **24b'**: MS (ESI+): $C_{26}H_{31}N_5O_5$. $[M+H]^+$ calcd./found 494.2/494.2.

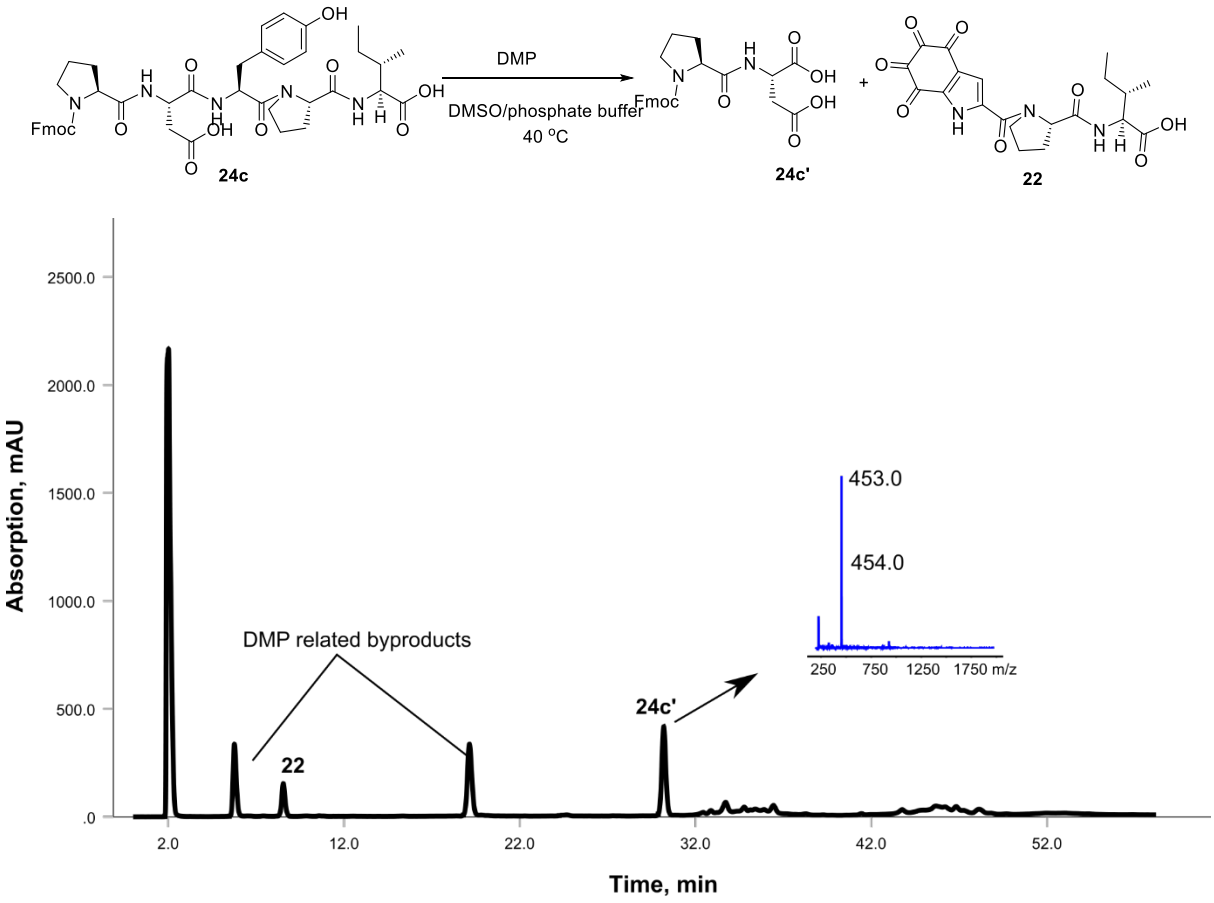

Figure S61. HPLC-MS profile of the DMP-mediated cleavage of **24c.** Waters Xterra MS C18 column (125 Å 4.6 mm × 150 mm, 5 µm) with a linear gradient of 5% B-65% B over 60 min (*ca.* 1 % B•min^{-1}) at a flow rate of 1 mL•min^{-1} (A = 0.1% TFA in H_2O and B = 0.1 %TFA MeCN). The UV-Vis detector was set at the wavelength of 254 nm. MS characterization of **24c'**: MS (ESI+): $C_{24}H_{24}N_2O_7$. $[M+H]^+$ calcd./found 453.2/453.0.

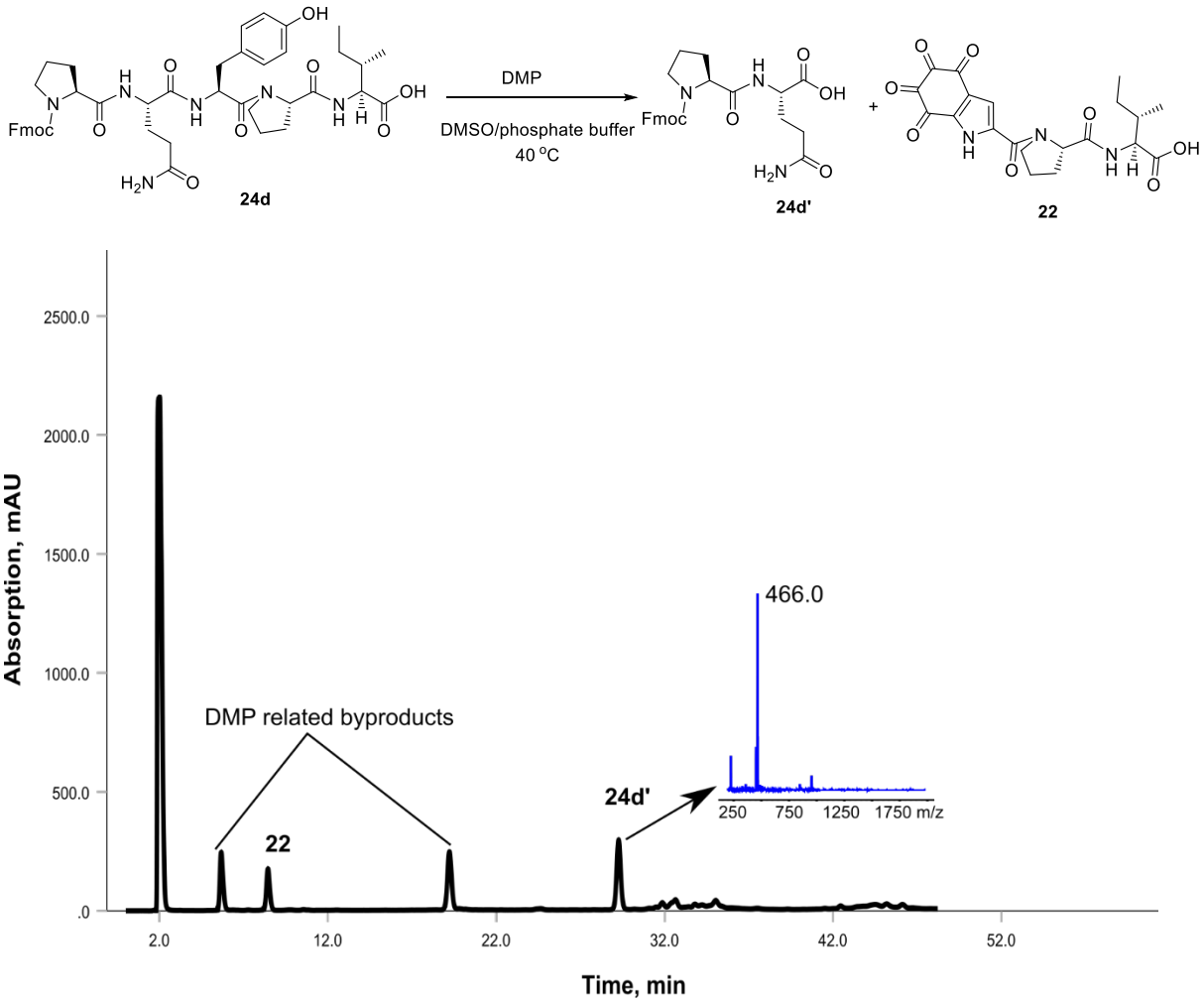

Figure S62. HPLC-MS profile of the DMP-mediated cleavage of **24d.** Waters Xterra MS C18 column (125 Å 4.6 mm × 150 mm, 5 µm) with a linear gradient of 5% B-65% B over 60 min (*ca.* 1 % B•min^{-1}) at a flow rate of 1 mL•min^{-1} (A = 0.1% TFA in H_2O and B = 0.1 %TFA MeCN). The UV-Vis detector was set at the wavelength of 254 nm. MS characterization of **24d'**: MS (ESI+): $C_{25}H_{27}N_3O_6$. $[M+H]^+$ calcd./found 466.2/466.0.

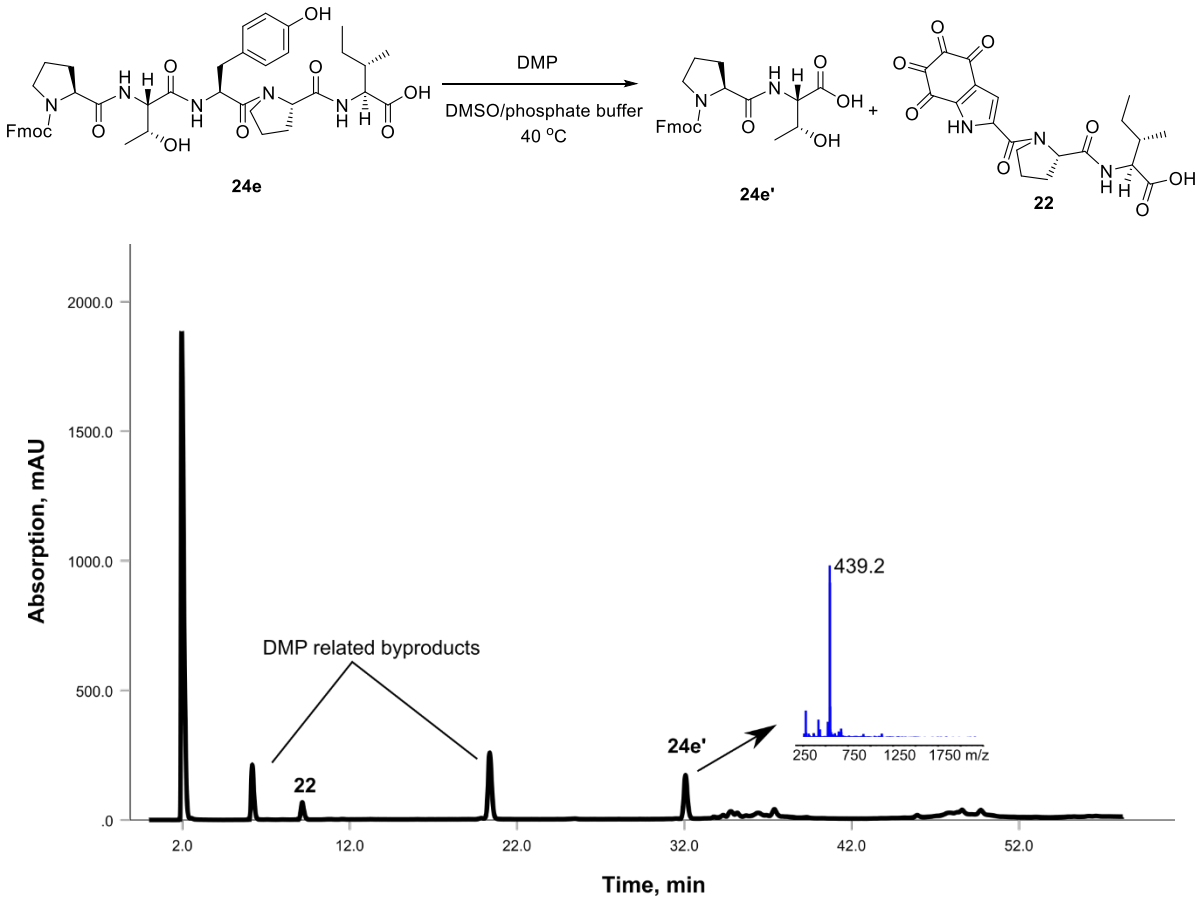

Figure S63. HPLC-MS profile of the DMP-mediated cleavage of **24e.** Waters Xterra MS C18 column (125 Å 4.6 mm × 150 mm, 5 µm) with a linear gradient of 5% B-65% B over 60 min (*ca.* 1 % B•min^{-1}) at a flow rate of 1 mL•min^{-1} (A = 0.1% TFA in H_2O and B = 0.1 %TFA MeCN). The UV-Vis detector was set at the wavelength of 254 nm. MS characterization of **24e'**: MS (ESI+): $C_{24}H_{26}N_2O_6$. $[M+H]^+$ calcd./found 439.2/439.2.

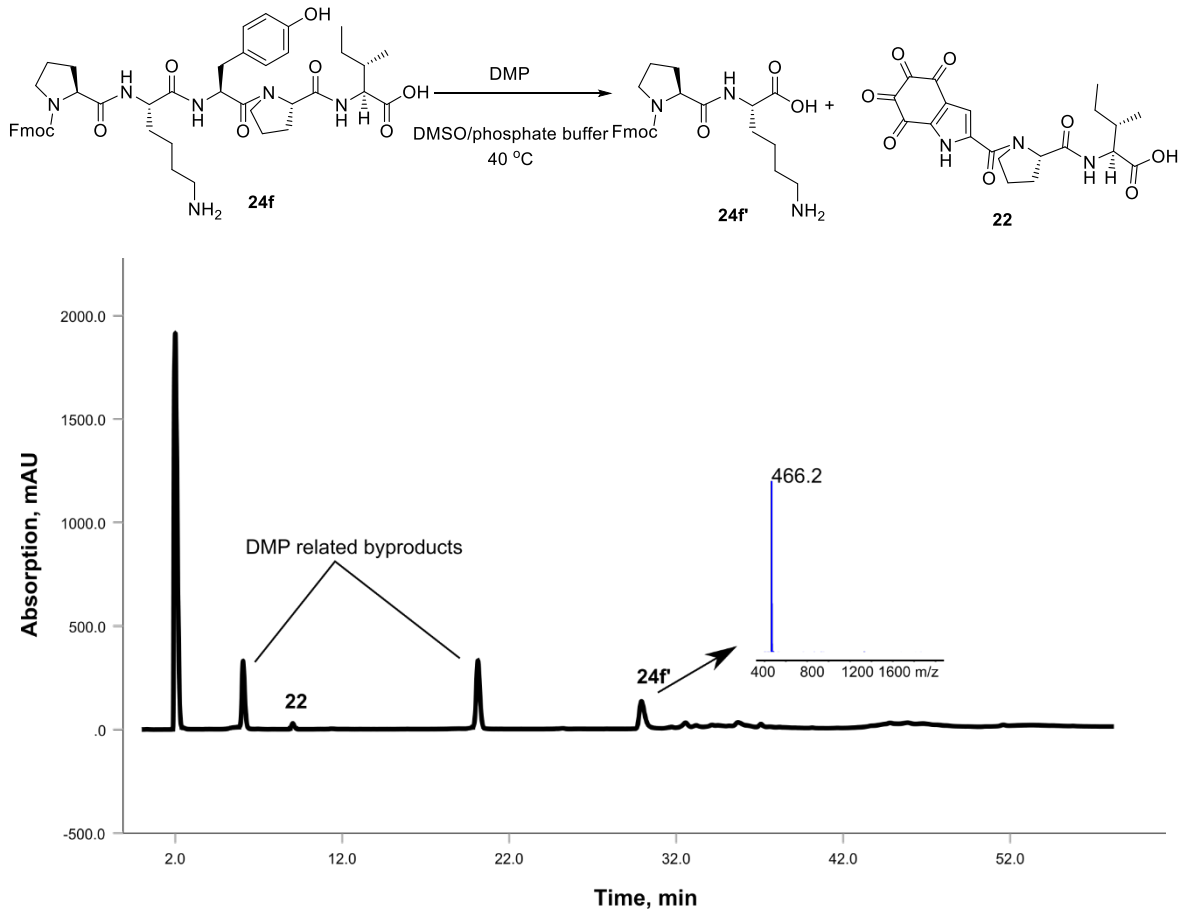

Figure S64. HPLC-MS profile of the DMP-mediated cleavage of **24f.** Waters Xterra MS C18 column (125 Å 4.6 mm × 150 mm, 5 µm) with a linear gradient of 5% B-65% B over 60 min (*ca.* 1 % B•min^{-1}) at a flow rate of 1 mL•min^{-1} (A = 0.1% TFA in H_2O and B = 0.1 %TFA MeCN). The UV-Vis detector was set at the wavelength of 254 nm. MS characterization of **24f'**: MS (ESI+): $C_{26}H_{31}N_3O_5$. $[M+H]^+$ calcd./found 466.2/466.2.

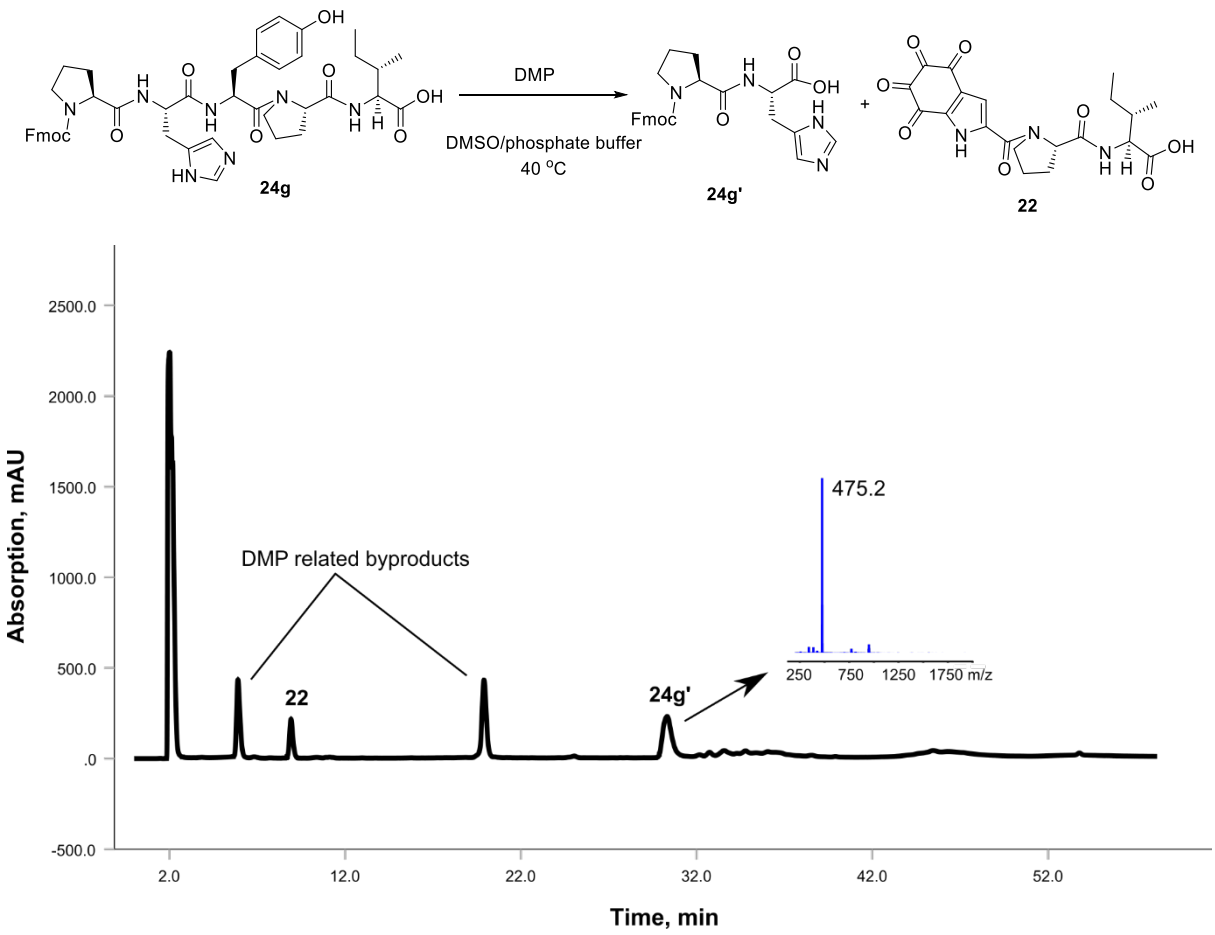

Figure S65. HPLC-MS profile of the DMP-mediated cleavage of **24g.** Waters Xterra MS C18 column (125 Å 4.6 mm × 150 mm, 5 µm) with a linear gradient of 5% B-65% B over 60 min (*ca.* 1 % B•min^{-1}) at a flow rate of 1 mL•min^{-1} (A = 0.1% TFA in H_2O and B = 0.1 %TFA MeCN). The UV-Vis detector was set at the wavelength of 254 nm. MS characterization of **24g'**: MS (ESI+): $C_{26}H_{26}N_4O_5$. $[M+H]^+$ calcd./found 475.2/475.2.

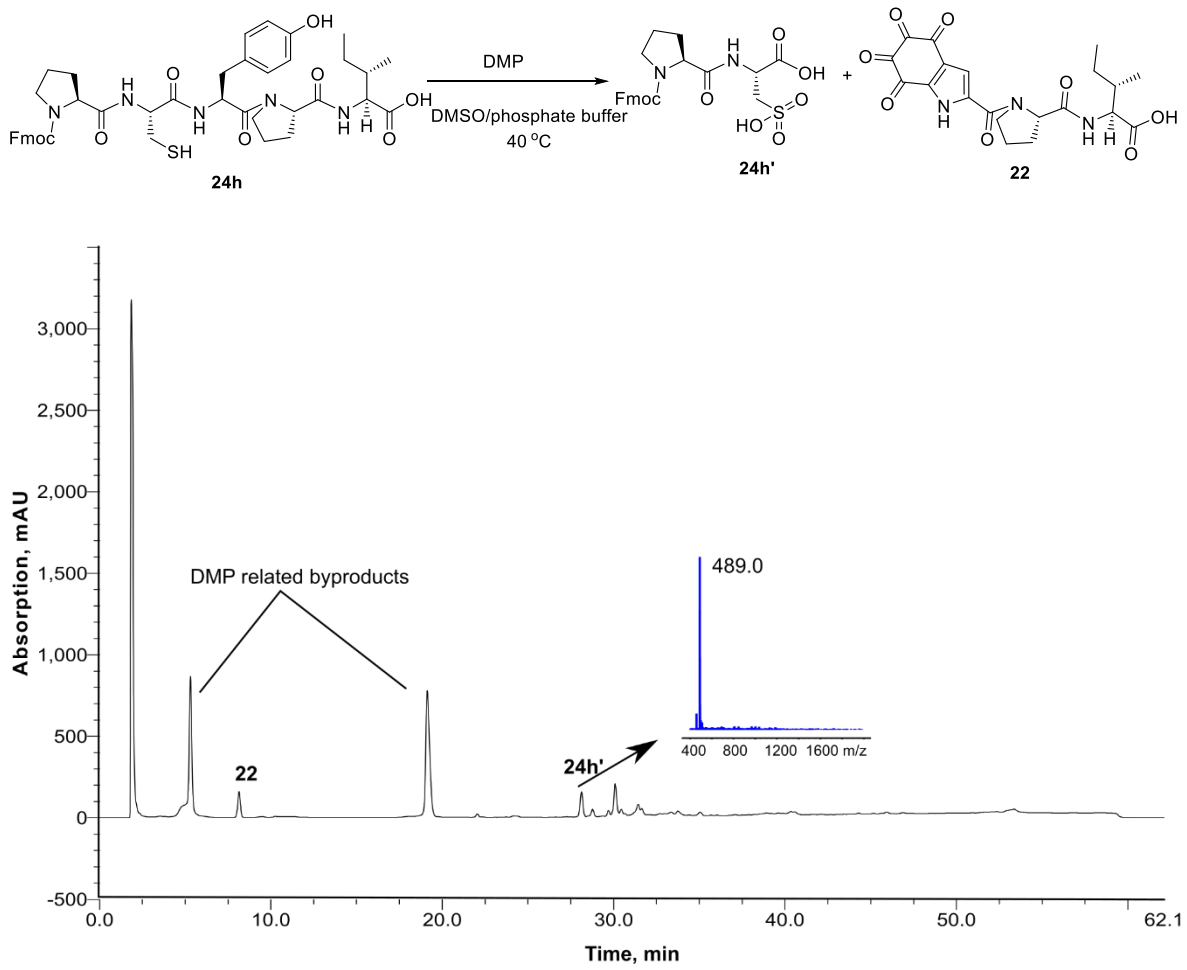

Figure S66. HPLC-MS profile of the DMP-mediated cleavage of **24h.** Waters Xterra MS C18 column (125 Å 4.6 mm × 150 mm, 5 µm) with a linear gradient of 5% B-65% B over 60 min (*ca.* 1 % B•min^{-1}) at a flow rate of 1 mL•min^{-1} (A = 0.1% TFA in H_2O and B = 0.1 %TFA MeCN). The UV-Vis detector was set at the wavelength of 254 nm. MS characterization of **24h'**: MS (ESI+): $C_{23}H_{24}N_2O_8S$. $[M+H]^+$ calcd./found 489.1/489.0.

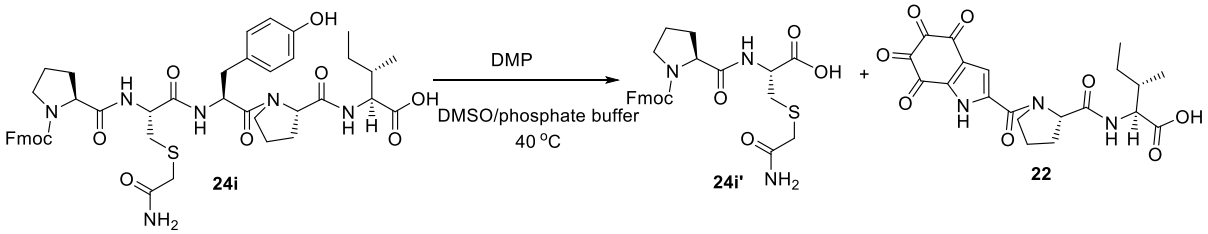

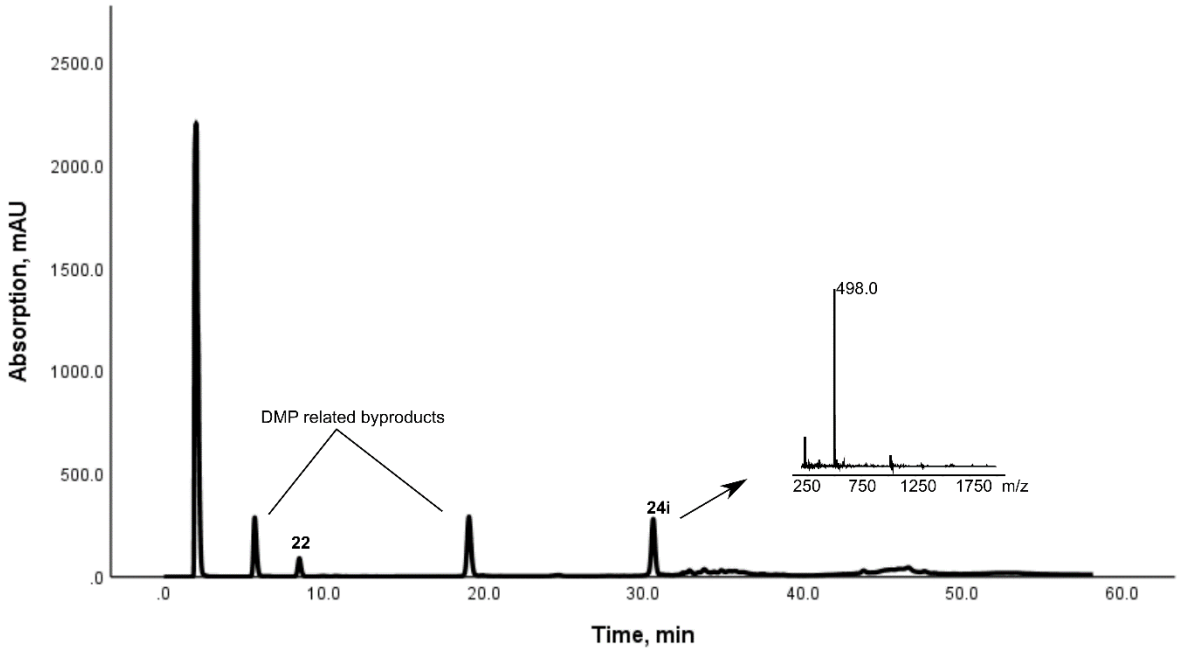

Figure S67. HPLC-MS profile of the DMP-mediated cleavage of **24i.** Waters Xterra MS C18 column (125 Å 4.6 mm × 150 mm, 5 µm) with a linear gradient of 5% B-65% B over 60 min (*ca.* 1 % B•min^{-1}) at a flow rate of 1 mL•min^{-1} (A = 0.1% TFA in H_2O and B = 0.1 %TFA MeCN). The UV-Vis detector was set at the wavelength of 254 nm. MS characterization of **24h'**: MS (ESI+): $C_{25}H_{27}N_3O_6S$. $[M+H]^+$ calcd./found 498.2/498.0.

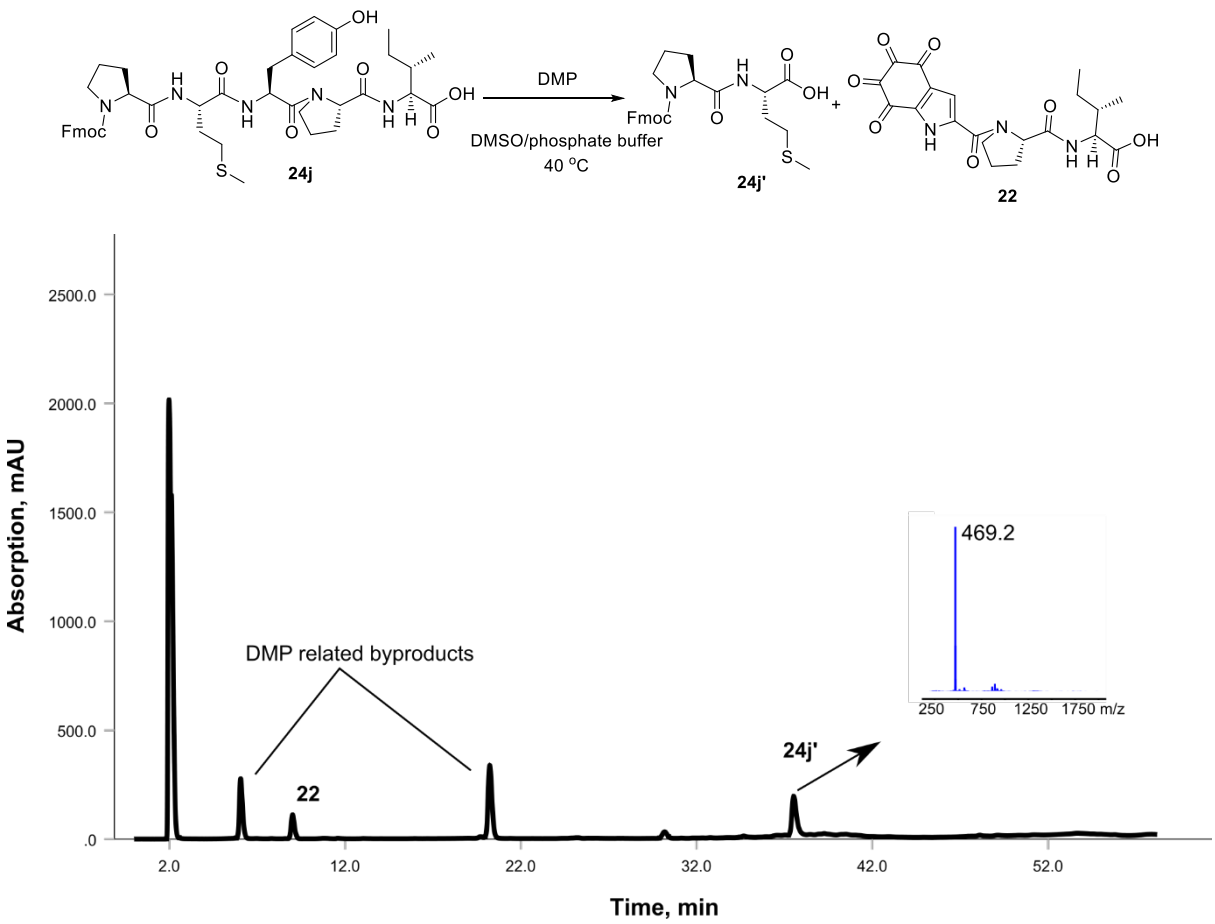

Figure S68. HPLC-MS profile of the DMP-mediated cleavage of **24j.** Waters Xterra MS C18 column (125 Å 4.6 mm × 150 mm, 5 µm) with a linear gradient of 5% B-65% B over 60 min (*ca.* 1 % B•min^{-1}) at a flow rate of 1 mL•min^{-1} (A = 0.1% TFA in H_2O and B = 0.1 %TFA MeCN). The UV-Vis detector was set at the wavelength of 254 nm. MS characterization of **24j'**: MS (ESI+): $C_{25}H_{28}N_2O_5S$. $[M+H]^+$ calcd./found 469.2/469.2.

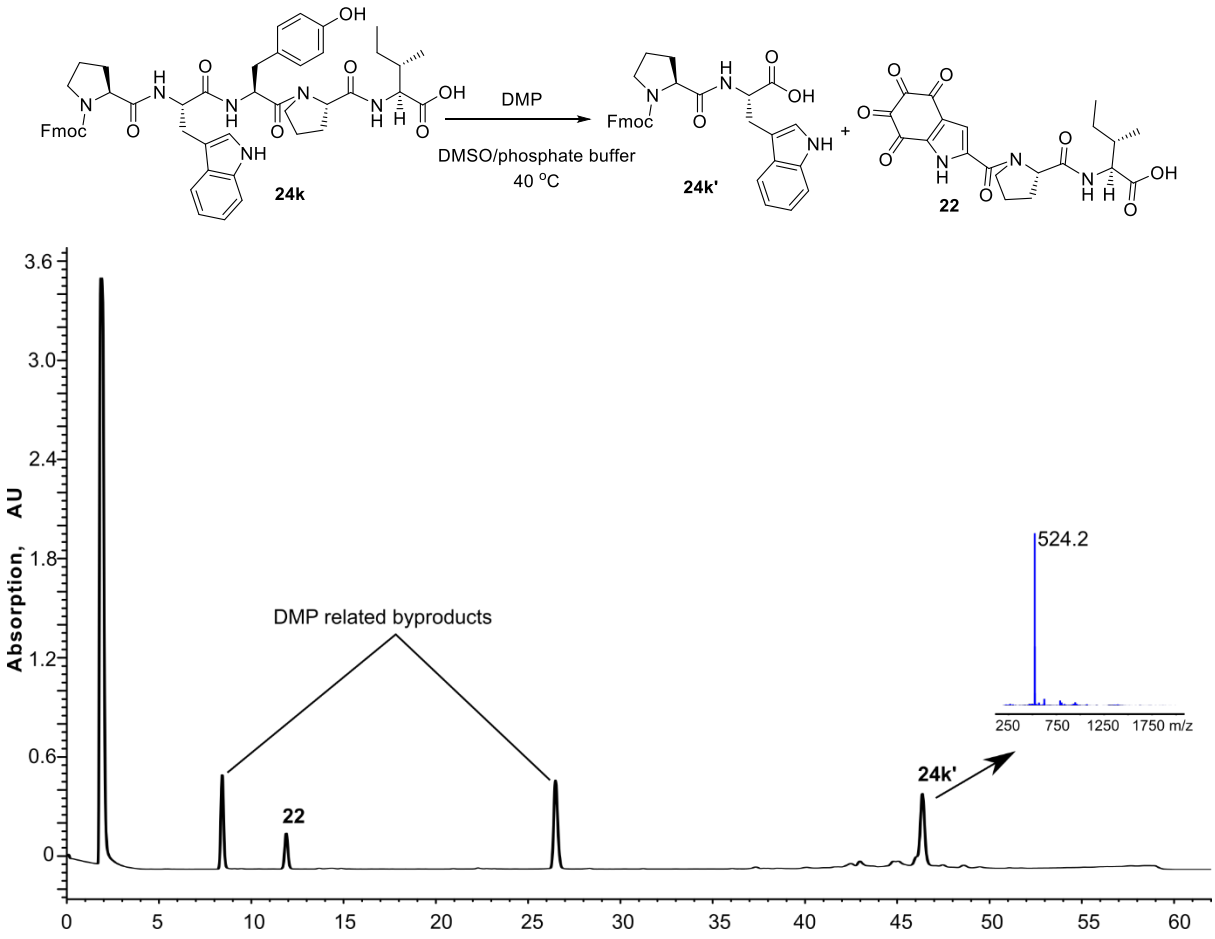

Figure S69. HPLC-MS profile of the DMP-mediated cleavage of **24k.** Waters Xterra MS C18 column (125 Å 4.6 mm × 150 mm, 5 µm) with a linear gradient of 5% B-65% B over 60 min (*ca.* 1 % B•min^{-1}) at a flow rate of 1 mL•min^{-1} (A = 0.1% TFA in H_2O and B = 0.1 %TFA MeCN). The UV-Vis detector was set at the wavelength of 254 nm. MS characterization of **24k'**: MS (ESI+): $C_{31}H_{29}N_3O_5$. $[M+H]^+$ calcd./found 524.2/524.2.

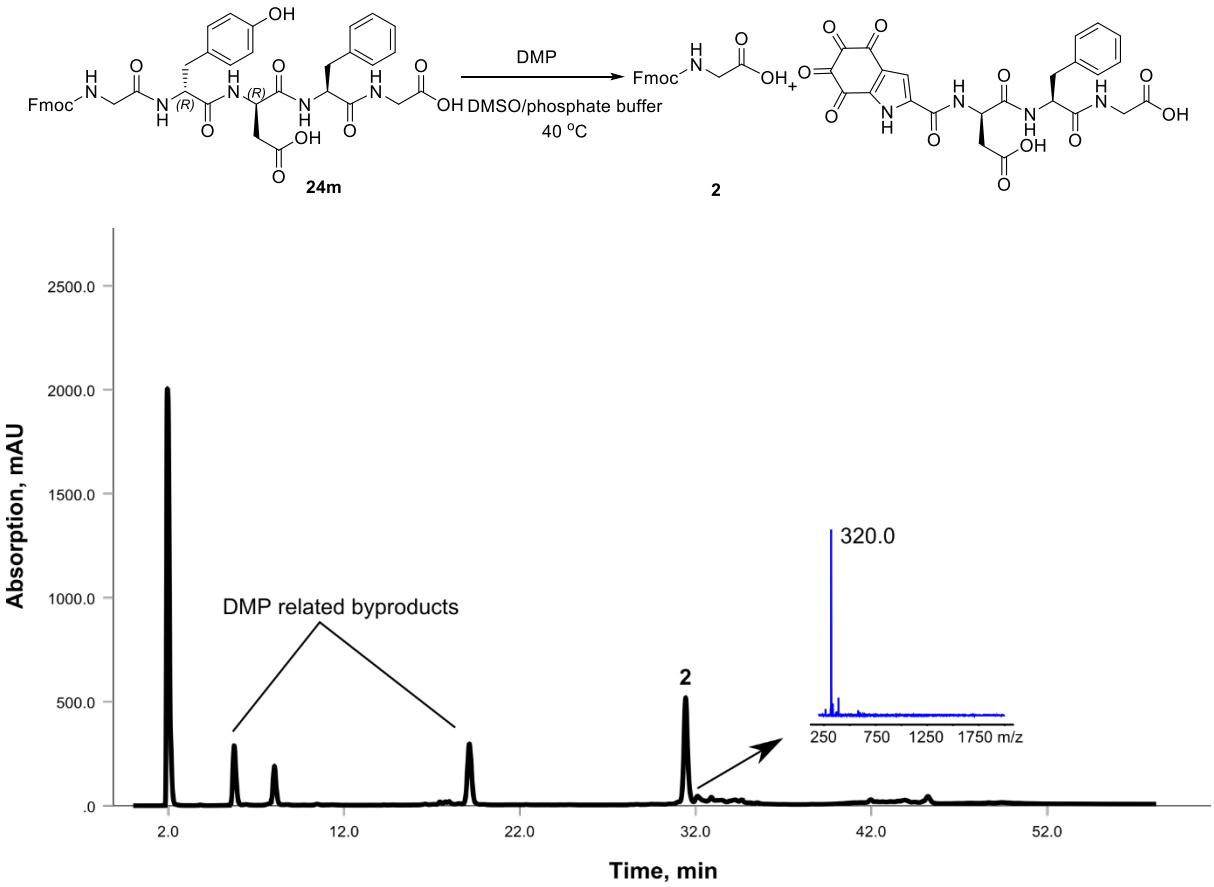

Figure S70. HPLC-MS profile of the DMP-mediated cleavage of **24m.** Waters Xterra MS C18 column (125 Å 4.6 mm × 150 mm, 5 µm) with a linear gradient of 5% B-65% B over 60 min (*ca.* 1 % B•min^{-1}) at a flow rate of 1 mL•min^{-1} (A = 0.1% TFA in H_2O and B = 0.1 %TFA MeCN). The UV-Vis detector was set at the wavelength of 254 nm. MS characterization of **24m'**: MS (ESI+): $C_{17}H_{15}NO_4Na$. $[M+Na]^+$ calcd./found 320.1/320.0.

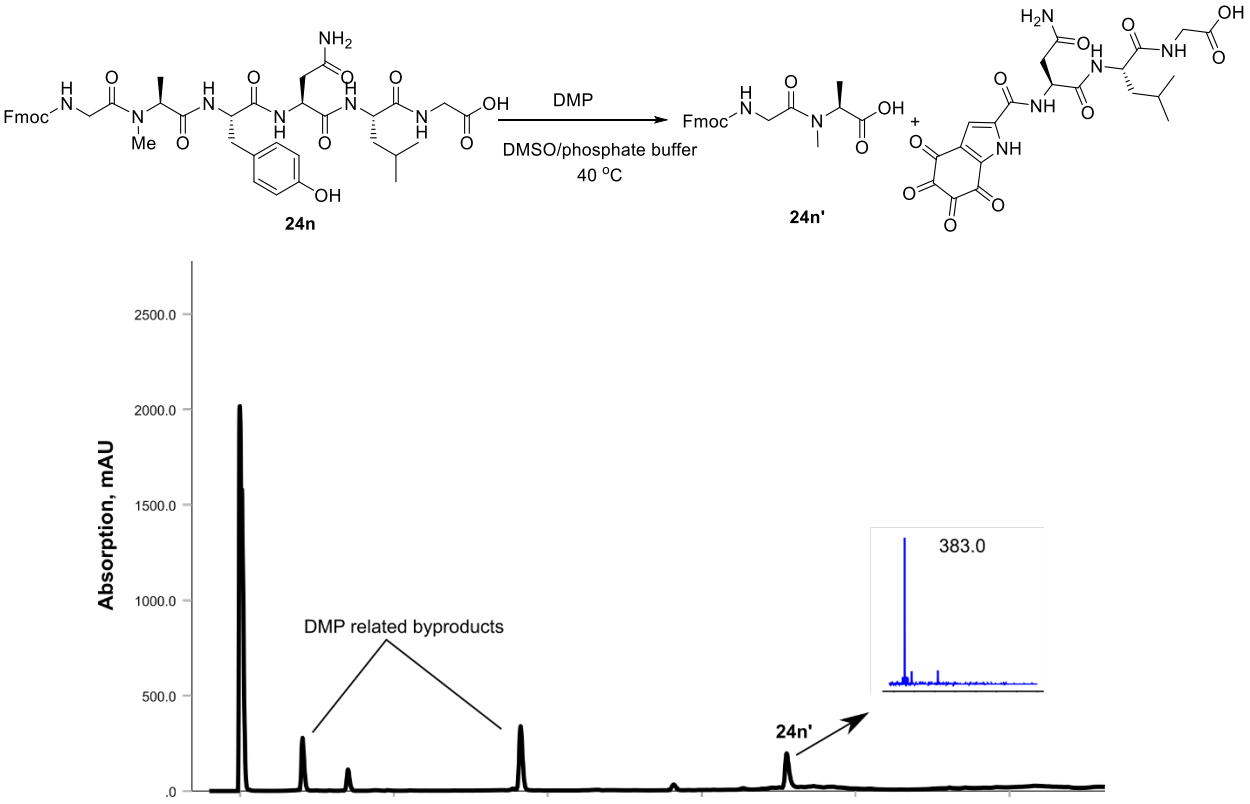

Figure S71. HPLC-MS profile of the DMP-mediated cleavage of **24n.** Waters Xterra MS C18 column (125 Å 4.6 mm × 150 mm, 5 µm) with a linear gradient of 5% B-65% B over 60 min (*ca.* 1 % B•min^{-1}) at a flow rate of 1 mL•min^{-1} (A = 0.1% TFA in H_2O and B = 0.1 %TFA MeCN). The UV-Vis detector was set at the wavelength of 254 nm. MS characterization of **24n'**: MS (ESI+): $C_{21}H_{22}N_2O_5$. $[M+H]^+$ calcd./found 383.1/383.0.

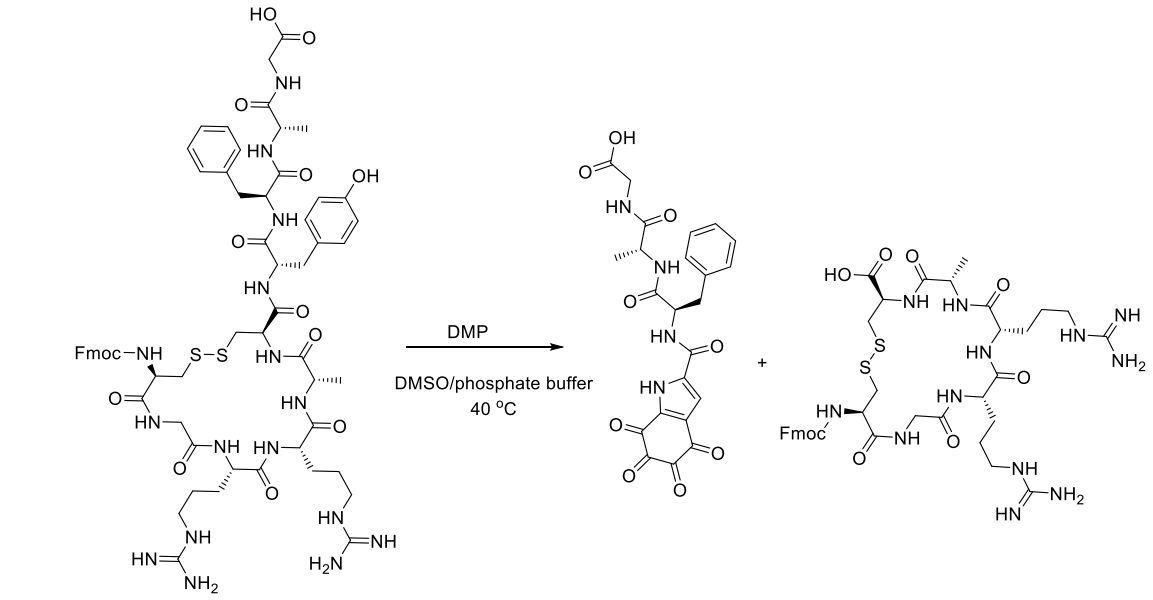

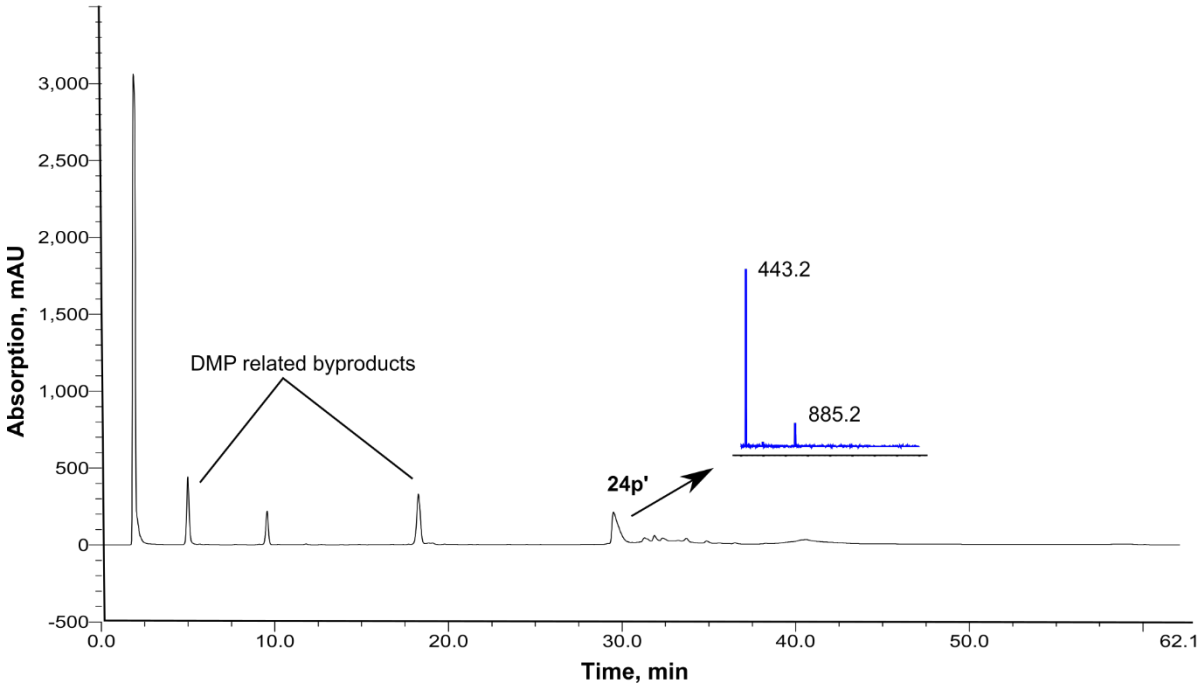

Figure S72. HPLC-MS profile of the DMP-mediated cleavage of **24p.** Waters Xterra MS C18 column (125 Å 4.6 mm × 150 mm, 5 µm) with a linear gradient of 5% B-65% B over 60 min (*ca.* 1 % B•min^{-1}) at a flow rate of 1 mL•min^{-1} (A = 0.1% TFA in H_2O and B = 0.1 %TFA MeCN). The UV-Vis detector was set at the wavelength of 254 nm. MS characterization of **24p'**: MS (ESI+): $C_{38}H_{52}N_{12}O_9S_2$. $[M+H]^+$ calcd./found 885.3/885.2, $[M+2H]^{2+}$ calcd./found 443.2/443.2

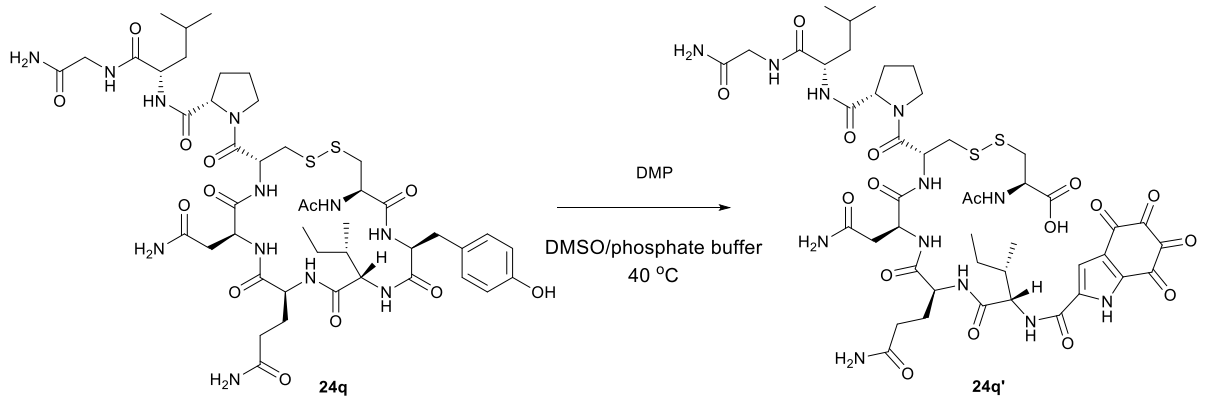

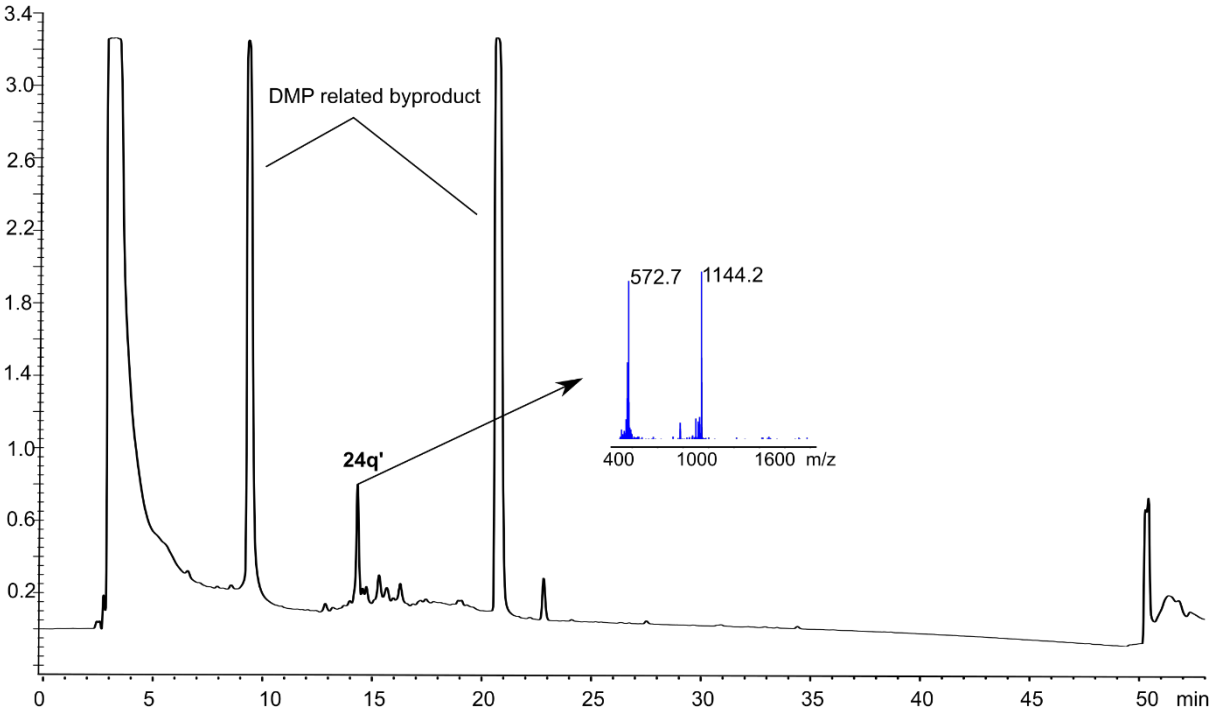

Figure S73. HPLC-MS profile of the DMP-mediated cleavage of **24q.** Phenomenex Luna, C_{18} column (100 Å, 4.6 x 250 mm, 5 µm) with using a linear gradient of 5% B-95% B over 45 min (ca. 2 % B•min^{-1}) at a flow rate of 1 mL•min^{-1} (A = 0.1% TFA in H_2O and B = 0.1 %TFA MeCN). The UV-Vis detector was set at the wavelength of 210 nm. MS characterization of **24q'**: MS (ESI+): $C_{45}H_{62}N_{12}O_{17}S_2$. $[M+2H_2O+H]^+$ calcd./found 1144.2/1144.2, $[M+2H_2O+2H]^{2+}$ calcd./found 572.6/572.7.

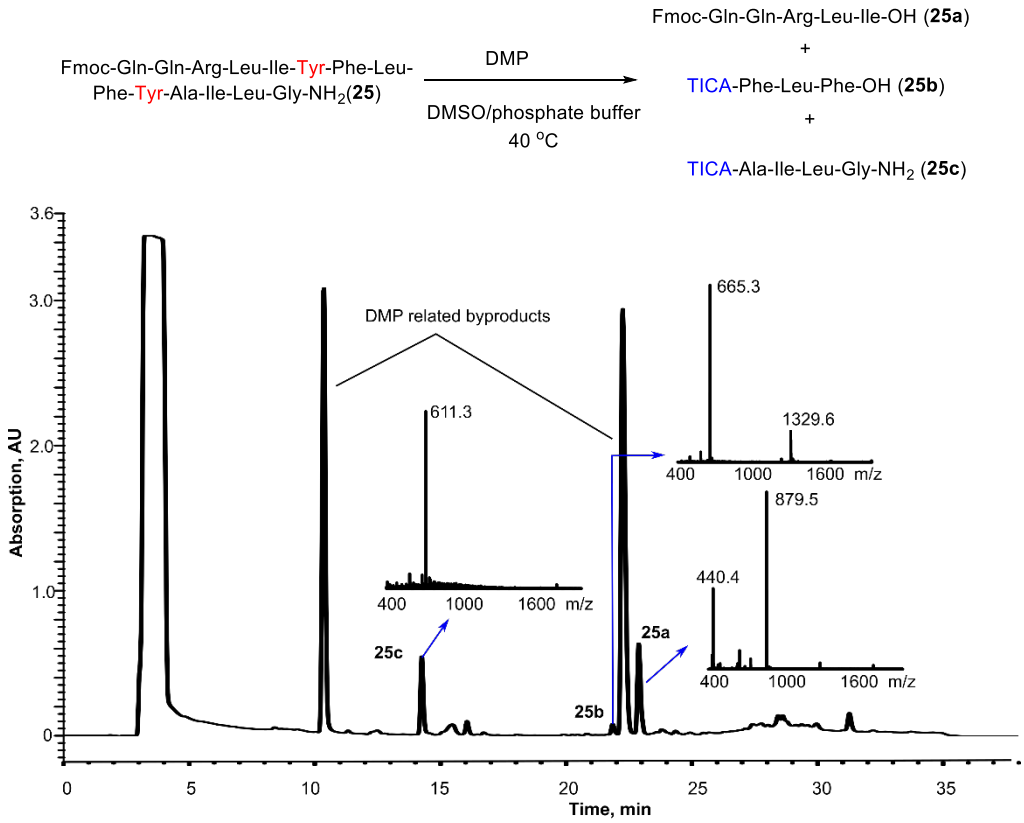

Figure S74. HPLC-MS profile of the DMP-mediated cleavage of **25.** Phenomenex Luna, C_{18} column (100 Å, 4.6 x 250 mm, 5 µm) with using a linear gradient of 5% B-65% B over 30 min (ca. 2 % B•min^{-1}) at a flow rate of 1 mL•min^{-1} (A = 0.1% TFA in H_2O and B = 0.1 %TFA MeCN). The UV-Vis detector was set at the wavelength of 254 nm. MS characterization of **25a**: MS (ESI+): $C_{43}H_{62}N_{10}O_{10}$. $[M+H]^+$ calcd./found 879.5/879.5; MS characterization of **25b**: MS (ESI+): $C_{33}H_{32}N_4O_9$. $[M+2H_2O+H]^+$ calcd./found 665.2/665.3; MS characterization of **25c**: MS (ESI+): $C_{26}H_{34}N_6O_9$. $[M+2H_2O+H]^+$ calcd./found 611.2/611.3.

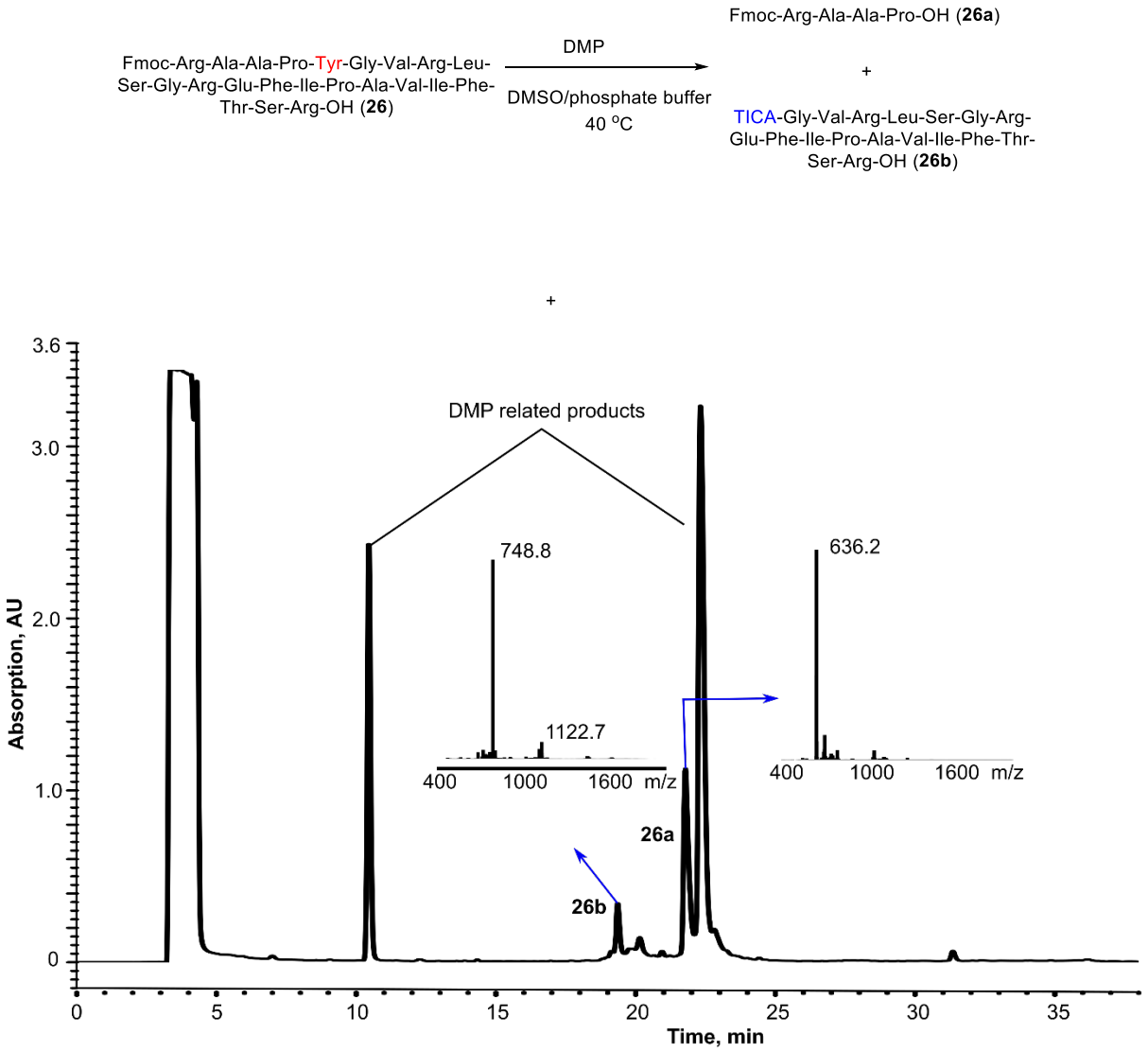

Figure S75. HPLC-MS profile of the DMP-mediated cleavage of **26.** Phenomenex Luna, C_{18} column (100 Å, 4.6 x 250 mm, 5 µm) with using a linear gradient of 5% B-65% B over 30 min (ca. 2 % B•min^{-1}) at a flow rate of 1 mL•min^{-1} (A = 0.1% TFA in H_2O and B = 0.1 %TFA MeCN). The UV-Vis detector was set at the wavelength of 254 nm. MS characterization of **26a**: MS (ESI+): $C_{32}H_{41}N_7O_7$. $[M+H]^+$ calcd./found 636.3/636.2; MS characterization of **26b**: MS (ESI+): $C_{100}H_{150}N_{28}O_{29}$. $[M+2H_2O+2H]^{2+}$ calcd./found 1123.0/1122.7, $[M+2H_2O+3H]^{3+}$ calcd./found 749.0/748.8.

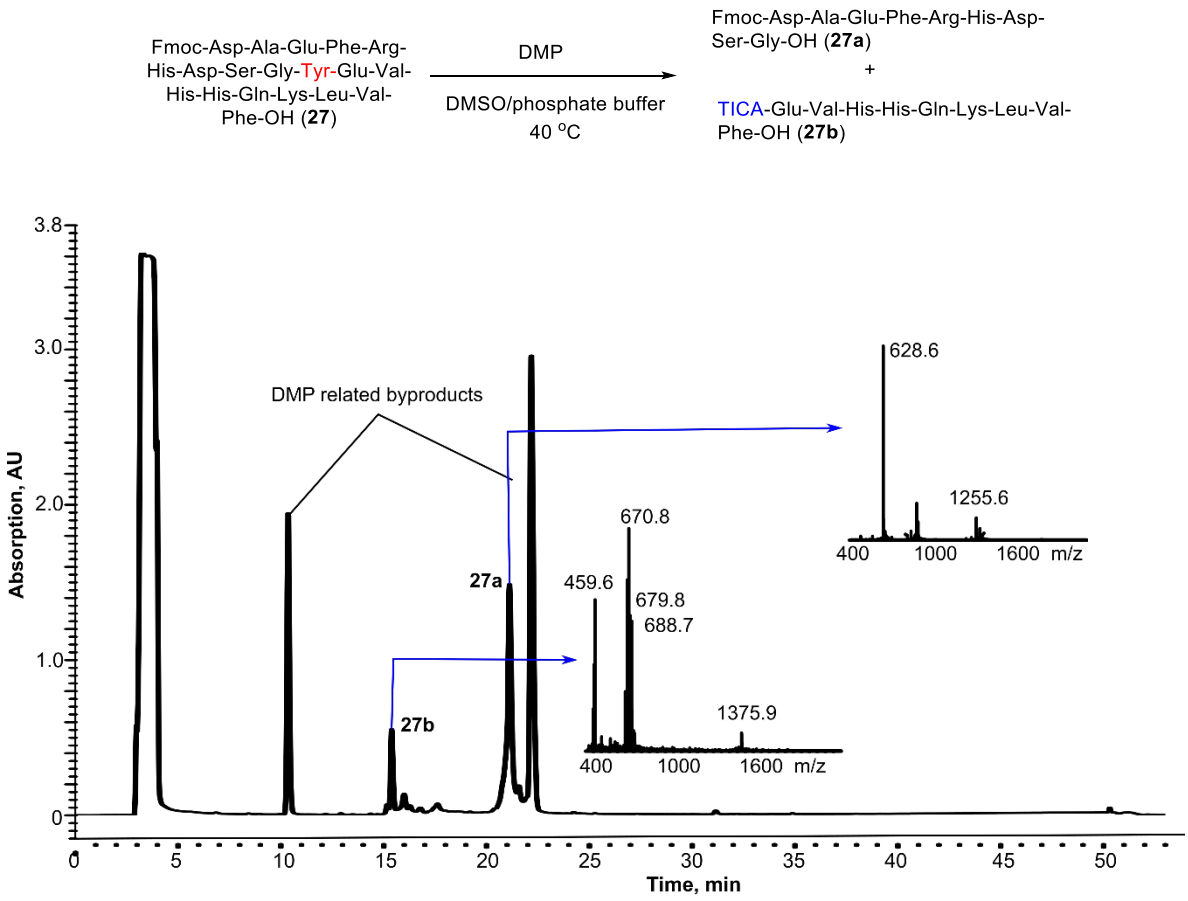

Figure S76. HPLC-MS profile of the DMP-mediated cleavage of **27.** Phenomenex Luna, C_{18} column (100 Å, 4.6 x 250 mm, 5 µm) with a linear gradient of 5% B-95% B over 45 min (*ca.* 2 % B•min^{-1}) at a flow rate of 1 mL•min^{-1} (A = 0.1% TFA in H_2O and B = 0.1 %TFA MeCN). The UV-Vis detector was set at the wavelength of 254 nm.MS characterization of **27a**: MS (ESI+): $C_{57}H_{70}N_{14}O_{19}$. $[M+H]^+$ calcd./found 1255.5/1255.6, $[M+2H]^{2+}$ calcd./found 628.3/628.6; MS characterization of **27b**: MS (ESI+): $C_{62}H_{82}N_{16}O_{18}$ $[M+2H_2O+H]^+$ calcd./found 1375.6/1375.9, $[M+2H_2O+2H]^{2+}$ calcd./found 688.3/688.7. $[M+2H_2O+3H]^{3+}$ calcd./found 459.2/459.6.

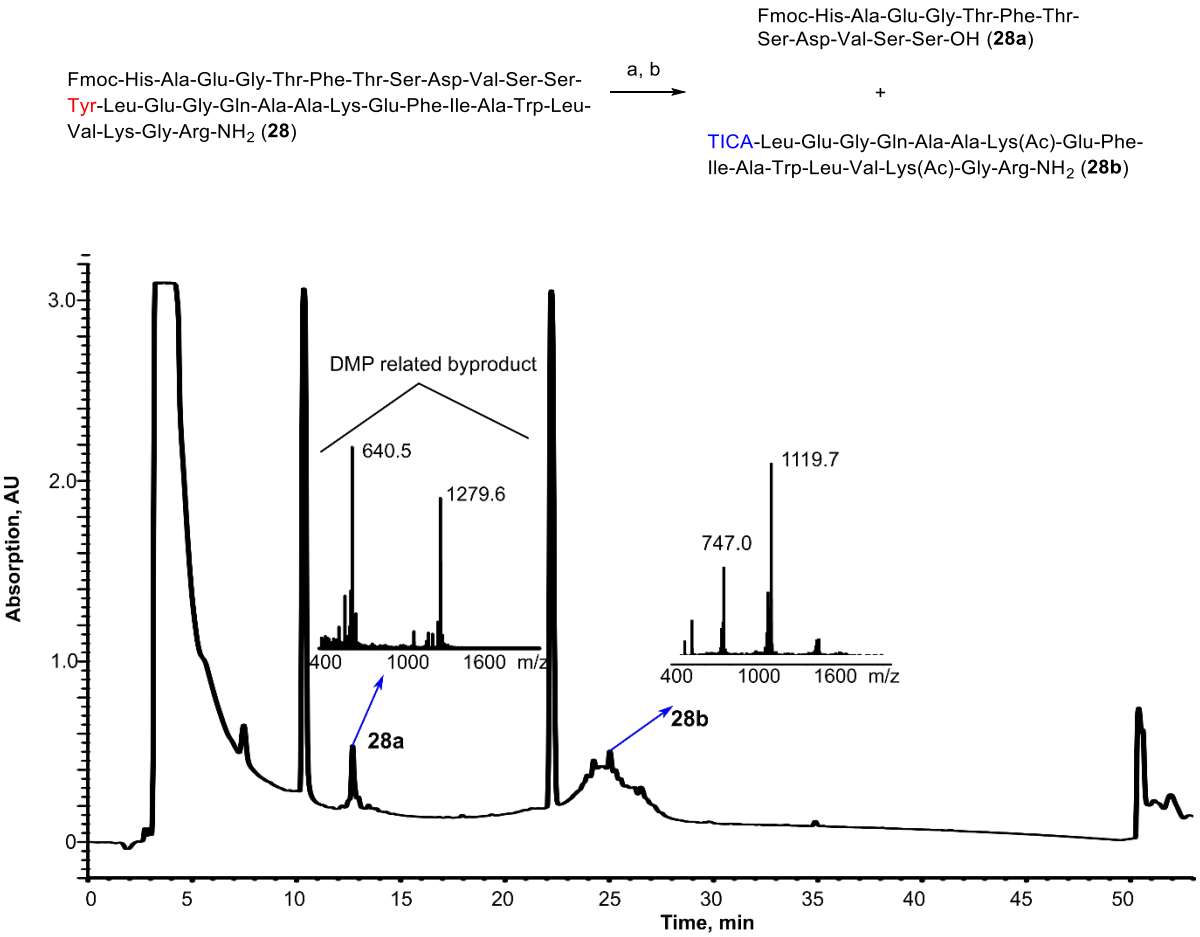

Figure S77. HPLC-MS profile of the DMP-mediated cleavage of **28.** Waters Xterra MS C18 column (125 Å 4.6 mm × 150 mm, 5 µm) with a linear gradient of 5% B-95% B over 45 min (*ca.* 2 % B•min^{-1}) at a flow rate of 1 mL•min^{-1} (A = 0.1% TFA in H_2O and B = 0.1 %TFA MeCN). The UV-Vis detector was set at the wavelength of 254 nm.MS characterization of **28a**: MS (ESI+): $C_{53}H_{78}N_{14}O_{23}$. $[M+H]^+$ calcd./found 1279.5/1279.6; MS characterization of **28b**: MS (ESI+): $C_{102}H_{147}N_{25}O_{30}$ $[M+2H_2O+2H]^{2+}$ calcd./found 1119.5/1119.7, $[M+2H_2O+3H]^{3+}$ calcd./found 746.7/747.0. Reaction conditions: (a) i) 50 equiv. of acetic anhydride, 30 equiv. of pyridine, DMSO, RT, 2 h; ii) 2 M hydroxylamine buffer (pH = 6), 4 h, RT; (b) 30 equiv. of DMP, 40 °C, DMSO/phosphate buffer at pH 7 (2:1, *v*/*v*), 3 h.

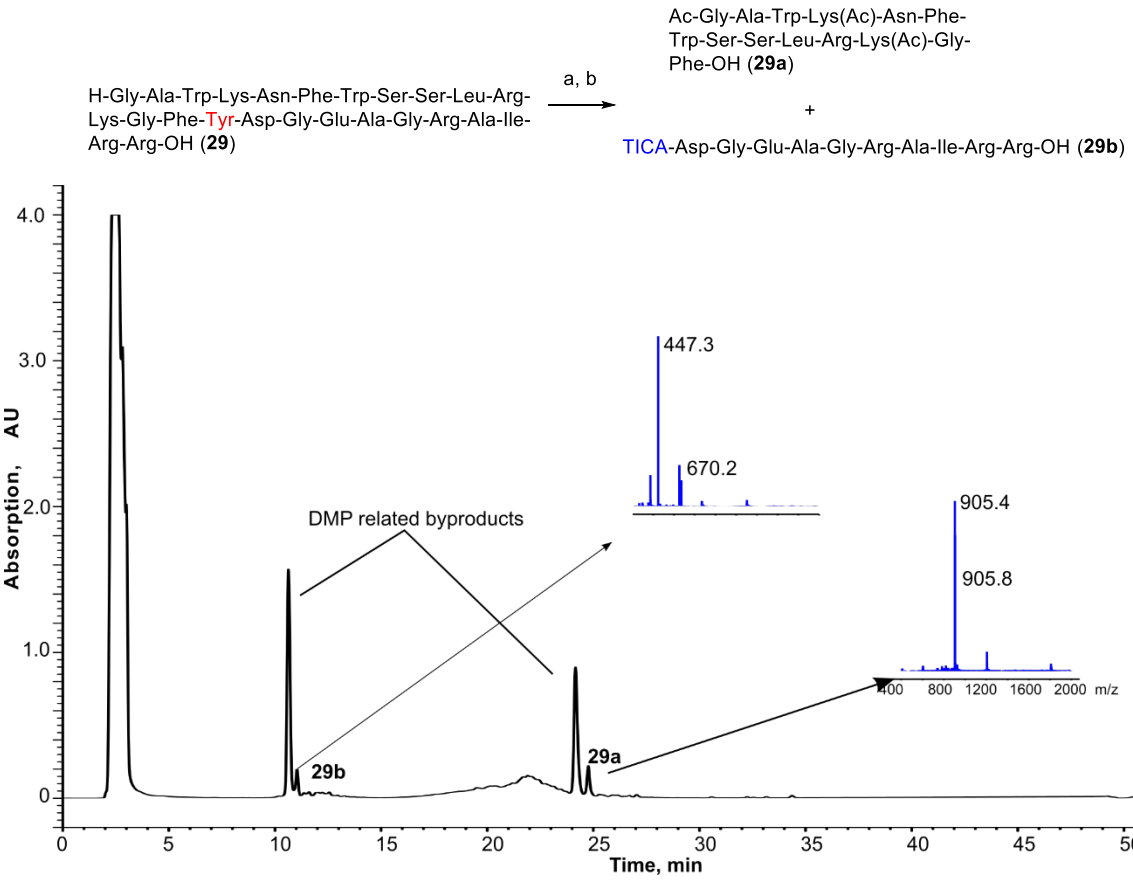

Figure S78. HPLC-MS profile of the DMP-mediated cleavage of **29.** Waters Xterra MS C18 column (125 Å 4.6 mm × 150 mm, 5 µm) with a linear gradient of 5% B-95% B over 45 min (*ca.* 2 % B•min^{-1}) at a flow rate of 1 mL•min^{-1} (A = 0.1% TFA in H_2O and B = 0.1 %TFA MeCN). The UV-Vis detector was set at the wavelength of 254 nm.MS characterization of **29a**: MS (ESI+): $C_{87}H_{120}N_{22}O_{21}$ $[M+2H]^{2+}$ calcd./found 905.4/905.4. MS characterization of **29b**: MS (ESI+): $C_{52}H_{78}N_{20}O_{20}$ $[M+2H_2O+2H]^{2+}$ calcd./found 670.3/670.2, $[M+2H_2O+3H]^{3+}$ calcd./found 447.2/447.3. Reaction conditions: (a) i) 50 equiv. of acetic anhydride, 30 equiv. of pyridine, DMSO, RT, 2 h; ii) 2 M hydroxylamine buffer (pH = 6), 4 h, RT; (b) 30 equiv. of DMP, 40 °C, DMSO/phosphate buffer at pH 7 (2:1, *v*/*v*), 3 h.

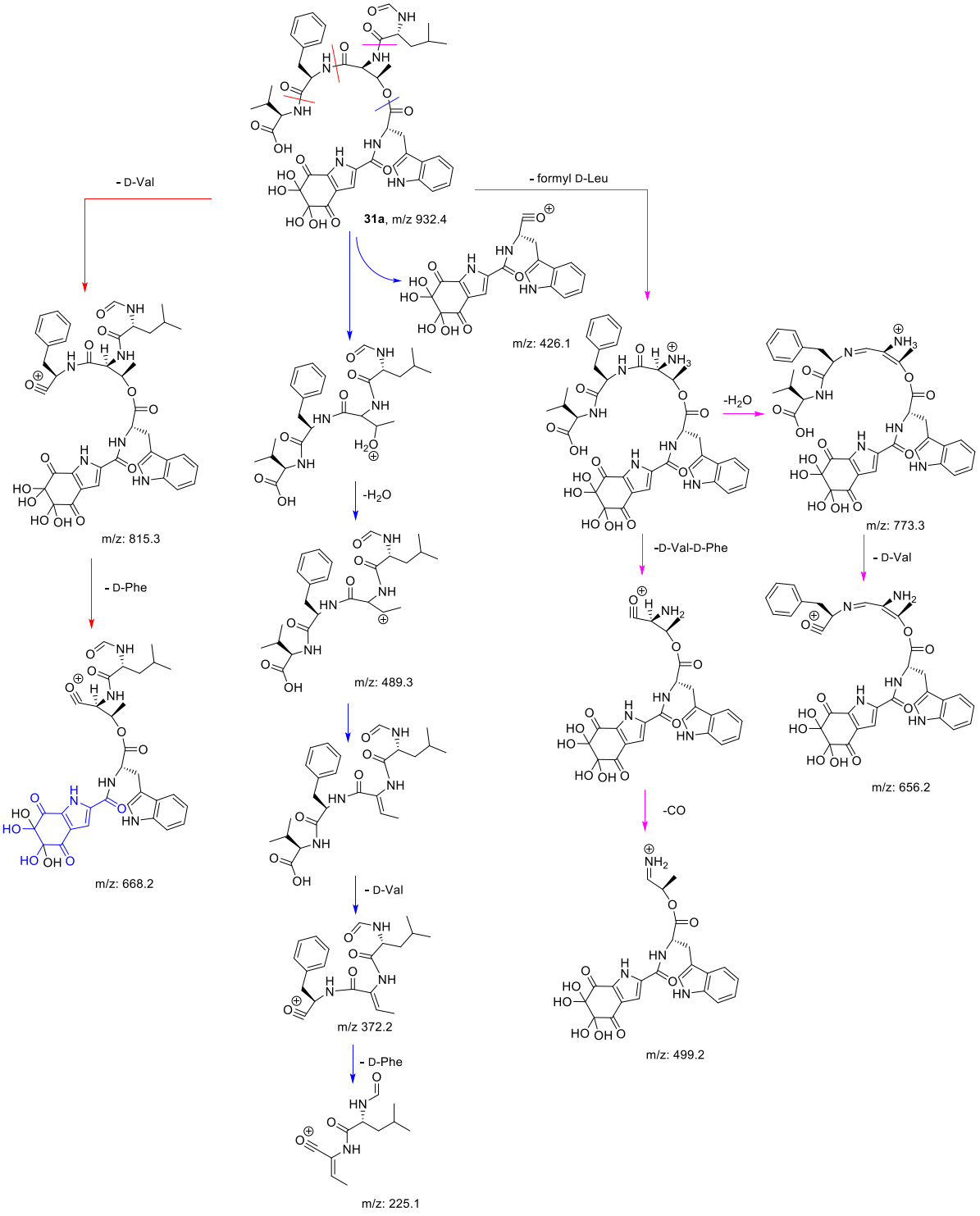

Figure S79. The MSMS fragmentation pattern of the linearized szentiamide (**31a**)

5. Structure Determination of the *C*-Terminal Fragment of a Tyr-selective Peptide Cleavage using DMP

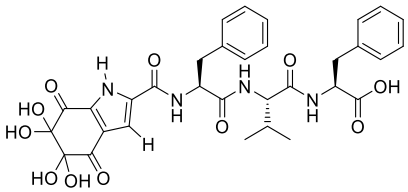

TICA-Phe-Val-Phe-OH (**3**): Linear peptide **1** (20.0 mg, 23 µmol) was treated with DMP (99 mg, 230 µmol) in DMSO (5 mL) at 40 ºC for two days. The resulting reaction mixture was diluted with water (45 mL), followed by semi-preparative RP-HPLC purification to afford **3** as a white powder (5.0 mg, 34%).

Alternatively, H-Tyr-Phe-Val-Phe-OH (**S1**) (17 mg, 30 µmol) was treated with DMP (125 mg, 300 µmol) in DMSO (5 mL) at 40 ºC for 0.5 h. The resulting reaction mixture was diluted with water (45 mL), followed by semi-preparative RP-HPLC purification to afford **3** as a white powder (9.6 mg, 53%). Anal. RP-HPLC: t_R = 18.8 min, purity: >95% (HPLC analysis at 210 nm).

^{1}H NMR (500 MHz, DMSO-d_6) of dihydrate **3** δ 13.14 (s, 1H), 8.63 (d, *J* = 8.5 Hz, 1H), 8.27 (d, *J* = 7.8 Hz, 1H), 8.02 (d, *J* = 9.1 Hz, 1H), 7.32 (d, *J* = 7.2 Hz, 2H), 7.23 (m, 6H), 7.20 (d, *J* = 1.2 Hz, 1H), 7.12 – 7.19 (m, 2H), 6.50 (s, 2H), 6.40 (s, 2H), 4.78 (m, 1H), 4.46 (m, 1H), 4.23 (dd, *J* = 9.0, 6.9 Hz, 1H), 2.99 – 3.10 (m, 2H), 2.82 – 2.93 (m, 2H), 1.96 (td, *J* = 13.5, 6.7 Hz, 1H), 0.83 (dd, *J* = 9.0, 6.7 Hz, 6H). ^{13}C NMR (125 MHz, DMSO-d_6) of of dihydrate **3a** δ 190.1, 185.6, 172.8, 170.9, 170.7, 158.6, 138.1, 137.5, 133.9, 132.6, 129.1, 129.1, 129.0, 129.0, 128.1, 128.1, 128.0, 128.0, 126.6, 126.4, 126.2, 109.3, 96.4, 96.2, 57.4, 54.1, 53.3, 37.2, 36.6, 30.9, 19.1, 18.1. Peptide decomposition took place on a small scale during the NMR experiment probably due to the instability of **3** when exposed to atmospheric oxygen[5]. MS (ESI+): $C_{32}H_{35}N_4O_{11}$ $[M+H]^+$ calcd./found 651.2302/651.2470.

^{1}H NMR (500 MHz, DMSO-d_6) of **3a** δ 13.61 (d, *J* = 1.5 Hz, 0.8H), 8.80 (d, *J* = 8.5 Hz, 0.8H), 8.29 (d, *J* = 7.8 Hz, 0.9H), 8.10 (d, *J* = 9.1 Hz, 0.9H), 7.40 (d, *J* = 2.1 Hz, 0.8H), 7.35 (m, 2H), 7.26 (m, 6H), 7.12 – 7.19 (m, 2H), 4.83 (ddd, *J* = 12.0, 8.6, 3.7 Hz, 1H), 4.47 (ddd, *J* = 9.0, 7.9, 5.3 Hz, 1H), 4.25 (dd, *J* = 9.0, 6.9 Hz, 1H), 3.01 – 3.10 (m, 2H), 2.84 – 2.94 (m, 2H), 1.97 (m, 1H), 0.85 (dd, *J* = 8.3, 6.9 Hz, 8H). ^{13}C NMR (125 MHz, DMSO-d_6) of **3a** δ 174.9, 174.2, 173.9, 172.8, 170.8, 170.7, 170.2, 158.4, 138.0, 137.5, 136.0, 134.1, 129.3, 129.1, 129.1, 129.0, 129.0, 128.2, 128.2, 128.1, 128.1, 126.4, 126.3, 110.6, 57.3, 54.2, 53.3, 37.3, 36.6, 30.9, 19.2, 18.1. A mixture of **3a** and **3** was observed in the NMR spectrum with a ratio of 1:4 (**3**:**3a**) after overnight storage of the NMR sample at RT.

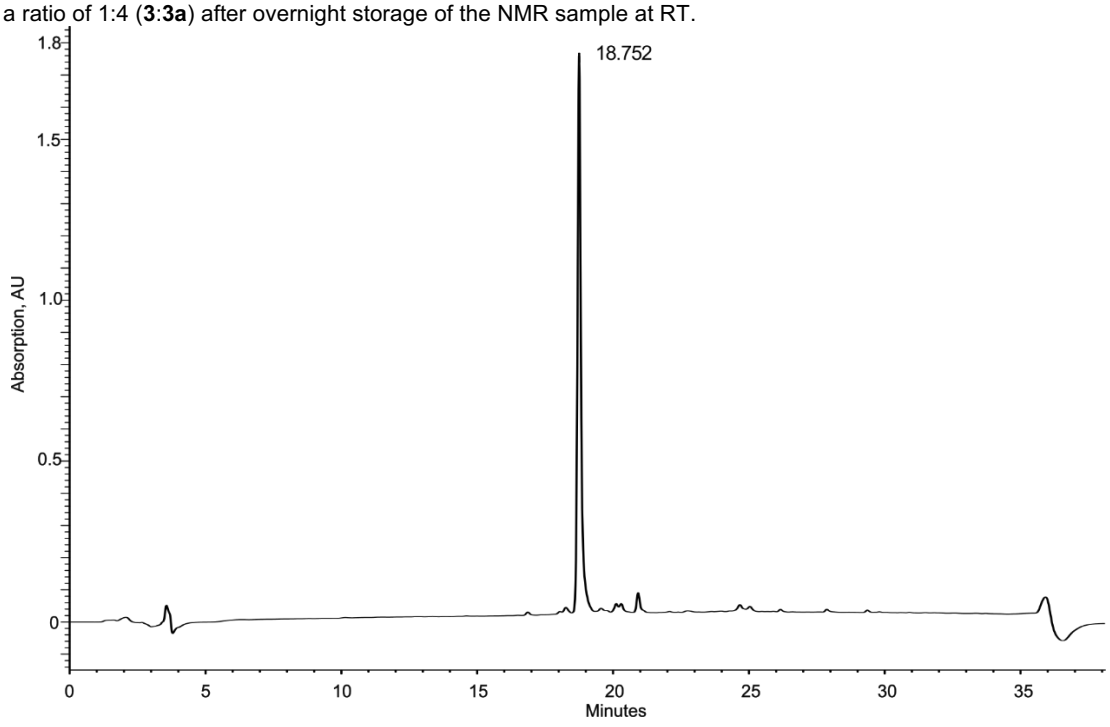

Figure S80. HPLC-MS profile of **3**, t_R = 18.8 min (purity >95% as judged by peak area of RP-HPLC at 210 nm); Waters XTerra MS C_{18} column (125 Å 4.6 mm × 150 mm, 5 µm) with using a linear gradient of 5% B-65% B over 30 min (ca. 2 % B•min^{-1}) at a flow rate of 1 mL•min^{-1} (A = 0.1% TFA in H_2O and B = 0.1 %TFA MeCN)

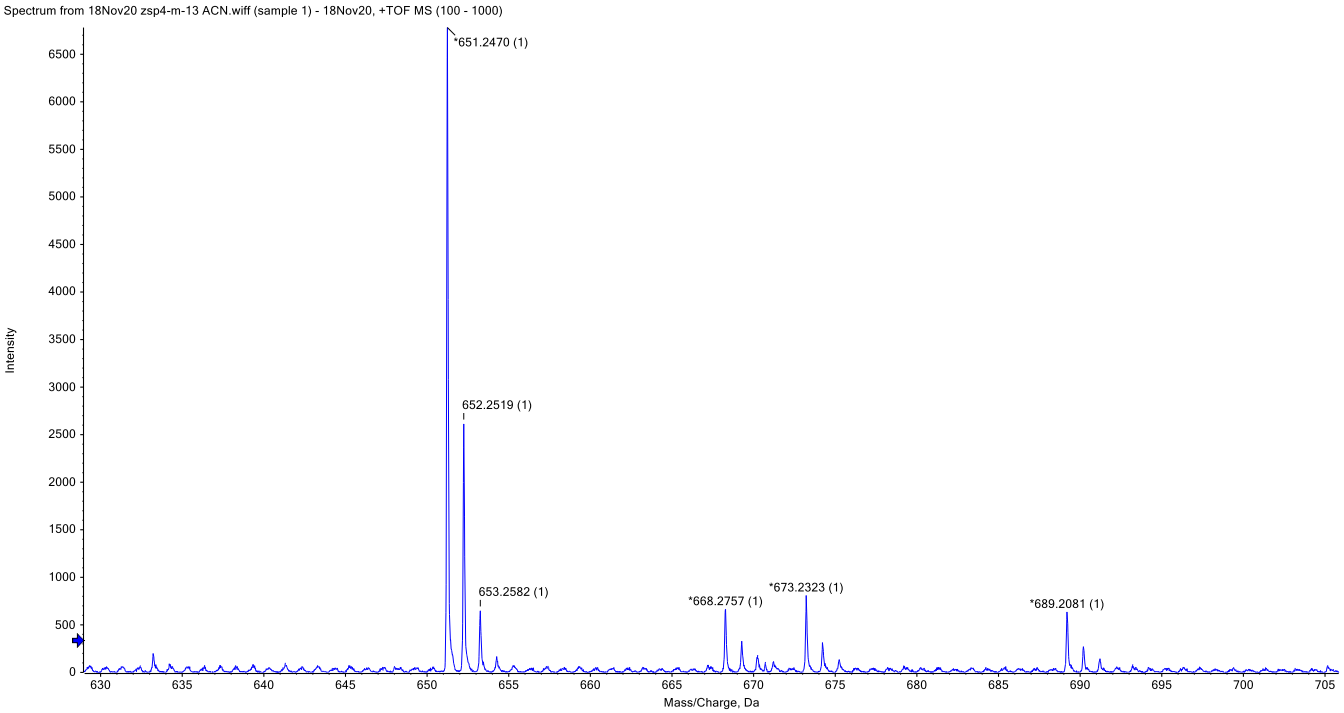

Figure S81. HRMS characterization of **3** in H_2O/MeCN (*v/v*, 1;1). MS (ESI+): $C_{32}H_{35}N_4O_{11}$ $[M+H]^+$ calcd./found 651.2302/651.2470.

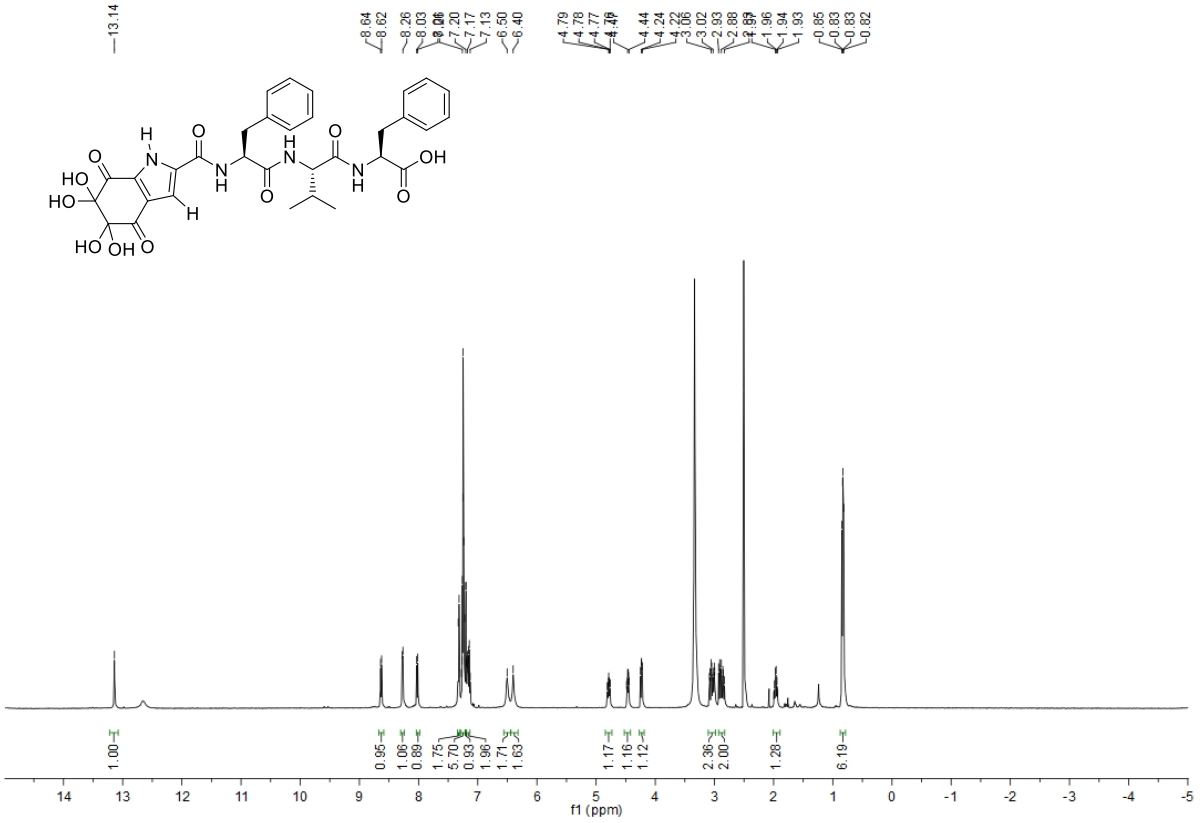

Figure S82. ^1H NMR (500 MHz, DMSO-d_6) of peptide dihydrate **3.**

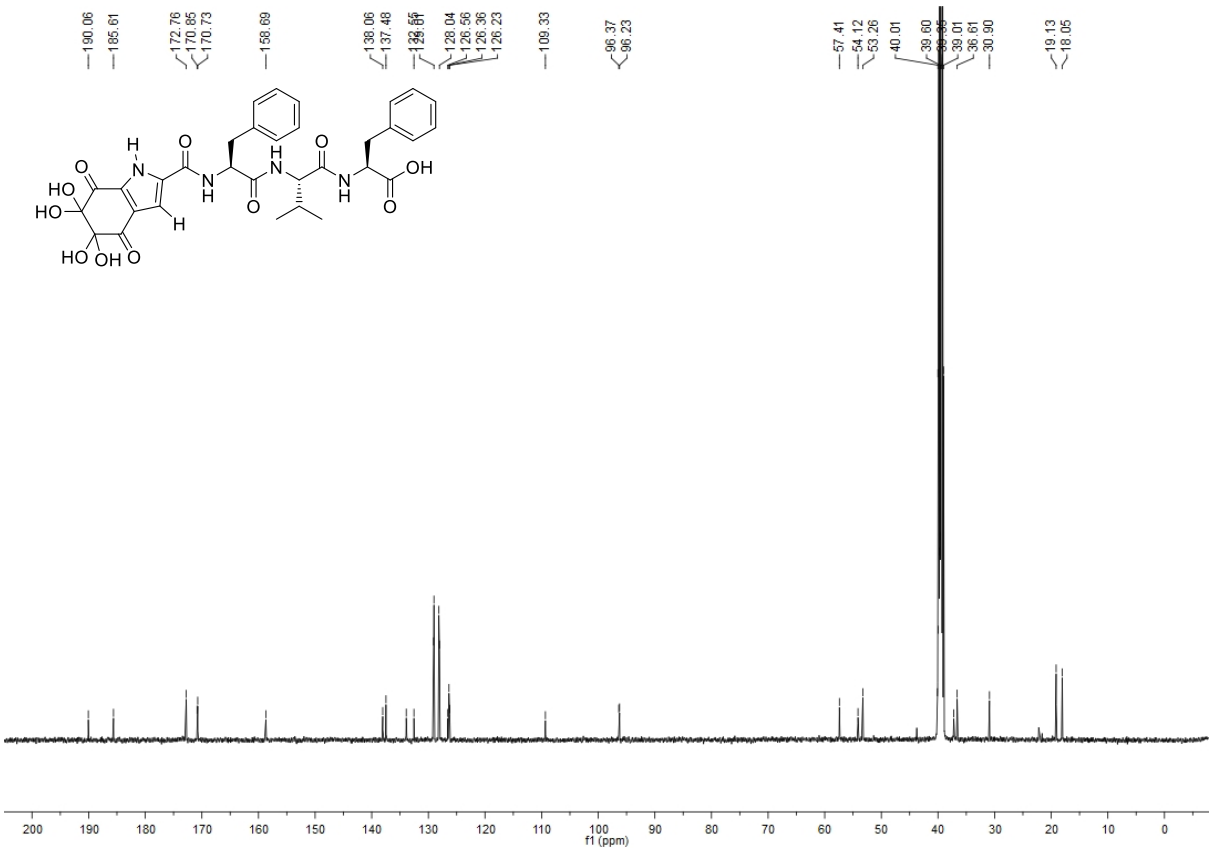

Figure S83. ^{13}C NMR (125 MHz, DMSO-d_6) of peptide dihydrate **3.**

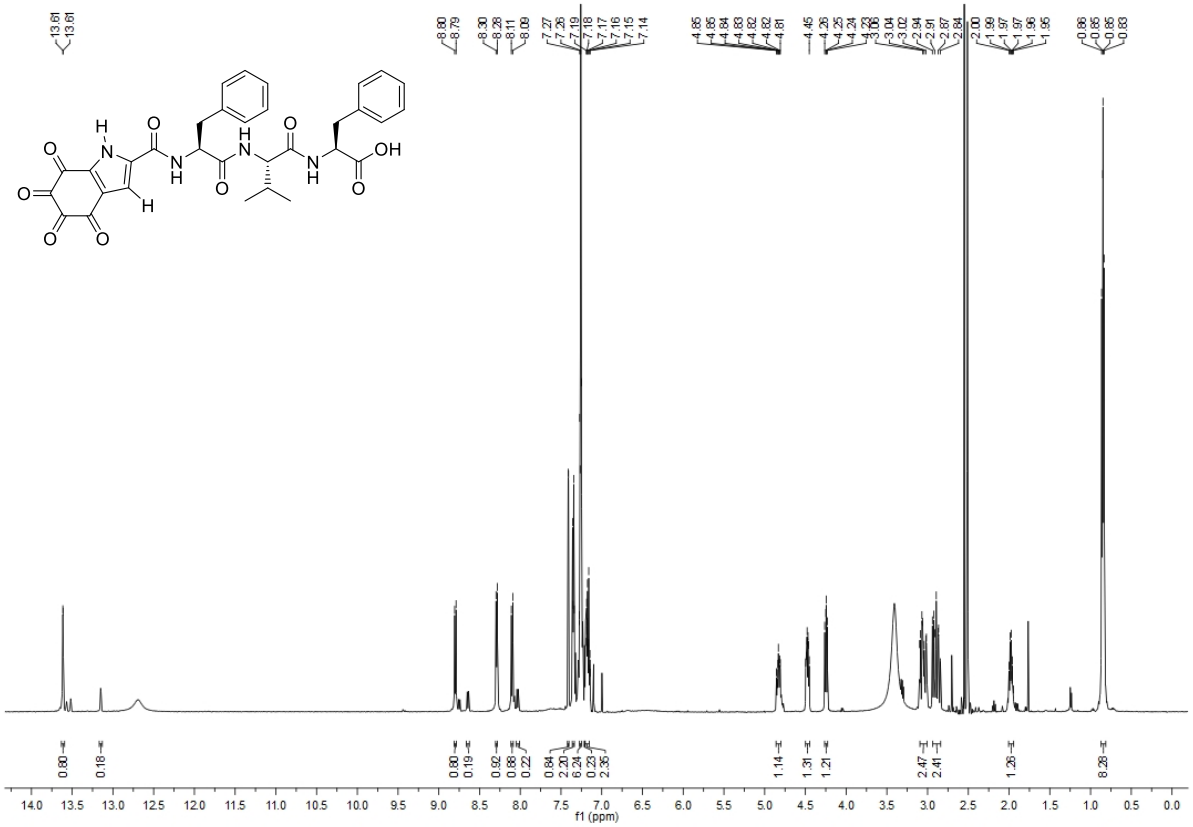

Figure S84. ^{1}H NMR (500 MHz, DMSO-d_6) of **3a.**

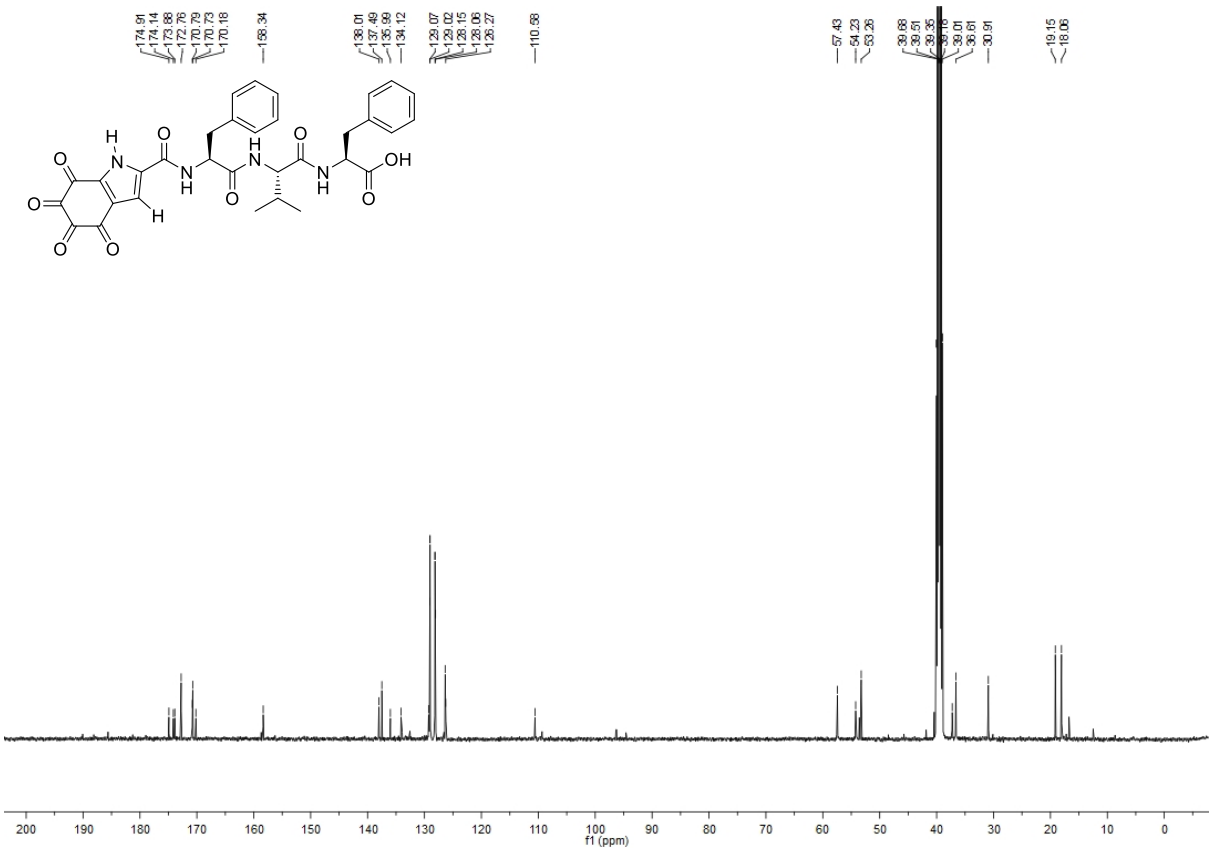

Figure S85. ^{13}C NMR (125 MHz, DMSO-d_6) of **3a.**

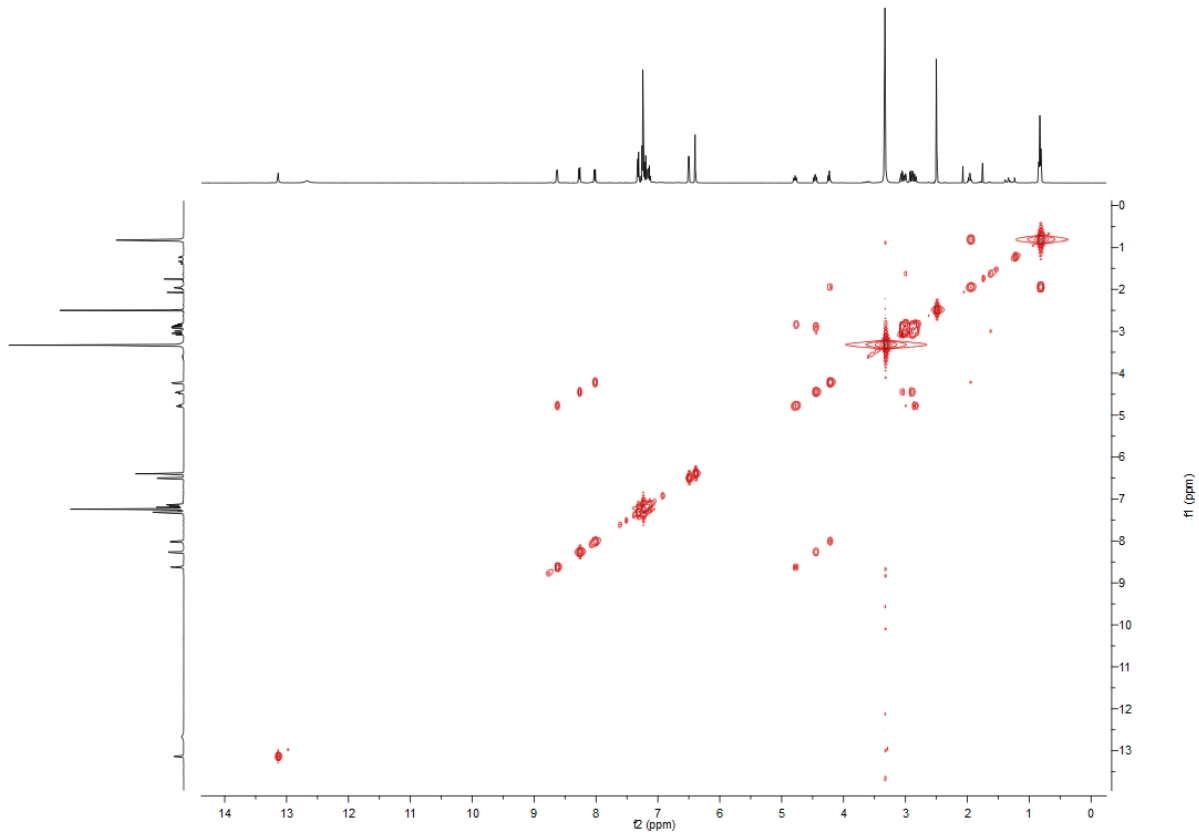

Figure S86. COSY spectrum (500MHz, DMSO-d_6) of **3**.

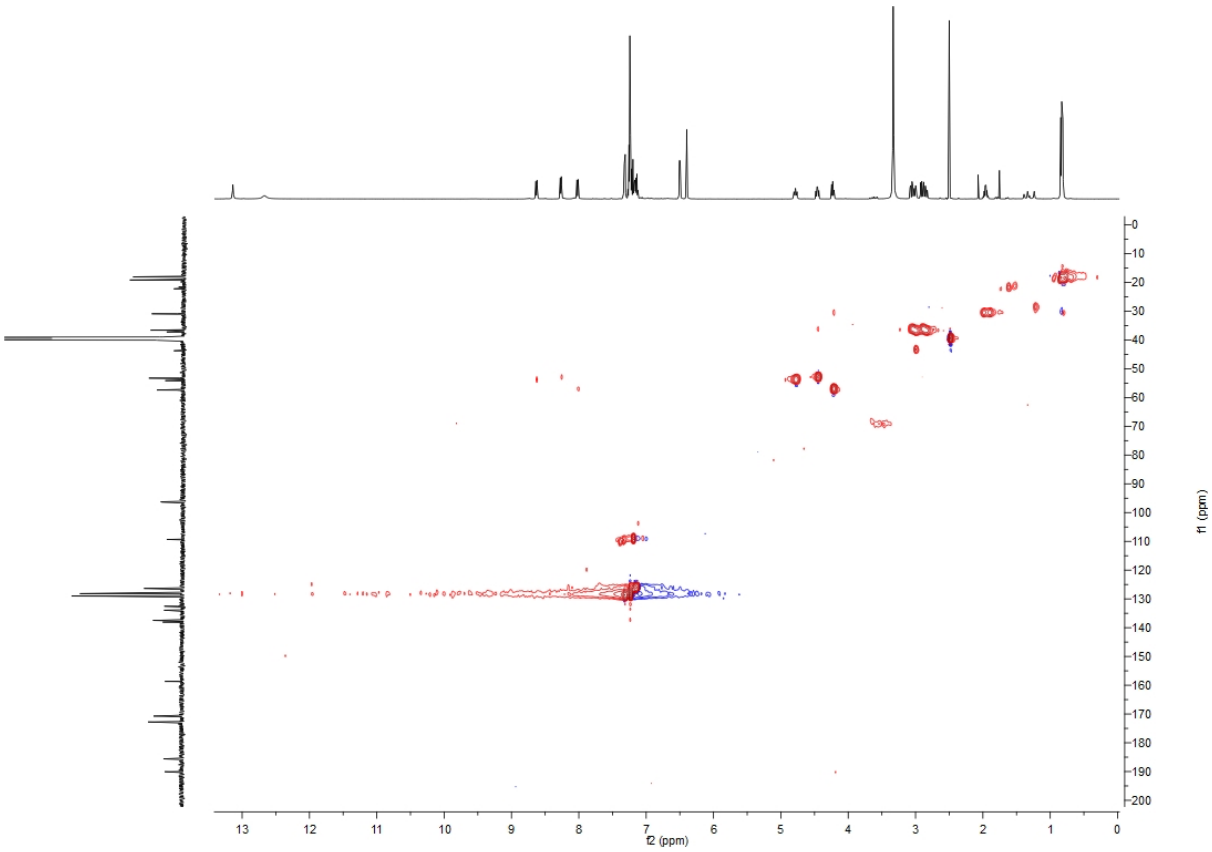

Figure S87. HSQC spectrum (500MHz, DMSO-d_6) of **3**.

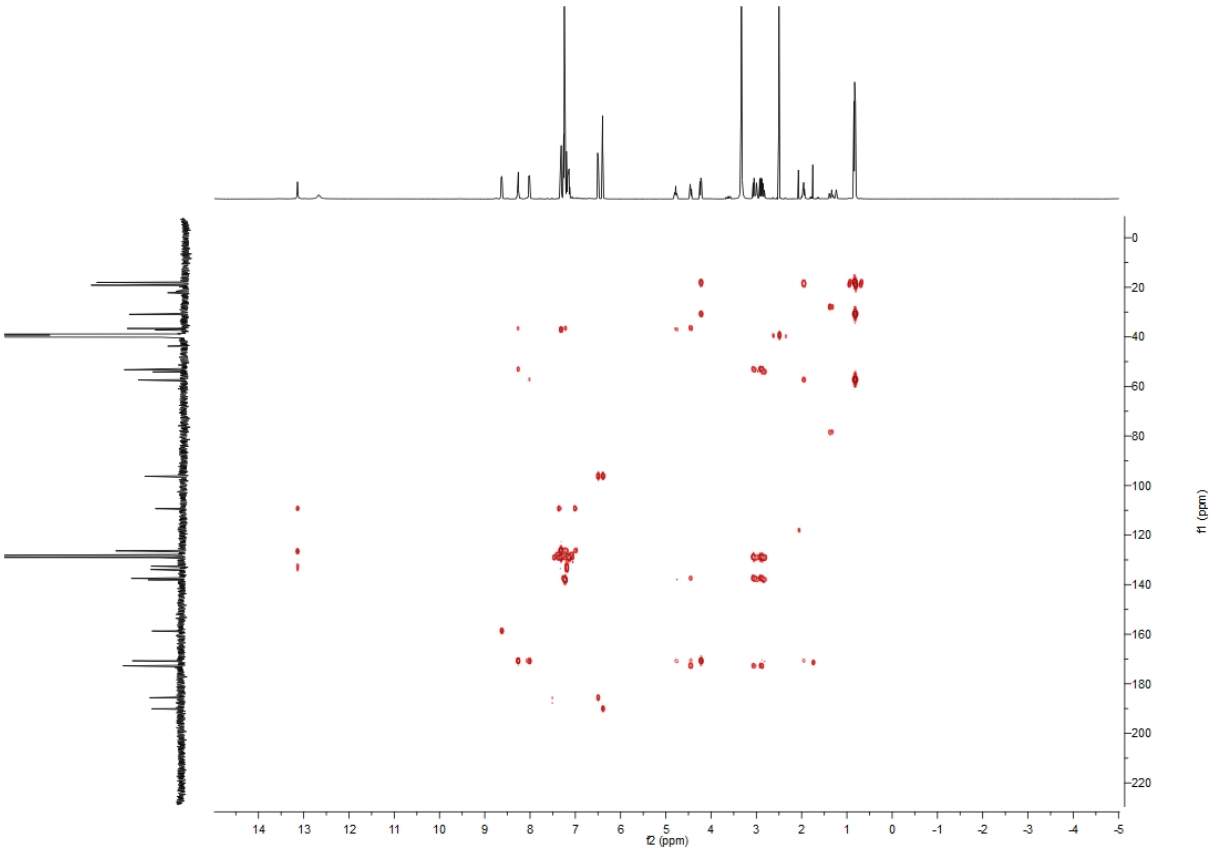

Figure S88. HMBC spectrum (500MHz, DMSO-d_6) of **3**.

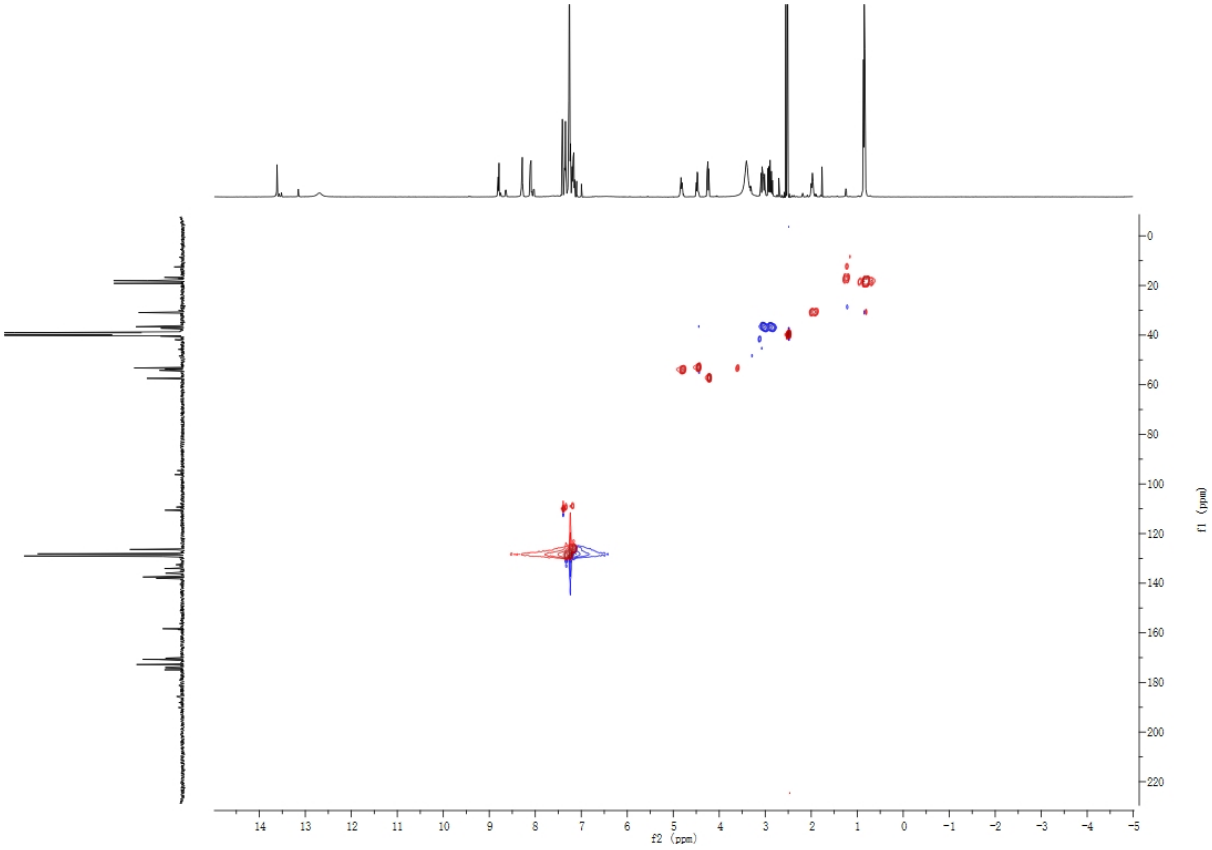

Figure S89. HSQC spectrum (500MHz, DMSO-d_6) of **3a**.

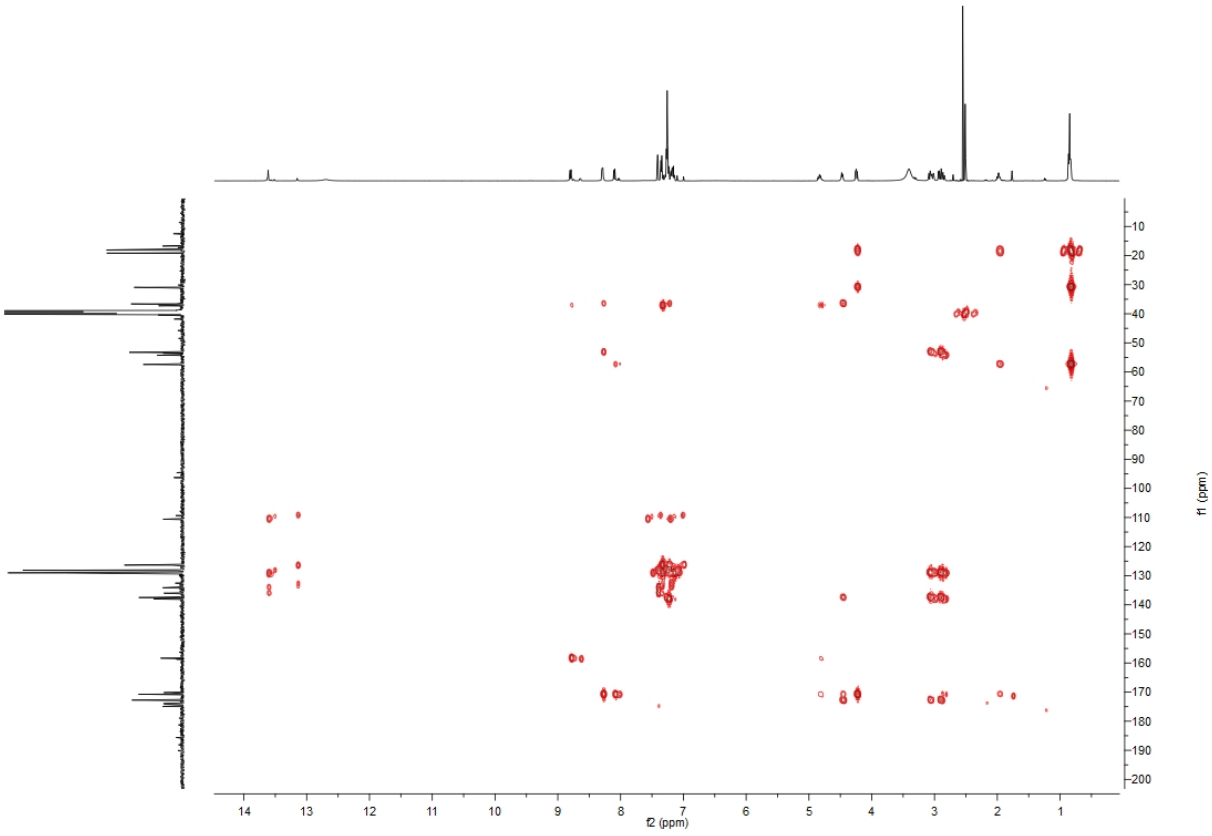

Figure S90. HMBC spectrum (500MHz, DMSO-d_6) of **3a**.

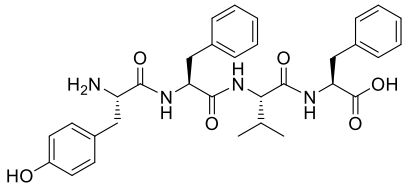

H-Tyr-Phe-Val-Phe-OH (**S1**). Peptide **S1** was prepared using Fmoc-SPPS as mentioned in section 3. Anal. RP-HPLC: t_R = 16.8 min, MS (ESI+): $C_{32}H_{39}N_4O_6$ $[M+H]^+$ calcd./found 575.3/575.3.Purity: >95% (HPLC analysis at 210 nm). ^{1}H NMR (500 MHz, DMSO-d_6) δ 8.69 (d, J = 8.2 Hz, 1H), 8.27 (d, J = 7.7 Hz, 1H), 8.16 (d, J = 9.1 Hz, 1H), 7.91 (s, 2H), 7.15 – 7.31 (m, 10H), 7.04 (d, J = 8.5 Hz, 2H), 6.66 (d, J = 8.5 Hz, 1H), 4.70 (m, 1H), 4.46 (m, 1H), 4.25 (dd, J = 9.0, 7.1 Hz, 1H), 3.87 (m, 1H), 3.04 (m, 2H), 2.92 (ddd, J = 13.9, 8.5, 3.8 Hz, 2H), 2.72 – 2.85 (m, 2H), 1.96 (dq, J = 13.6, 6.7 Hz, 1H), 0.85 (dd, J = 8.3, 6.9 Hz, 6H). ^{13}C NMR (125 MHz, DMSO-d_6) of **S1** δ 172.8, 170.7, 170.5, 168.0, 156.6, 137.5, 137.5, 130.7, 130.7, 129.2, 129.2, 129.0, 129.0, 128.2, 128.2, 128.1, 128.1, 126.3, 126.3, 124.3, 115.3, 57.4, 53.9, 53.3, 53.2, 37.6, 36.6, 36.0, 31.0, 19.1, 18.1.

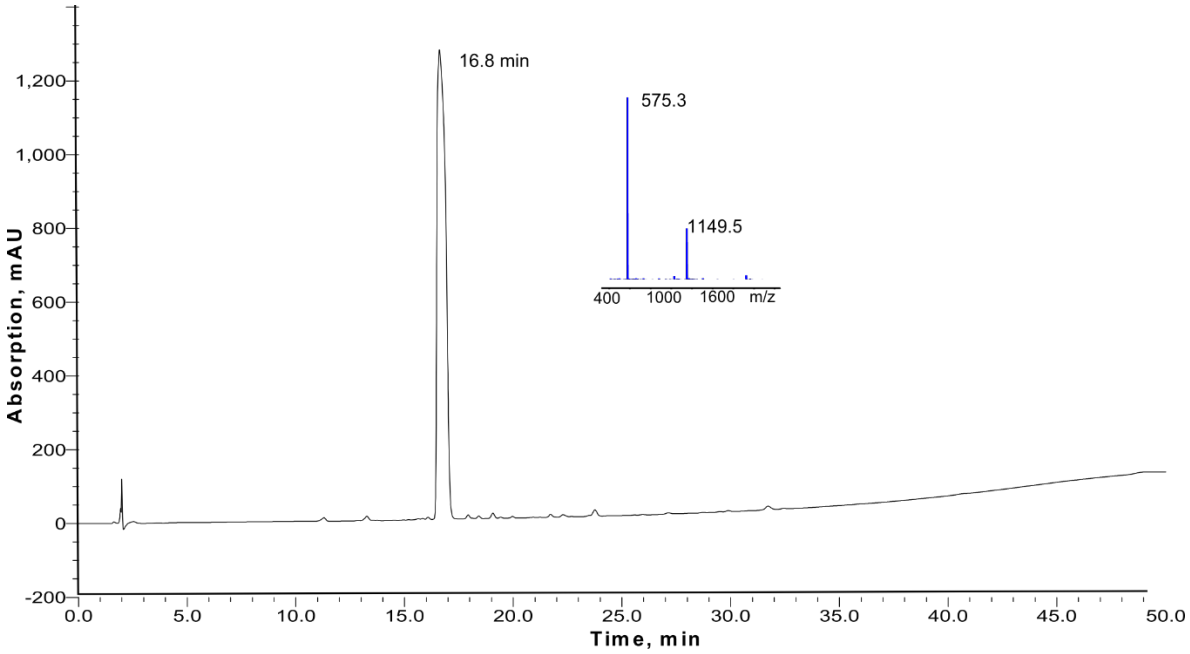

Figure S91. HPLC-MS profile of **S1**, t_R = 16.8 min (purity >95% as judged by peak area of RP-HPLC at 210 nm); Waters XTerra MS C18 column (125 Å 4.6 mm × 150 mm, 5 µm) with a linear gradient of 5% B-95% B over 45 min (*ca.* 2 % B•min^{-1}) at a flow rate of 1 mL•min^{-1} (A = 0.1% TFA in H_2O and B = 0.1 %TFA MeCN).

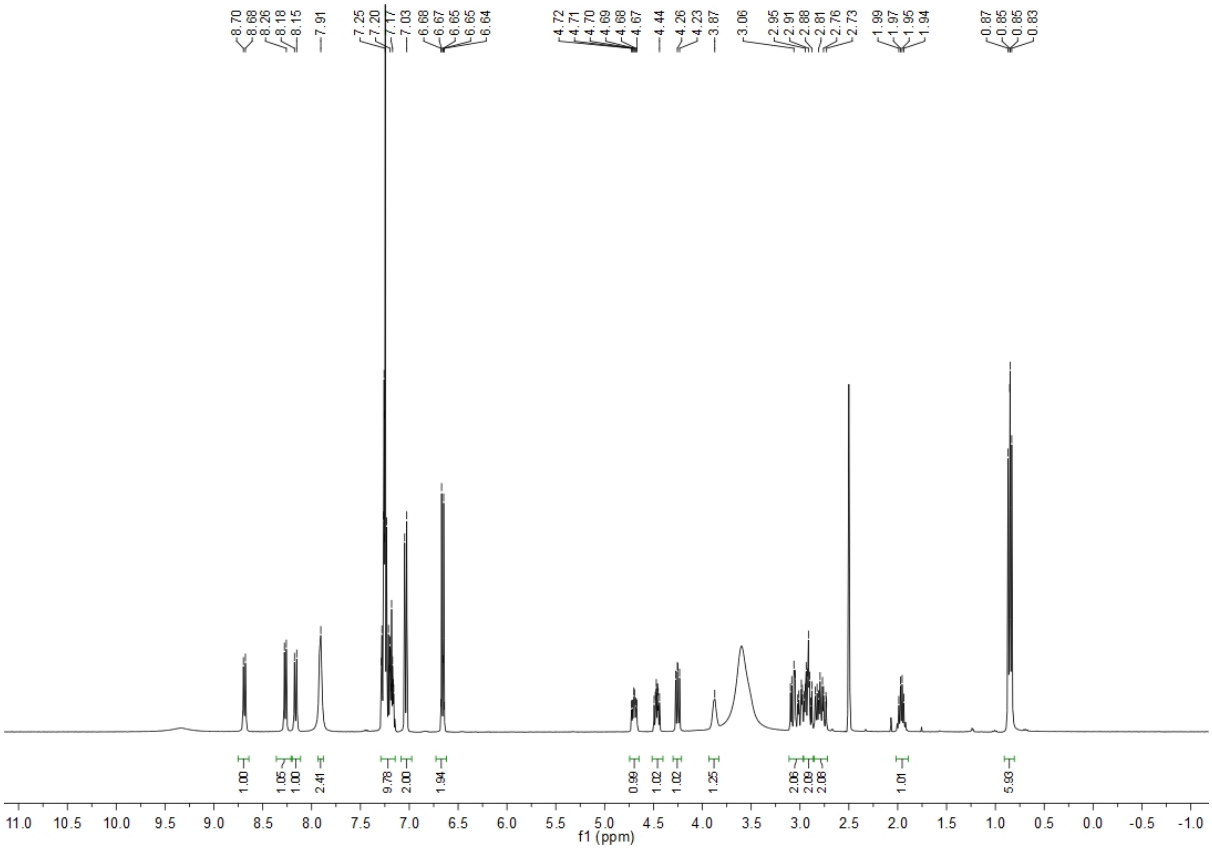

Figure S92. ^{1}H NMR (125 MHz, DMSO-d_6) of **S1**.

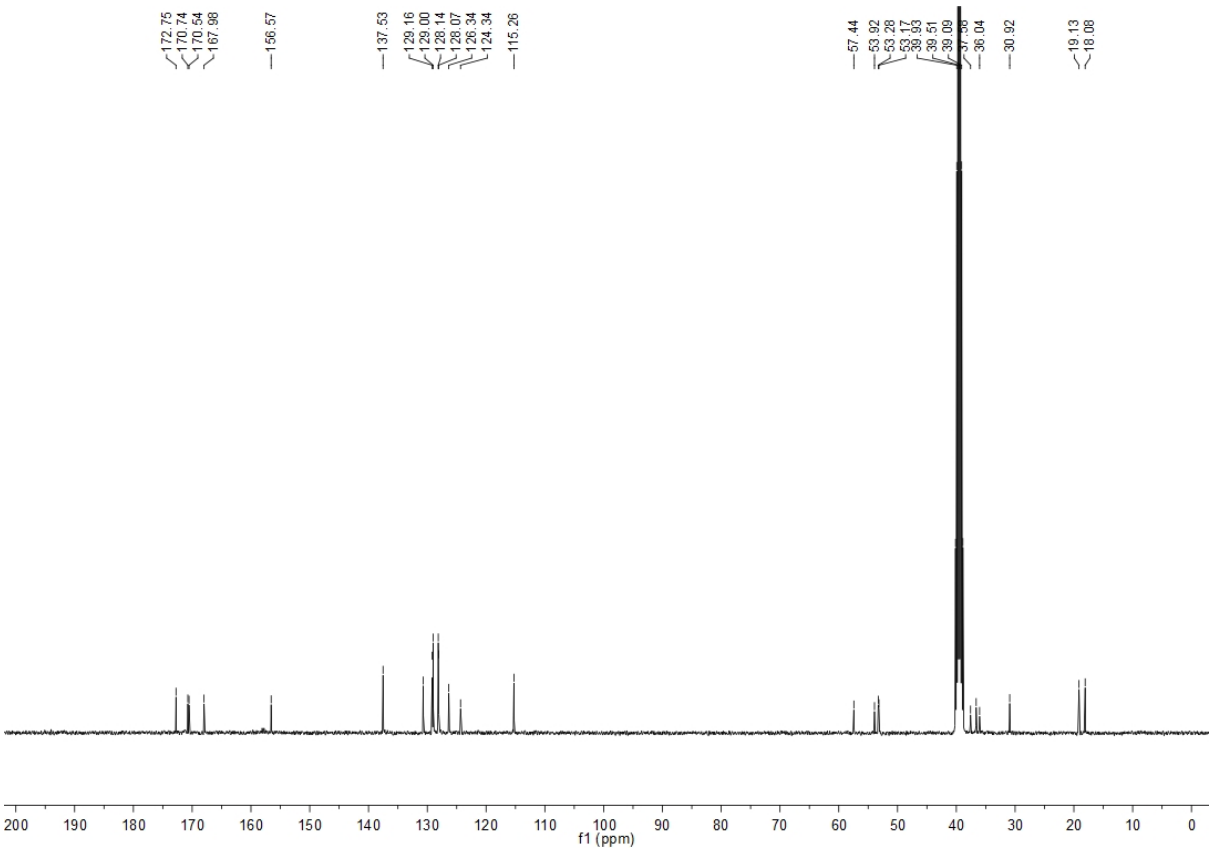

Figure S93. ^{13}C NMR (125 MHz, DMSO-d_6) of **S1**.

6. References

1. M. A. Pullar, D. Barker and B. R. Copp, *Tetrahedron Lett.*, 2015, **56**, 5604-5606.
2. H. Morita, T. Iizuka, C.-Y. Choo, K.-L. Chan, H. Itokawa and K. Takeya, *J. Nat. Prod.*, 2005, **68**, 1686-1688.
3. F. I. Nollmann, A. Dowling, M. Kaiser, K. Deckmann, S. Grösch, R. ffrench-Constant and H. B. Bode, *Beilstein J. Org. Chem.*, 2012, **8**, 528-533.
4. B. Ohlendorf, S. Simon, J. Wiese and J. F. Imhoff, *Nat. Prod. Commun.*, 2011, **6**, 1247-1250.
5. V. L. Novikov, O. P. Shestak, N. P. Mishchenko, S. A. Fedoreev, E. A. Vasileva, V. P. Glazunov and A. A. Artyukov, *Russ. Chem. Bull.*, 2018, **67**, 282-290.